Walter A. Rosenblith New Investigator Award
RESEARCH REPORT

HEALTH EFFECTS INSTITUTE

Number 164
December 2011

Pulmonary Particulate Matter and Systemic Microvascular Dysfunction

Timothy R. Nurkiewicz, Dale W. Porter, Ann F. Hubbs, Samuel Stone, Amy M. Moseley, Jared L. Cumpston, Adam G. Goodwill, Stephanie J. Frisbee, Peter L. Perrotta, Robert W. Brock, Jefferson C. Frisbee, Matthew A. Boegehold, David G. Frazer, Bean T. Chen, and Vincent Castranova

Pulmonary Particulate Matter and Systemic Microvascular Dysfunction

Timothy R. Nurkiewicz, Dale W. Porter, Ann F. Hubbs, Samuel Stone, Amy M. Moseley, Jared L. Cumpston, Adam G. Goodwill, Stephanie J. Frisbee, Peter L. Perrotta, Robert W. Brock, Jefferson C. Frisbee, Matthew A. Boegehold, David G. Frazer, Bean T. Chen, and Vincent Castranova

with a Critique by the HEI Health Review Committee

Research Report 164

Health Effects Institute

Boston, Massachusetts

Trusted Science • Cleaner Air • Better Health

Publishing history: This document was posted at *www.healtheffects.org* in December 2011.

Citation for document:

Nurkiewicz TR, Porter DW, Hubbs AF, Stone S, Moseley AM, Cumpston JL, Goodwill AG, Frisbee SJ, Perrotta PL, Brock RW, Frisbee JC, Boegehold MA, Frazer DG, Chen BT, Castranova V. 2011. Pulmonary Particulate Matter and Systemic Microvascular Dysfunction. Research Report 164. Health Effects Institute, Boston, MA.

 Asterisk Typographics, Barre, Vt., Compositor. Printed by Recycled Paper Printing, Boston, Mass. Library of Congress Catalog Number for the HEI Report Series: WA 754 R432.

Cover paper: made with at least 55% recycled content, of which at least 30% is post-consumer waste; free of acid and elemental chlorine. Text paper: made with 100% post-consumer waste recycled content; acid free; no chlorine used in processing. The book is printed with soy-based inks and is of permanent archival quality.

CONTENTS

Research Report 164

ABOUT HEI

The Health Effects Institute is a nonprofit corporation chartered in 1980 as an independent research organization to provide high-quality, impartial, and relevant science on the effects of air pollution on health. To accomplish its mission, the institute

- Identifies the highest-priority areas for health effects research;
- Competitively funds and oversees research projects;
- Provides intensive independent review of HEI-supported studies and related research;
- Integrates HEI's research results with those of other institutions into broader evaluations; and
- Communicates the results of HEI's research and analyses to public and private decision makers.

HEI typically receives half of its core funds from the U.S. Environmental Protection Agency and half from the worldwide motor vehicle industry. Frequently, other public and private organizations in the United States and around the world also support major projects or research programs. HEI has funded more than 280 research projects in North America, Europe, Asia, and Latin America, the results of which have informed decisions regarding carbon monoxide, air toxics, nitrogen oxides, diesel exhaust, ozone, particulate matter, and other pollutants. These results have appeared in the peer-reviewed literature and in more than 200 comprehensive reports published by HEI.

HEI's independent Board of Directors consists of leaders in science and policy who are committed to fostering the public–private partnership that is central to the organization. The Health Research Committee solicits input from HEI sponsors and other stakeholders and works with scientific staff to develop a Five-Year Strategic Plan, select research projects for funding, and oversee their conduct. The Health Review Committee, which has no role in selecting or overseeing studies, works with staff to evaluate and interpret the results of funded studies and related research.

All project results and accompanying comments by the Health Review Committee are widely disseminated through HEI's Web site (*www.healtheffects.org*), printed reports, newsletters and other publications, annual conferences, and presentations to legislative bodies and public agencies.

ABOUT THIS REPORT

Research Report 164, *Pulmonary Particulate Matter and Systemic Microvascular Dysfunction*, presents a research project funded by the Health Effects Institute and conducted by Dr. Timothy R. Nurkiewicz of the West Virginia University School of Medicine, Morgantown, and his colleagues. This research was funded under HEI's Walter A. Rosenblith New Investigator Award Program, which provides support to promising scientists in the early stages of their careers. The report contains three main sections.

The HEI Statement, prepared by staff at HEI, is a brief, nontechnical summary of the study and its findings; it also briefly describes the Health Review Committee's comments on the study.

The Investigators' Report, prepared by Nurkiewicz and colleagues, describes the scientific background, aims, methods, results, and conclusions of the study.

The Critique is prepared by members of the Health Review Committee with the assistance of HEI staff; it places the study in a broader scientific context, points out its strengths and limitations, and discusses remaining uncertainties and implications of the study's findings for public health and future research.

This report has gone through HEI's rigorous review process. When an HEI-funded study is completed, the investigators submit a draft final report presenting the background and results of the study. This draft report is first examined by outside technical reviewers and a biostatistician. The report and the reviewers' comments are then evaluated by members of the Health Review Committee, an independent panel of distinguished scientists who have no involvement in selecting or overseeing HEI studies. During the review process, the investigators have an opportunity to exchange comments with the Review Committee and, as necessary, to revise their report. The Critique reflects the information provided in the final version of the report.

HEI STATEMENT
Synopsis of Research Report 164

Pulmonary Particulate Matter and Systemic Microvascular Dysfunction

INTRODUCTION

Ambient particulate matter (PM) is a complex mixture of solid and liquid airborne particles, ranging from approximately 5 nm to 100 µm in aerodynamic diameter. To protect the general population and those considered most vulnerable to adverse effects from PM, the U.S. Environmental Protection Agency has promulgated National Ambient Air Quality Standards for PM with an aerodynamic diameter $\leq$ 2.5 µm ($PM_{2.5}$, also referred to as fine particles). Particles in this size range can deposit in the lower airways. Epidemiologic and toxicologic studies show an association between $PM_{2.5}$ exposure and a number of cardiac, vascular, and pulmonary outcomes. Current and past research on PM has aimed at identifying the pathophysiologic mechanisms involved and the characteristics of PM (including size and chemical composition) most responsible for the health effects. Some scientists believe that the subset of $PM_{2.5}$ made up of particles less than 100 nm in diameter (referred to here as nano-PM) may be especially toxic because, although these particles are small, they can be present in large numbers and have a high surface area per unit mass.

Dr. Timothy R. Nurkiewicz (of West Virginia University School of Medicine) submitted an application under the "Walter A. Rosenblith New Investigator Award" to evaluate and compare the effect of fine and nano-titanium dioxide (TiO_2) particles on endothelium-dependent vascular dilation and the underlying mechanisms. This type of PM was chosen because it is used as a nanomaterial in many consumer products. The HEI Research Committee recommended the proposal for funding because they believed the project was innovative and would contribute to understanding the pathophysiologic mechanisms by which PM of different size fractions could cause adverse effects.

APPROACH

Groups of rats were exposed by inhalation to fine and nano-TiO_2 (at concentrations ranging from 0.5 to 20 mg/m^3) or filtered air for up to 12 hours. The primary size of nano-TiO_2 was 21 nm; that of fine TiO_2 was 1000 nm. All observations were made 24 hours after the end of the exposure. To account for differences in deposition patterns between inhaled fine and nano-PM, the investigators used the measured mass of particles deposited in the lungs as the primary exposure metric.

Vascular dilation was evaluated in anesthetized rats by intravital microscopy of the microvasculature in the exteriorized spinotrapezius muscle enclosed in a tissue bath and perfused for the duration of the experiment. A vascular dilator (A23187) was injected into selected microvessels (1–3 per rat) for 2-minute periods. The effect of previous PM exposure was measured as the change in the ability of vessels from PM-exposed rats to dilate in response to A23187, compared with the ability of vessels from filtered air–exposed rats. Arterial dilation was quantified on the basis of video images of each experiment. Because vascular dilation is in large part mediated by nitric oxide (NO), Nurkiewicz and colleagues also evaluated whether PM exposure inhibited NO production or the ability of the vessels to dilate in response to endogenous NO.

The investigators measured oxidative stress, which is thought to mediate the effects of PM on the cardiovascular system, in the microvasculature and in the lung. They also measured lung inflammation and systemic inflammation (cytokines and chemokines), both shown to be linked to oxidative stress, and some markers of coagulation in blood.

RESULTS AND INTERPRETATION

Measurements inside the exposure chamber showed that the peak of the number-based size distribution of nano-PM was 100 nm, indicating that the nano-TiO_2 did not consist of single primary particles but rather of agglomerates of the primary particles. The number-based size distribution of fine PM was bimodal and had a major peak at 710 nm and a minor peak at 100 nm. The measured deposited PM

This Statement, prepared by the Health Effects Institute, summarizes a research project funded by HEI and conducted by Dr. Timothy R. Nurkiewicz of the West Virginia University School of Medicine, Morgantown, and colleagues. Research Report 164 contains both the detailed Investigators' Report and a Critique of the study prepared by the Institute's Health Review Committee.

mass at the same TiO_2 concentration and exposure duration was lower after exposure to nano-PM than to fine PM. Inhalation of either fine- or nano-TiO_2 particles impaired arteriolar dilation, and the effect was dose dependent. At similar measured deposited PM mass, nano-PM produced greater inhibition of microvascular dilation (more than sixfold) than did fine PM.

NO production by the microvascular endothelium was inhibited as a function of different doses of fine and nano-PM, indicating that vascular dilation was dependent on NO. Consistent with this finding was the observation that when a NO donor was added to the perfusate, arterial dilation in response to A23187 was the same in vessels from PM-exposed and filtered air–exposed rats. This result also indicated that endothelial sensitivity to NO was not altered after exposure to either fine or nano-PM.

Other intravital microscopy experiments showed that NO production increased in the presence of radical scavengers in the perfusate and that radical scavengers (in the presence of A23187) partially reduced the inhibition of arterial dilation caused by PM exposure. These findings were consistent with the observed increase in arteriolar ethidium bromide fluorescence and in staining for nitrotyrosine after exposure to either fine or nano-PM. Together, these results demonstrate that the impairment in microvascular function observed after exposure to TiO_2 is likely to be related to enhanced oxidative stress (that is, to the formation of reactive oxygen species) in the microvasculature and the lung.

Results of analyses of markers of lung and systemic inflammation were largely negative: the only statistically significant effect was a small increase in some inflammatory cytokines in the blood of rats exposed to fine PM. Markers of coagulation were for the most part unaffected by the exposure. The investigators measured these markers because they have been associated with exposure to PM and are involved in the processes leading to clot formation. However, no mechanistic interpretation linking them to arteriolar dilation is provided by the authors.

CONCLUSIONS

In its independent review of the study, the HEI Review Committee thought that, overall, this was a thorough and well-conducted study. Each of the specific aims was achieved. The use of intravital microscopy to measure vascular dilation and oxidative stress is a novel approach and may be useful in future investigations. A potential drawback of this procedure is that the use of general anesthesia and surgical manipulations used to obtain measurements may themselves affect microvascular function. Another strength of the study is the measurement of the PM mass deposited in the lung after each exposure condition and the use of this metric for comparing effects of nano- and fine PM.

The concentrations used in the study are very high in relation to the PM levels that are generally encountered in ambient air; however, they are not far from the current occupational exposure limits for TiO_2 recommended by the National Institute for Occupational Safety and Health.

An important finding reported by Nurkiewicz and colleagues is that acute high-dose–inhalation exposure to nano- and fine-TiO_2 particles impairs the ability of the skeletal-muscle microvasculature to dilate in response to a stimulus and that this effect is mediated by decreased NO production by endothelial cells. Also important is the finding that at the same pulmonary mass deposition, nano-PM produced significantly greater systemic microvascular dysfunction than fine PM. The impairment in NO production appears to be related to enhanced oxidative stress in both lung tissue and the vasculature. Although oxidative stress has been linked to both lung and systemic inflammation in several studies, evidence of lung inflammation was weak in this study, and a role of systemic inflammatory mediators was not clearly established.

The study provides insights into the pathophysiologic vascular changes after inhalation of nano-TiO_2. This type of PM is relatively insoluble and is considered to have low reactivity. It should not be considered to be representative of nanoengineered particles in general and of PM in ambient air, which contains a variety of reactive metals, polycyclic aromatic hydrocarbons, and other organic compounds. The Review Committee further cautioned against extrapolating from the effects and mechanisms observed in rats after short-term exposure to high concentrations of the TiO_2 PM to effects in humans after either short-term or long-term exposure to lower concentrations and to different types of PM. Future mechanistic studies might usefully focus on addressing the effects of lower concentrations of ambient and engineered nano-PM not only on the systemic resistance vessels but also on coronary endothelial function.

INVESTIGATORS' REPORT

Pulmonary Particulate Matter and Systemic Microvascular Dysfunction

Timothy R. Nurkiewicz, Dale W. Porter, Ann F. Hubbs, Samuel Stone, Amy M. Moseley, Jared L. Cumpston, Adam G. Goodwill, Stephanie J. Frisbee, Peter L. Perrotta, Robert W. Brock, Jefferson C. Frisbee, Matthew A. Boegehold, David G. Frazer, Bean T. Chen, and Vincent Castranova

The Center for Cardiovascular and Respiratory Sciences (T.R.N., A.G.G., S.J.F., R.W.B., J.C.F., M.A.B.), the Department of Physiology and Pharmacology (T.R.N., D.W.P., A.G.G., R.W.B., J.C.F., M.A.B., D.G.F.), Department of Neurobiology and Anatomy (T.R.N.), Department of Pathology (P.L.P.), and Department of Community Medicine (S.J.F.), West Virginia University School of Medicine, Morgantown; and the Pathology and Physiology Research Branch, Health Effects Laboratory Division, National Institute for Occupational Safety and Health, Morgantown, West Virginia (D.W.P., A.F.H., S.S., A.M.M., J.L.C., D.G.F., B.T.C., V.C.)

ABSTRACT

Pulmonary particulate matter (PM*) exposure has been epidemiologically associated with an increased risk of cardiovascular morbidity and mortality, but the mechanistic foundations for this association are unclear. Exposure to certain types of PM causes changes in the vascular reactivity of several macrovascular segments. However, no studies have focused upon the systemic microcirculation, which is the primary site for the development of peripheral resistance and, typically, the site of origin for numerous pathologies. Ultrafine PM — also referred to as nanoparticles, which are defined as ambient and engineered particles with at least one physical dimension less than 100 nm (Oberdorster et al. 2005) — has been suggested to be more toxic than its larger counterparts by virtue of a larger surface area per unit mass. The purpose of this study was fourfold: (1) determine whether particle size affects the severity of postexposure microvascular dysfunction; (2) characterize alterations in microvascular nitric oxide (NO) production after PM exposure; (3) determine whether alterations in microvascular oxidative stress are associated with NO production, arteriolar dysfunction, or both; and (4) determine whether circulating inflammatory mediators, leukocytes, neurologic mechanisms, or a combination of these play a fundamental role in mediating pulmonary PM exposure and peripheral microvascular dysfunction. To achieve these goals, we created an inhalation chamber that generates stable titanium dioxide (TiO_2) aerosols at concentrations up to 20 mg/m^3.

TiO_2 is a well-characterized particle devoid of soluble metals. Sprague Dawley and Fischer 344 (F-344) rats were exposed to fine or nano-TiO_2 PM (primary count modes of approximately 710 nm and approximately 100 nm in diameter, respectively) at concentrations of 1.5 to 16 mg/m^3 for 4 to 12 hours to produce pulmonary loads of 7 to 150 µg in each rat. Twenty-four hours after pulmonary exposure, the following procedures were performed: the spinotrapezius muscle was prepared for in vivo microscopy, blood samples were taken from an arterial line, and various tissues were harvested for histologic and immunohistochemical analyses. Some rats received a bolus dose of cyclophosphamide 3 days prior to PM exposure to deplete circulating neutrophils and bronchoalveolar lavage (BAL) was performed in separate groups of rats exposed to identical TiO_2 loads. No significant differences in BAL fluid composition based on PM size or load were found in these rats. Plasma levels of interleukin (IL)-2, IL-18, IL-13, and growth-related oncogene (GRO) (also known as keratinocyte-derived-chemokine [KC]) were altered after PM exposure. In rats exposed to fine TiO_2, endothelium-dependent arteriolar

This Investigators' Report is one part of Health Effects Institute Research Report 164, which also includes a Critique by the Health Review Committee and an HEI Statement about the research project. Correspondence concerning the Investigators' Report may be addressed to Dr. Timothy R. Nurkiewicz, Center for Cardiovascular and Respiratory Sciences, Robert C. Byrd Health Sciences Center, 1 Medical Center Drive, West Virginia University, Morgantown, WV 26506-9105.

Although this document was produced with partial funding by the United States Environmental Protection Agency under Assistance Award CR–83234701 to the Health Effects Institute, it has not been subjected to the Agency's peer and administrative review and therefore may not necessarily reflect the views of the Agency, and no official endorsement by it should be inferred. The contents of this document have not been reviewed by private party institutions, including those that support the Health Effects Institute; therefore, it may not reflect the views or policies of these parties, and no endorsement by them should be inferred.

* A list of abbreviations and other terms appears at the end of the Investigators' Report.

dilation was significantly decreased, and this dysfunction was robustly augmented in rats exposed to nano-TiO_2. This effect was not related to an altered smooth-muscle responsiveness to NO because arterioles in both groups dilated comparably in response to the NO donor sodium nitroprusside (SNP). Endogenous microvascular NO production was similarly decreased after inhalation of either fine or nano-TiO_2 in a dose-dependent manner. Microvascular oxidative stress was significantly increased among both exposure groups. Furthermore, treatment with antioxidants (2,2,6,6-tetramethylpiperdine-*N*-oxyl [TEMPOL] plus catalase), the myeloperoxidase (MPO) inhibitor 4-aminobenzoic hydrazide (ABAH), or the nicotinamide adenine dinucleotide phosphate oxidase (NADPH oxidase) inhibitor apocynin partially restored NO production and normalized arteriolar function in both groups. Neutrophil depletion restored dilation in PM-exposed rats by as much as 42%. Coincubation of the spinotrapezius muscle with the fast sodium (Na^+) channel antagonist tetrodotoxin (TTX) restored arteriolar dilation by as much as 54%, suggesting that sympathetic neural input may be affected by PM exposure.

The results of these experiments indicate that (1) the size of inhaled PM dictates the intensity of systemic microvascular dysfunction; (2) this arteriolar dysfunction is characterized by a decreased bioavailability of endogenous NO; (3) the loss of bioavailable NO after PM exposure is at least partially caused by elevations in local oxidative stress, MPO activity, NADPH oxidase activity, or a combination of these responses; and (4) circulating neutrophils and sympathetic neurogenic mechanisms also appear to be involved in the systemic microvascular dysfunction that follows PM exposure. Taken together, these mechanistic studies support prominent hypotheses that suggest peripheral vascular effects associated with PM exposure are due to the activation of inflammatory mechanisms, neurogenic mechanisms, or both.

INTRODUCTION

THE RESISTANCE VASCULATURE AND RESISTANCE GENERATION

Just as a resistor governs the flow of current in an electrical circuit, so do resistance vessels in the vascular circuit. Vascular resistance is defined as the opposition to blood flow that must be overcome in order to propel blood through the peripheral circulation (Zweifach 1991). This resistance is generated almost entirely by microvascular arterioles (Zweifach 1974; Zweifach and Lipowsky 1977). Small resistance arteries (the arterial segments immediately outside a target tissue) also contribute to the generation of vascular resistance but to a much lesser extent than the arterioles (Zweifach 1974; Zweifach and Lipowsky 1977). The dynamic mechanism by which vascular resistance is altered is via a change in vessel diameter. Arteriolar constriction can be so powerful that the vessel lumen can close. Although macrovascular segments or "conduit arteries," such as the aorta and brachial artery, are capable of generating wall tension or even mild constrictions in a very limited regard, they do not substantially contribute to vascular resistance (Zweifach 1974, 1991; Zweifach and Lipowsky 1977, 1984). As such, the primary function of conduit arteries is to channel blood flow to target organs and tissues with as little resistance as possible, thus providing rapid delivery of nutrients. By contrast, the primary function of the resistance vasculature is to regulate and distribute blood flow within an organ. This in turn regulates the delivery of nutrients (such as oxygen [O_2]) and removal of metabolic byproducts (such as carbon dioxide [CO_2]) from the organ. Furthermore, such regulation also contributes to the maintenance of capillary hydrostatic pressure and therefore capillary fluid exchange. Although a tremendous amount of research is regularly performed with conduit arteries, such vessels are anatomically and physiologically different from resistance arteries and, moreover, from arterioles. To truly explore the consequences of particulate matter (PM) exposure upon vascular function, researchers must study the appropriate blood vessels.

PM BURDENS AND RISKS

PM is one of the six air pollutants whose ambient levels are regulated by the U.S. Environmental Protection Agency (U.S. EPA). Major sources of primary PM include fossil fuel combustion, industrial operations, and fires (U.S. EPA 2002), and secondary PM is formed through atmospheric reactions between nitrogen oxides and sulfur oxides. In 2001, PM with an aerodynamic diameter ≤ 2.5 μm ($PM_{2.5}$) constituted approximately 23% of the national ambient PM burden of approximately 31.5×10^5 tons (U.S. EPA 2002). In the past 10 years, evidence has linked PM to pulmonary morbidity and mortality and also to adverse systemic effects and disease. The relationship between PM exposure and mortality is well established (Fairley 1990; Samet et al. 2000a, 2000b; Dockery 2001), and deaths due to cardiovascular dysfunction have emerged as a subgroup of these PM-associated deaths (Samet et al. 2000a; Goldberg et al. 2001). Ambient PM is associated with hospital admissions for patients with preexisting cardiovascular diseases (Burnett et al. 1999; Morris 2001). Moreover, ambient PM exposure increases emergency department visits associated with cardiovascular complications (Metzger

et al. 2004). Alarmingly, $PM_{2.5}$ emissions decreased only about 10% from 1992 to 2001, and this nominal decrease does not consider secondary $PM_{2.5}$ formation, which accounts for a large portion of $PM_{2.5}$ (U.S. EPA 2002).

The U.S. population, including the population groups most susceptible to complications associated with PM exposure (those who are overweight, obese, or hypertensive as well as children and senior citizens), continues to increase. At least two-thirds of our population is obese or overweight and one-third is hypertensive (Fields et al. 2004; Hedley et al. 2004). Children and senior citizens comprise approximately 40% of the total U.S. population, and this figure is projected to swiftly increase in the coming years (U.S. Census Bureau 2004). Perhaps the greater concern is that although the most susceptible population groups continue to increase, the mechanisms by which PM increases morbidity and mortality remain largely unknown. Microvascular dysfunction is typically at the root of almost every pathological process in mammalian systems, and normal microvascular function supports the development or maintenance of tissue homeostasis. If the above-mentioned populations are to be protected or the consequences of PM exposure are to be ameliorated, it is critical to first identify the common microvascular mechanisms or pathways that are perturbed by PM exposure.

PM AND CARDIOVASCULAR EFFECTS

Ischemic heart disease (Schwartz and Morris 1995; Goldberg et al. 2000) and the risk of myocardial infarction (Peters et al. 2001) increase within hours after increases in environmental PM concentrations. Similarly, the risk of cardiac readmission in survivors of myocardial infarction increases after increases in PM (von Klot et al. 2005). Pulmonary inflammation, bradycardia, and cardiac arrhythmias have been proposed as mechanisms for cardiovascular mortality associated with PM (Godleski et al. 2000; Watkinson et al. 2001), but changes in the peripheral vasculature may also be important in this regard. We have reported that pulmonary exposure to either residual oil fly ash or TiO_2 abolishes endothelium-dependent arteriolar dilation in the rat spinotrapezius muscle (Nurkiewicz et al. 2004), and exposure to ambient PM near highways induces systemic inflammation, significantly increases C-reactive protein, and alters cardiac rhythm in healthy human subjects (Riediker et al. 2004). After exposure to diesel exhaust particles, healthy rats also display abnormal cardiac rhythms and their coronary arteries become more sensitive to endothelin, endogenous vasoconstrictor released from the endothelium (Campen et al. 2005). Constriction of the brachial artery has been observed in humans exposed to PM and ozone (O_3) (Brook et al. 2002), and air pollution increases systolic blood pressure in individuals with increased blood viscosity and heart rate (Ibald-Mulli et al. 2001). Conversely, telemetry experiments in rats exposed to PM indicate that heart rate and blood pressure decrease in a dose- and time-dependent fashion (Wichers et al. 2004). In vitro, PM elicits the relaxation of aortic rings but not small arteries (Knaapen et al. 2001; Bagate et al. 2004a). Aortic rings treated with PM extracted from motorcycle exhaust show endothelium-dependent dilation (via a superoxide-dependent mechanism) and agonist-induced vasoconstriction (Cheng and Kang 1999). However, the relevance of these latter in vitro findings is unclear because they rely on the assumption that PM enters the systemic circulation and directly interacts with the vasculature. In normal rats, the serum endothelin concentration increases after PM exposure (Kang et al. 2002). PM exposure also decreases messenger RNA (mRNA) of endothelin-1 and angiotensin-converting enzyme in rat lung tissue; the lower levels of endothelin-1 and angiotensin may reflect endothelial damage in pulmonary blood vessels (Ulrich et al. 2002).

PM AND INFLAMMATION

Numerous hypotheses have been advanced to explain how inhaled PM can elicit a systemic response, but inflammation stands out as the most frequently cited among these hypotheses (National Research Council 1998; Donaldson et al. 2001; Yeates and Mauderly 2001; Kodavanti et al. 2002). Stimulation of the hematopoietic system is a component of systemic inflammatory responses. Cultured human alveolar macrophages (AMs) produce tumor necrosis factor α (TNF α) and proinflammatory cytokines after phagocytosing PM, and circulating IL-1 is elevated in humans exposed to PM (van Eeden et al. 2001). The release of leukocytes from bone marrow is a major component of the inflammatory response. Acute exposure to PM accelerates the transit of polymorphonuclear leukocytes (PMNLs) through bone marrow and into the systemic circulation, whereas chronic exposure increases the size of the bone marrow PMNL pool (van Eeden and Hogg 2002). Blood samples from healthy humans exposed to PM reveal a systemic inflammatory response in the form of elevated levels of immature PMNLs (Tan et al. 2000), neutrophils, and platelets (Salvi et al. 1999). PM exposure has also been shown to accelerate the formation of atherosclerotic lesions and increase cell turnover in plaques (Suwa et al. 2002). Unfortunately, these findings do not provide much insight into the effects of PM exposure at the systemic microvascular level, where most peripheral resistance occurs (Zweifach et al. 1981; Zweifach and Lipowsky 1984).

PM deposited in the lungs may influence systemic microvascular function through the release of factors or cells that exit the lungs and enter the systemic circulation. The pulmonary inflammatory cascade triggered by PM can activate and release such factors and cells into the systemic circulation, but their ultimate destinations and effects are not well understood. Following PM deposition in the lungs, circulating PMNLs increase as a result of AM stimulation of the bone marrow (Terashima et al. 1997). PM exposure stimulates AM cytokine production (Brody and Bonner 1991; Driscoll and Maurer 1991; Brody et al. 1992; Driscoll et al. 1993, 1995) and also stimulates human bronchial epithelial cells to release proinflammatory cytokines (Fujii et al. 2001). Within 24 hours of PM exposure, circulating cytokines induce systemic neutrophilia via increased PMNL mobilization into the circulating pool and accelerated PMNL release from the postmitotic pool (Suwa et al. 2000). Cytokines can also directly alter microvascular tone or permeability (Matsuki et al. 1993; Mayhan 2002). For example, IL-1, IL-6, and TNF α acutely dilate skeletal-muscle arterioles and increase microvascular sensitivity to arginine-vasopressin (Vicaut et al. 1991; Baudry et al. 1996; Brian and Faraci 1998; Matsuki and Duling 2000). However, it is not known whether PM exposure actually triggers an effect of PMNLs on microvascular function; one aim of this study was to determine whether it does.

Generation of reactive oxygen species (ROS) during PM-induced inflammation could also lead to systemic effects (Donaldson et al. 2001). PM generates ROS in cell-free systems (Gilmour et al. 1996), cultured cells (Carter et al. 1997; Jimenez et al. 2000), and animals (Costa and Dreher 1997; Kadiiska et al. 1997), and ROS in the pulmonary system can initiate a systemic cytokine response via NF-κB (nuclear factor kappa-light-chain enhancer of activated B cells) (Rahman and MacNee 1998). Some ROS are membrane permeable and could theoretically exit the immediate pulmonary area, but this is unlikely because they are also highly reactive and short-lived (Kohen and Nyska 2002). Alternatively, active PMNLs, which have access to the entire system of circulation, release significant amounts of ROS (Fantone and Ward 1982; Yoshioka and Ichikawa 1989; Hampton et al. 1996; Carreras et al. 1997). PMNL activation in the kidney constricts the efferent arteriole, but this effect is absent in the presence of ROS scavengers (Yoshioka and Ichikawa 1989). In obese subjects, the antioxidant troglitazone reduces the generation of ROS by PMNLs and improves flow-dependent dilation of the brachial artery (Garg et al. 2000). However, there is no information on whether the generation of ROS by PMNLs affects microvascular blood flow after PM exposure. At the microvascular level, it is likely that ROS derived from PMNLs would first influence the endothelium, where the ROS rapidly oxidize endothelium-derived NO and nullify its influence on vascular tone (Gryglewski et al. 1986; Rubanyi and Vanhoutte 1986), and it has recently been shown that ROS attenuate endothelium-dependent dilation in spinotrapezius-muscle arterioles (Lenda et al. 2000). Another aim of this study is to determine whether pulmonary PM influences endothelium-dependent regulation of arteriolar tone via reactive species.

During the course of an inflammatory response, the PMNL may also deposit hemoproteins, such as MPO, that may play an important role in host defense (Klebanoff 1991; Vogt 1996). MPO uses hydrogen peroxide (H_2O_2) derived from a neutrophil's respiratory burst to catalyze hypochlorous acid (HOCl) formation, which also produces substantial amounts of ROS (Podrez et al. 2000; Winterbourn et al. 2000; Eiserich et al. 2002; Gaut et al. 2002). These MPO-dependent ROS have been found to drive NO catabolism to nitrite (Eiserich et al. 2002; Gaut et al. 2002; Hazen et al. 1999). Following leukocyte degranulation, MPO has been shown to concentrate in endothelial cells and the subendothelial matrix (Baldus et al. 2001, 2002; Eiserich et al. 2002). This strategic location within the vascular wall ideally positions MPO to oxidize NO and thereby negate its relaxing effect on vascular smooth muscle (VSM) (Hazen et al. 1999; Abu-Soud and Hazen 2000; Eiserich et al. 2002; Gaut et al. 2002). As expected, MPO impairs vascular responsiveness to endothelium-dependent vasodilators such as acetylcholine and the calcium (Ca^{2+}) ionophore A23187, which exert an effect via NO synthase stimulation (Eiserich et al. 2002; Zhang et al. 2001a). Additionally, MPO catalyzes the oxidation of chlorides (Cl^-) by H_2O_2 (Eiserich et al. 1998), which produces the HOCl that has been shown to inhibit endothelial NO production by chlorinating L-arginine (Zhang et al. 2001a,b). Although the adverse effects of MPO on endothelium-dependent dilation have been documented in larger conduit arteries, studies have not been performed at the microvascular level, and the potential association with systemic effects of PM exposure has not been explored.

NANOTECHNOLOGY

Nanotechnology has firmly rooted itself in multiple aspects of our daily lives, and people are more likely to experience exposure via inhalation than other major routes of exposure. As a result, and in the absence of proper characterization of the biologic effects of exposure to nano-PM, these particles may become the asbestos of the 21st century (Gwinn and Vallyathan 2006). Certainly, countless types of nano-PM exist, and nano-TiO_2 is not characteristic of the collective nano-PM pool. But because it is not

practical to attempt a single study of all nano-PM, we focused on nano-TiO_2 particles, which are metal oxides and, as such, are representative of commonly used spherical metal-oxide nano-PM. Nano-TiO_2 particles are among the smallest nano-PM used in commercial and industrial applications and are regularly used as photocatalysts to clean air and water (Sun et al. 2004), antibacterial agents on glass and steel (Shieh et al. 2006), and components of numerous cosmetics and sunscreens. Despite the widespread use of nano-TiO_2, little is known about its biologic effects, although nano-TiO_2 is known to cause airway inflammation and injury in a dose-dependent manner (Chen et al. 2006b; de Haar et al. 2006; Grassian et al. 2007). Furthermore, nano-TiO_2 can enter the systemic circulation (Geiser et al. 2005). We have previously shown that systemic microvascular dysfunction follows deposition of fine-TiO_2 particles in the lungs (Nurkiewicz et al. 2004, 2006). Although many of the widespread applications of nanotechnology are clearly beneficial, such benefits cannot be fully realized until the biologic effects of nano-PM exposure are fully defined (Maynard et al. 2006).

COAGULATION STUDIES

The rationale for performing coagulation studies is that common human diseases, including myocardial infarction and stroke, are caused by abnormalities of blood coagulation that predispose people to thrombosis (blood clots). These diseases are influenced by environmental factors; however, not all risk factors for clotting disorders are known. Nanomaterials that enter the workplace could enter the body through inhalation, and these exposures could alter the blood coagulation system. Although in vitro studies of the effects of nanosized materials on blood coagulation proteins can be performed, in vivo studies are needed because the effects on blood clotting cannot be predicted with certainty with in vitro experiments alone.

SPECIFIC AIMS

The central hypothesis of this study was that the size of inhaled particles dictates the intensity of subsequent systemic microvascular dysfunction, and this dysfunction is mediated by inflammation. This hypothesis was tested through the completion of three specific aims:

SPECIFIC AIM 1

Determine the severity of systemic microvascular dysfunction after PM exposure and characterize the influence of particle size in this dysfunction. Rats were exposed via inhalation to various loads of fine TiO_2 (a primary particle size of 1 μm) and nano-TiO_2 (a primary particle size of 21 nm). Endothelium-dependent arteriolar dilation was subsequently evaluated by intraluminal infusion of an endothelial agonist into a single arteriole. Specific Aim 1B reanalyzed the data generated from Specific Aim 1A to determine whether deposited particle surface area is a more appropriate dose metric than particle mass burden.

1A. Define the dose–response relationships between particle exposure and microvascular dysfunction.

1B. Determine whether particle surface area is a stronger predictor than mass of the microvascular dysfunction associated with particle exposure.

SPECIFIC AIM 2

Determine whether PM exposure reduces endothelium-dependent microvascular NO production or VSM NO sensitivity. Rats were exposed to fine and nano-TiO_2 aerosols at concentrations that produced 50% impairment of arteriolar dilation 24 hours after exposure (EC_{50}). Endothelium-dependent NO production was stimulated while simultaneously measuring microvascular concentration or [NO] with a NO-sensitive microelectrode.

2A. Measure microvascular NO during endothelial stimulation in rats exposed to PM.

2B. Determine whether VSM NO sensitivity is altered by PM exposure.

SPECIFIC AIM 3

Determine whether systemic inflammation is associated with the microvascular dysfunction after PM exposure. Rats were exposed to fine and nano-TiO_2 at doses described in Specific Aim 2 (EC_{50}). Fluorescent intravital microscopy was used to measure oxidative stress in the arteriolar wall, and histologic techniques were used to characterize microvascular inflammation. Specific radical scavengers and inhibitors of MPO and NADPH oxidase were used to determine the contribution of these factors to the microvascular dysfunction associated with PM exposure.

3A. Characterize ROS generation in the systemic microcirculation after PM exposure.

3B. Determine whether an increased ROS presence in the arteriolar wall contributes to the microvascular dysfunction associated with PM exposure.

3C. Identify changes in MPO activity in the arteriolar wall after PM exposure and determine whether any such change contributes to the inherent microvascular dysfunction.

METHODS

LABORATORY ANIMALS

Specific pathogen-free male Sprague Dawley (Hla:(SD) CVF) rats (6 to 7 weeks old) were purchased from Hilltop Laboratories (Scottsdale, PA) and housed in an animal facility approved by the Association for Assessment and Accreditation of Laboratory Animal Care International at the National Institute for Occupational Safety and Health (NIOSH). Rats were housed in laminar flow cages under controlled temperature and humidity conditions and a 12 hour light/12 hour dark cycle. Food and water were provided ad libitum. Rats were acclimated for 5 days before use and certified free of endogenous viral pathogens, parasites, mycoplasms, *Helicobacter*, and cilia-associated respiratory (CAR) bacillus. To ensure that all methods were performed humanely and with regard for alleviation of suffering, the Animal Care and Use Committees of NIOSH and West Virginia University approved all experimental procedures. A flowchart is provided in Figure 1 that provides an overview of all experimental procedures performed and endpoints measured.

INHALATION EXPOSURE

An inhalation exposure system, consisting of a fluidized-bed powder generator, an animal chamber, and several aerosol monitoring devices, was developed for continuous generation and monitoring of fine or nano-TiO_2 aerosols for rodent exposure (Chen et al. 2006a). Bronze beads were used in the bed of the generator to enhance particle dispersion and aerosolization; a schematic diagram of the system is presented in Figure 2. The system was designed based on the criteria of simplicity, ability to disperse TiO_2 aerosols, and ease of maintenance. The fine and nano-TiO_2 powders were obtained from Sigma-Aldrich (titanium [IV] oxide, 224227, primary particle size 1 μm, St. Louis, MO) and DeGussa (aeroxide TiO_2, P25, primary particle size 21 nm, Parsippany, NJ), respectively. To reduce the potential formation of aggregates from van der Waals force, we carefully prepared the TiO_2 powders for generation by sieving (to remove the big aggregates), drying (to avoid aggregate formation because of high humidity), and storage (in a jar inside a dessicator to prevent aggregate attraction through contact charges). A fluidized-bed aerosol generator (TSI Inc., Shoreview, MN) was used in this study because it was able to disperse powders effectively.

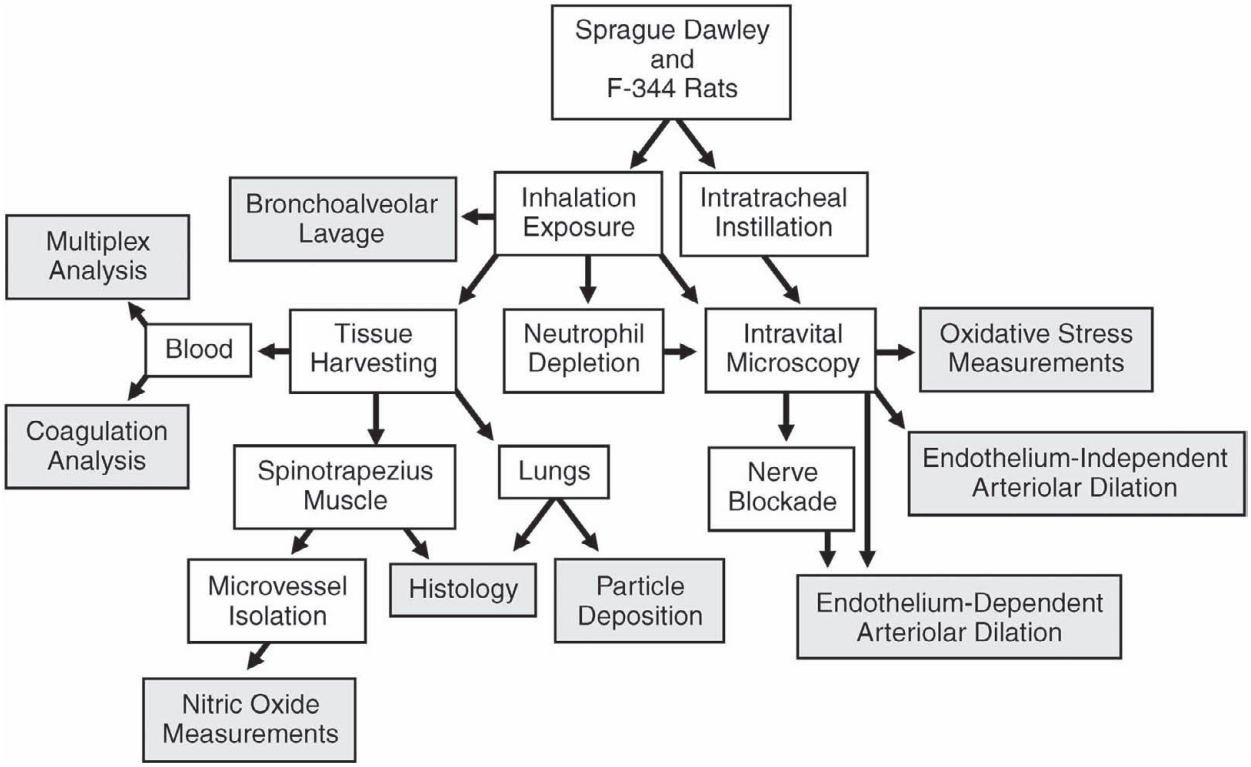

Figure 1. Schematic diagram of overall study design. White boxes represent fundamental techniques and components of the study that are described in Methods. Shaded boxes represent endpoints in animal experiments from which data in Results were generated.

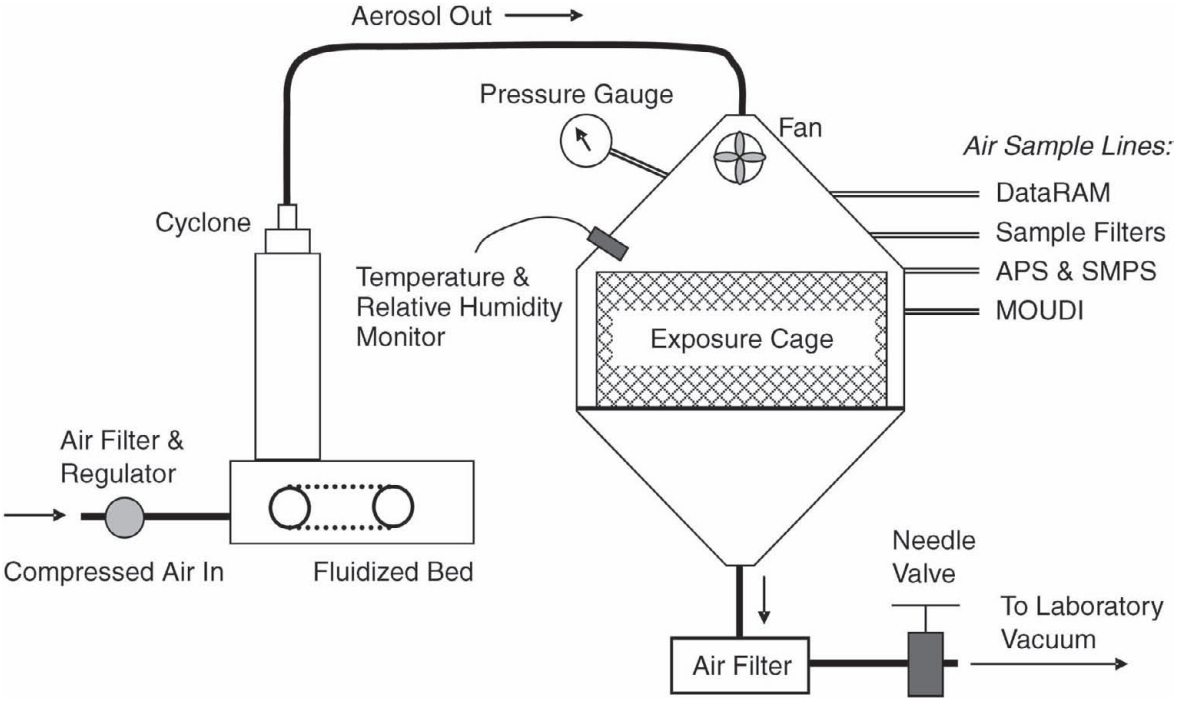

Figure 2. Schematic diagram of the TiO_2 inhalation exposure system. The system includes data-logging real-time aerosol monitor (DataRAM), APS, SMPS, and micro-orifice uniform deposit impactors (MOUDI). (Reprinted from Nurkiewicz et al. 2008).

A 19-L metabolism chamber that contains an animal cage was modified for use as the whole-body exposure chamber. The cage can accommodate three rats for each exposure. During exposure, TiO_2 mass concentrations were continuously monitored with a Data RAM (DR-40000 Thermo Electron Co., Franklin, MA) and gravimetrically measured with Teflon filters. Aerosol concentrations between 1.5 and 20 mg/m^3 were achieved by adjusting the powder feed rate in the generator. Pulmonary deposition was estimated by the following formula: Pulmonary Load = aerosol concentration × minute ventilation × exposure duration × deposition fraction, where minute ventilation and deposition fraction were estimated to be 200 cc/min and 10%, respectively. The particle-size distributions of TiO_2 aerosols were measured with a micro-orifice uniform deposit impactor ([MOUDI] MSP Co., Shoreview, MN), a scanning mobility particle sizer (SMPS, TSI Inc.), and an aerodynamic sizing instrument (APS, TSI Inc.). The impactor was used for measuring mass-based, aerodynamic size distributions, whereas the latter two sizing devices were combined for determining number-based mobility size distributions. In addition, temperature, relative humidity, and pressure in the chamber were monitored throughout the exposure.

INTRATRACHEAL INSTILLATION

To determine whether the systemic microvascular effects of pulmonary particle exposure were affected by different exposure methods, a separate group of Sprague Dawley rats that were the same age and weight as other rats used in this study were lightly anesthetized by an intraperitoneal (i.p.) injection of sodium methohexitol (Brevital) and instilled intratracheally (i.t.) with 100 µg of fine TiO_2 (in a 300-µL sterile saline suspension) according to previously established methods (Brain et al. 1976).

TIME FRAME

All experimental procedures described from this point forward were performed 24 hours after the end of either inhalation exposure or i.t. instillation.

INTRAVITAL MICROSCOPY

Animals were anesthetized with sodium thiopental (100 mg/kg, i.p.) and placed on a heating pad to maintain a 37°C rectal temperature. The trachea was intubated to ensure a patent airway and the right carotid artery was cannulated to measure arterial pressure. The right

spinotrapezius muscle was then exteriorized for microscopic observation, leaving its innervation and all feed vessels intact. After exteriorization, the muscle was gently secured over an optical pedestal at its in situ length (i.e., after exteriorization, the muscle was gently secured over an optical pedestal as it normally occurs) and immersed in a tissue bath for transillumination and observation. Throughout the surgery and subsequent experimental period, the muscle was continuously superfused with an electrolyte solution (119 mM sodium chloride [NaCl], 25 mM sodium bicarbonate [$NaHCO_3$], 6 mM potassium chloride [KCl], and 3.6 mM calcium chloride [$CaCl_2$]), warmed to 35°C, and equilibrated with 95% nitrogen (N_2) and 5% CO_2 (pH = 7.35–7.40). Superfusate flow rate was maintained at 4 to 6 mL/min to minimize equilibration with atmospheric O_2 (Boegehold and Bohlen 1988). A schematic diagram of the intravital microscopy preparation is depicted in Figure 3. In the reported experiments, arterial pressure and arteriolar diameter were measured with video calipers or digitally captured, and digital images were captured for fluorescence analysis (described below under the Measurement of Microvascular Oxidative Stress section).

MEASUREMENT OF PULMONARY PARTICLE DEPOSITION AND SURFACE AREA

Lungs were removed, weighed, frozen at −80°C, and then lyophilized. Sample digestion was initiated by placing the tissue into a 15-mL glass centrifuge tube with 10 mL of concentrated sulfuric acid. The tubes were then put into an aluminum block and placed into a muffle furnace at ambient temperature. The temperature of the furnace was increased to 100°C, and the samples were allowed to heat at this temperature for 15 minutes. The furnace temperature was then increased to 125°C, and once this temperature was reached, the samples were allowed to heat for 1 hour, slowly

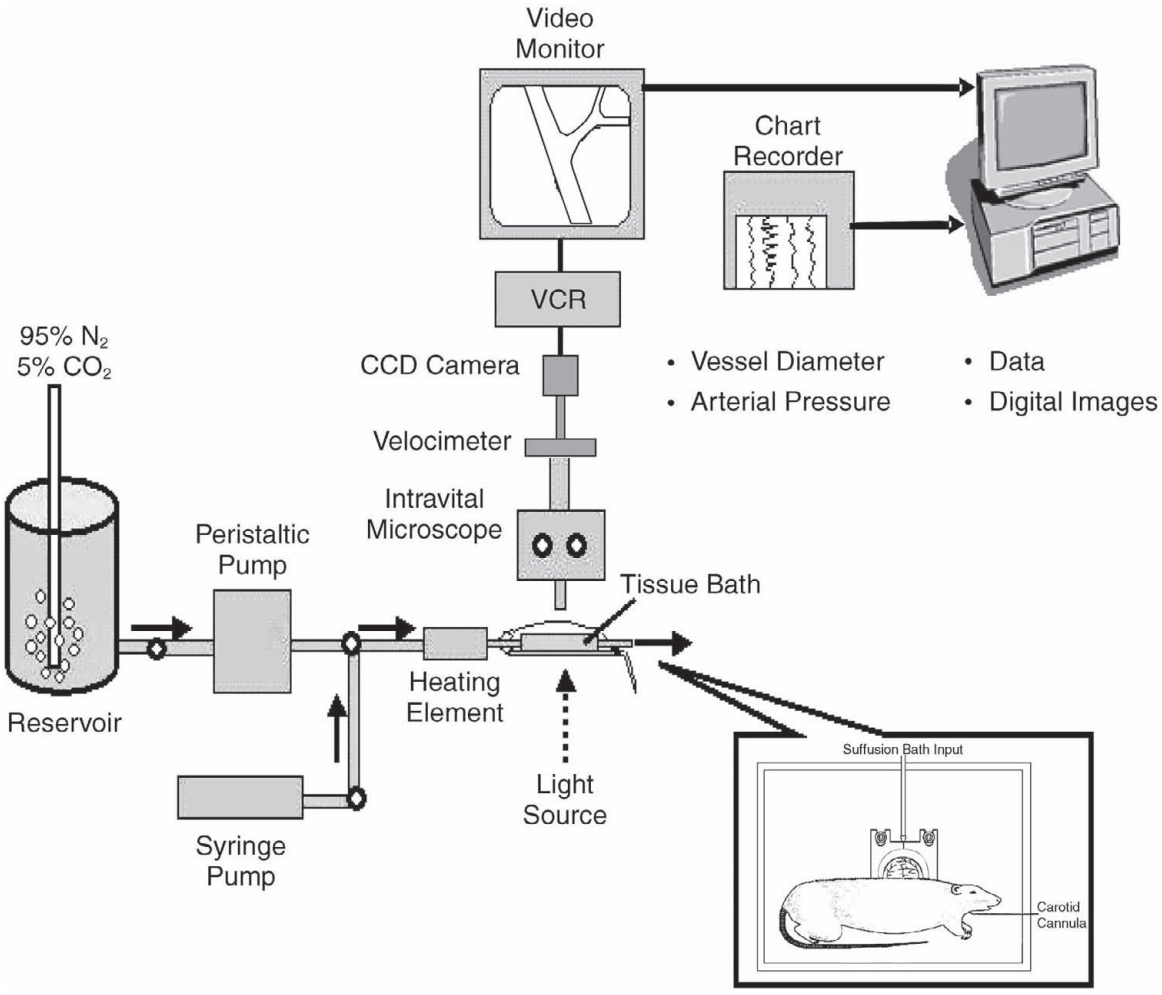

Figure 3. Schematic diagram of the intravital microscopy system.

digesting the lung tissue. After this time period, the muffle furnace was heated at 50°C increments. Each time a higher temperature level was reached in the furnace, the samples were held for 15 minutes before the next temperature increase until a final temperature of 250°C was reached. Once the furnace temperature was at 250°C, the samples were allowed to heat for 1 hour. The muffle furnace was turned off and allowed to cool to near room temperature. The samples were removed from the furnace and allowed to finish cooling to room temperature before proceeding to the next steps.

Once the test tubes had been equilibrated at room temperature, the contents of the tubes were transferred into 50-mL centrifuge tubes that had been placed into a pan filled with cold tap water. The test tubes were each rinsed with a solution of 10% (vol/vol) sulfuric acid. The rinsates were added to the centrifuge tube. A total of four rinses were performed on each test tube. After the final rinse, the samples were allowed to cool in the water bath before bringing the samples up to a final volume of 40 mL. Each sample was filtered through a 1-μm filter, then capped and inverted several times to ensure mixing of the sample before analysis by inductively-coupled plasma-atomic emission spectroscopy. The samples were analyzed with a Perkin Elmer Optima 3200XL ICP (Cleveland, OH). Lung TiO_2 burden was expressed as total lung burden (μg).

Assuming that the particles are spherical, the specific surface area for the fine and nano-TiO_2 particles are determined to be 2.0 and 15.8 m^2/g, respectively, indicating that nano-TiO_2 had approximately eight times more surface area per unit mass than fine TiO_2. The particle densities used in the calculation are 4.23 and 3.8 g/cm^3, respectively.

BRONCHOALVEOLAR LAVAGE

At 24-hours postexposure, rats were euthanized with sodium pentobarbital (≥100 mg/kg, i.p.). The abdomen was opened, and whole blood was collected from the renal vein with a Vacutainer blood collection tube containing sodium ethylenediamine tetraacetate (Na_2EDTA) as an anticoagulant. A tracheal cannula was inserted and ice-cold Ca^{2+}–magnesium (Mg^{2+})-free phosphate-buffered saline (PBS) was performed through the cannula. The first lavage was with 6 mL of PBS and was kept separate from the rest of the lavage fluid. Subsequent lavages used 8 mL of PBS until a total of 80 mL of lavage fluid was collected. The samples were centrifuged, and the first supernatant was saved for lactate dehydrogenase (LDH) activity and protein assays. Cells were combined and resuspended in 4-(2-hydroxyethyl)-1-piperazineethanesulfonic acid (HEPES)-buffered media to determine cell counts as well as AM activity by cultured liquids as described previously (Porter et al. 2001, 2002). Blood cell differentials were determined with a Cell Dyne counter and BAL cells were counted with an electronic cell counter equipped with a cell-sizing attachment.

HISTOPATHOLOGIC ANALYSIS

At 24-hours postexposure, lungs from other rats were rapidly removed and inflated with 6 mL 10% neutral-buffered formalin, routinely processed overnight in an automated tissue processor, embedded in paraffin, sectioned at 5 μm, and stained with hematoxylin and eosin (H&E). The left lung lobe pathology was evaluated by a board-certified veterinary pathologist in a blinded fashion.

NITRIC OXIDE MEASUREMENT

The left and right spinotrapezius muscles from the same animal were excised and placed in Ca^{2+}-free Dulbecco's PBS. The excised muscles were pinned out on a Sylgard-coated petri dish, and microvessels were dissected from the tissue at 4°C. The microvessels were lightly homogenized during collection and then lightly centrifuged to form a loose pellet. The pellet was then placed into a four-port, water-jacketed (34°C), biosensing chamber (World Precision Instruments Inc., Sarasota, FL) that contained 2 mL Dulbecco's PBS with Ca^{2+} (3.6 mM), L-arginine (0.2 mM), and tetrahydrobiopterin (BH_4, 4 μM). Two of the chamber ports contained ISO-NOP NO sensors (World Precision Instruments Inc., Sarasota, FL), the third contained a temperature probe, and the fourth was left open to add reagents to the chamber via digital micropipette (Ranin, Woburn, MA). The ISO-NOP sensors were connected to an Apollo 4000 Free Radical Analyzer (World Precision Instruments, Sarasota Inc., FL) to make electrochemical NO measurements in real time (Zhang 2004; Davies and Zhang 2008). Prior to each use, electrodes were calibrated from the decomposition of *S*-nitroso-*N*-acetyl-D, L-penicillamine (SNAP) to NO in a copper catalyst solution (cuprous chloride, 0.1 M). Data were collected at a rate of 10 values per second, and measurements were made only during steady-state responses that were at least 30 seconds in duration. Because the amount of microvascular tissue that was dissected varied between experiments, data were normalized to tissue mass (nM/mg).

MEASUREMENT OF MICROVASCULAR OXIDATIVE STRESS

ROS, such as O_2, were quantified in the microvascular wall via hydroethidine (HE) oxidation. HE was added to the muscle superfusate (described in the Intravital Microscopy section) at a concentration of 1×10^{-3} M, and the

spinotrapezius muscle was continuously exposed to this HE-containing superfusate for 30 minutes in complete darkness to prevent HE photodestruction. HE has been extensively used for the detection of O_2^- (Morgan et al. 1979; Bindokas et al. 1996; Benov et al. 1998); it easily permeates cell membranes and, when oxidized by O_2^-, is converted to fluorescent ethidium bromide that intercalates into nuclear DNA (Morgan et al. 1979; Benov et al. 1998). In theory, any differences among vessels in the extent of cellular HE loading could also lead to differences in ethidium bromide fluorescence that would be erroneously interpreted as differences in O_2^- activity. To circumvent this problem, we calculated the ratio of oxidized-to-unoxidized substrate in the arteriolar wall from paired fluorescence intensity measurements at the peak emission wavelengths for ethidium bromide and HE, respectively. Tissue autofluorescence at each of these wavelengths was measured before HE exposure and then subtracted from signals measured after HE exposure to determine specific ethidium bromide and HE fluorescence intensities. After the 30-minute exposure period, the muscle was rinsed with normal superfusate for 15 minutes to remove extracellular HE and then briefly (1–2 seconds) illuminated with a mercury lamp with appropriate excitation and emission filters for detection of ethidium bromide fluorescence (480- to 550-nm bandpass, 590-nm barrier), and HE fluorescence (330- to 385-nm bandpass, 420-nm barrier). Fluorescence images were acquired, stored, and analyzed with Metamorph 6.01 imaging software (Universal Imaging, Dowington, PA).

MULTIPLEX ANALYSIS

Whole blood was collected via the carotid artery cannula from live animals directly into tubes containing ethylenediaminetetraacetic acid dipotassium salt (K_2 EDTA) and immediately centrifuged for 10 minutes at 2500 × *g*. The plasma layer (supernatant) was then transferred into 1.5-mL microcentrifuge tubes. These tubes were snap-frozen in liquid nitrogen before being placed at −80°C for long-term storage (less than 6 months). When plates were to be analyzed, samples were slow-thawed and placed on ice. Analysis was performed with multiplex suspension bead array immunoassays on a Luminex 200 system (Luminex Corporation, Austin, TX). The levels of 26 cytokines that were part of the Rat Cytokine and Rat Cardiovascular Disease-2 panels (Millipore, St. Charles, MO) were measured: IL-1α, IL-1β, IL-2, IL-4, IL-5, IL-6, IL-9, IL-10, IL-12, IL-13, IL-17, IL-18, eotaxin, granulocyte colony-stimulating factor (G-CSF), granulocyte macrophage colony-stimulating factor (GM-CSF), GRO-KC, interferon (IFN)-γ, chemokine ligand 10 (IP-10), leptin, monocyte chemoattractant protein (MCP)-1, macrophage inflammatory protein (MIP)-1a, RANTES (regulated upon activation, normal T-cell expressed, and secreted), sE-Selectin, soluble intercellular adhesion molecule (sICAM-1), TNF α, and vascular endothelial growth factor (VEGF). Samples were diluted following manufacturer's recommendations and assayed in duplicate in accordance with manufacturer's instructions. In brief, plates were blocked with a nonspecific protein (i.e., with milk) and then assay buffer, samples, and an antibody-immobilized bead cocktail was added to each well, with plates being kept in the dark for all steps subsequent to the addition of bead cocktail to minimize the effects of photobleaching. Plates were then incubated for 18 to 20 hours at 4°C with agitation, washed, and treated with detection antibody. After a 2-hour room temperature incubation with agitation, strepavidin-conjugated phycoerythrin (a fluorescent detection reagent) was added to the wells and a final 30-minute room temperature incubation with agitation was performed. Wells were thoroughly washed, beads were resuspended in sheath fluid, and the plate was analyzed. Concentrations of each cytokine were calculated based on a standard curve generated on the same plate by logistic fit analysis on Luminex 100 IS software version 2.3.182 (Luminex Corporation, Austin, TX).

COAGULATION ANALYSIS

Whole blood was drawn via the carotid cannula from filtered air–exposed and TiO_2-exposed rats into sodium citrate anticoagulant (0.105 M, 3.2%, 1:10 ratio citrate to whole blood). Platelet-poor plasma was prepared by centrifugation at 4°C and stored at −80°C until use. Plasma prepared in this way was used for all studies described in this section.

Endogenous thrombin potential (ETP) of the rat plasma was measured with a kit (Technothrombin TGA, Diapharma Group, Columbus, OH) containing a phospholipid micelle reagent (TGA RC High Reagent, Diapharma Group) and a fluorogenic thrombin substrate (Z-GGR-AMC). Plasma (40 µL) diluted with buffer was added to black-bottom 96-well microplates after which the TGA reagent and TGA substrate (50 µL) were added. Fluorometric measurements were made at 60-second intervals for up to 1 hour with a kinetic plate reader (Beckman Coulter DTX 880, Fullerton, CA) prewarmed to 37°C and set to appropriate wavelengths (excitation 390 nm, emission 465 nm). A thrombin calibration curve was generated with known concentrations of thrombin according to the kit protocol in order to quantify thrombin generation. The intra-assay and inter-assay variability of the ETP assay for thrombin generation were measured at 9% and 6%, respectively.

A customized kit (LINCOplex Rat CVD Panel, Millipore, St. Charles, MO) was used to quantify specific analytes in

rat plasma including fibrinogen, von Willebrand factor (vWF), troponin I, and troponin T. This technology allows multiplexed detection of proteins from a single sample. This 96-well microplate immunoassay utilizes distinct color microsphere beads coated with protein-specific capture antibody. Sample is added to these beads and the protein is captured, after which a fluorescent detection antibody is added. The Luminex analyzer lasers detect both bead dyes' spectral properties and the flourescence of the tagged detection antibody. Analyte concentrations are calculated with the built-in software. Fibrinogen was also quantified in rat plasma with an enzyme-linked immunosorbent assay (ELISA) (AssayMax Rat Fibrinogen, AssayPro, St. Charles, MO) according to manufacturer's instructions.

STUDY DESIGN

Except where indicated, all experimental techniques were performed 24 hours after the end of PM exposure. Five doses were chosen for both the fine and nano-TiO_2 groups in order to ensure that an effective dose–response curve would be generated and to allow for overlap in calculated mass deposition between groups. The concentration used to achieve these estimated doses ranged between 1.5 and 16 mg/m^3. The exposure duration ranged between 4 and 12 hours. The experiments conducted are divided into three groups on the basis of protocol and endpoints.

EXPERIMENTAL PROTOCOL 1

Age- and exposure-matched rats in all groups were used to harvest tissues in order to measure pulmonary particle deposition and collect lung tissue samples and BAL fluid for the analysis of inflammation and injury and blood for the analyses of systemic inflammation and clotting potential as described in Protocol 3.

Arteriolar endothelium-dependent dilation was evaluated by intravital microscopy in all groups of rats by assessing the capacity for Ca^{2+}-dependent endothelial NO formation in response to intraluminal infusion of A23187 (Sigma Chemical). Glass micropipettes were beveled to a 23° to 25° angle and a 2- to 4-mm inner tip diameter. One mg of A23187 was dissolved in 50 µL of dimethylsulfoxide (DMSO) and then serially diluted in PBS to produce a 10^{-7} M solution that was loaded into the micropipettes. A23187 increases endothelial NO synthase activity, which produces NO and therefore relaxes exposed vessels (Schneider et al. 2003). The micropipette was inserted into the lumen of the selected arteriole approximately 100 µm upstream from the diameter measurement site, and A23187 was then infused directly into the flow stream. A Picospritzer II pressure system (General Valve Corporation, Fairfield, NJ) was used to continuously infuse A23187 for 2-minute periods at net ejection pressures of 5-, 10-, 20-, and 40-pounds per square inch (psi). In preliminary tests, we verified that the amount of agonist ejected from the pipette tip was directly proportional to the ejection pressure. The order in which the different ejection pressures were applied was randomized in each experiment, and a 2-minute recovery period followed each ejection. Given the resistance of the pipette tips, the fluid volumes ejected at these pressures are relatively small and increase total arteriolar volume flow by no more than 10% (T.R.N. and M.A.B., unpublished observations). This technique does not produce artifacts that influence vascular tone and the A23187 vehicle is not vasoactive (Nurkiewicz et al. 2004). At the end of each experiment, adenosine (ADO) was added via a syringe pump to the superfusate at a final concentration of 10^{-4} M to fully dilate the microvascular network and determine the passive diameter of each arteriole studied. We previously showed that the magnitude of arteriolar dilation induced by 10^{-4} M ADO is not further augmented by subsequent exposure to SNP and nifedipine in a Ca^{2+}-free superfusate, indicating that 10^{-4} M ADO completely abolishes arteriolar tone in the exteriorized spinotrapezius muscle without altering systemic arterial pressure (Nurkiewicz and Boegehold 2000).

EXPERIMENTAL PROTOCOL 2

The EC_{50} from Experimental Protocol 1 dose responses was determined to be 67 µg for fine TiO_2 and 10 µg for nano-TiO_2, which were produced by exposure conditions reported in Table 1. These doses were used throughout the remainder of the experiments in this study. To evaluate arteriolar responsiveness to NO, we applied the NO donor SNP iontophoretically to individual arterioles in rats exposed to either 67 µg fine or 10 µg nano-TiO_2 (and filtered air–exposed rats). Glass micropipettes were prepared as above and filled with a 0.05-M solution of SNP in distilled water. The pipette tip was placed in light contact with the arteriolar wall, and a current programmer (model 260, World Precision Instruments, New Haven, CT) was used to deliver continuous 2-minute ejection currents of 5, 10, and 20 nA. A recovery period of at least 2 minutes followed each application. The order of the 5- and 10-nA ejection currents was randomized, but the 20-nA ejection current was always delivered last because of a considerably slower recovery from this stimulus. At the end of each experiment, ADO was added to the superfusate at a final concentration of 10^{-4} M to determine the passive diameter of each arteriole studied.

Table 1. TiO_2 Aerosol Exposure Profiles and Group Depositions[a]

Particle Type	Aerosol Concentration (mg/m^3)	Exposure Time (min)	Calculated Deposition (μg)	Actual Deposition (μg)[b]
Control	0	240	0	0
Nano	10	720[c]	150	37.60 ± 1.90
Nano	12	240	60	19.17 ± 0.36
Nano	6	240	30	9.48 ± 0.32
Nano	3	240	15	6.38 ± 0.13
Nano	1.5	240	7	3.70 ± 0.08
Fine	15	480	150	89.80 ± 6.92
Fine	16	300	100	66.50 ± 3.82
Fine	12	240	60	36.33 ± 0.69
Fine	6	240	30	19.67 ± 1.07
Fine	3	240	15	8.26 ± 0.29

[a] Analysis of the filter samples collected from the exposure chamber does not indicate any detectable quantity of copper or tin (two major components of bronze beads used in the fluidized-bed aerosol generator). This indicates that the exposure environment does not have detectable levels of contaminants from the bronze beads used to disperse the bulk TiO_2 samples.

[b] Values are mean ± SE.

[c] Exposure was 4 hours/day for 3 days.

NO measurements were made (as described in Methods) in Experimental Protocol 2. Endogenous microvascular NO formation was directly measured in suspensions of excised microvessels from each of the exposure groups (including the filtered air–exposed group). NO production was stimulated by introducing a 20-μL bolus dose of A23187 (10^{-3} M) into the biosensing chamber (10^{-5} M final concentration). In these exposure dose–response experiments, NO synthase (NOS) activity was then competitively inhibited by coincubation with N^G-monomethyl-L-arginine (L-NMMA, 10^{-4} M final superfusate concentration), and the microvessels were stimulated again with A23187. In other experiments with a different group of animals, superoxide and H_2O_2 were scavenged with the superoxide dismutase mimetic TEMPOL (with a 10^{-4} M final bath concentration) and catalase (with a 50-U/mL final bath concentration), respectively. MPO was inhibited by tissue superfusion with ABAH (10 μM final superfusate concentration) for 20 minutes prior to repeating any experimental procedures. NADPH oxidase was inhibited by tissue superfusion with apocynin (10^{-4} M final superfusate concentration) for 20 minutes prior to repeating any experimental procedures. Time course studies indicated that the microvessels produced reliable NO signals for multiple stimulations over 2 to 3 hours. Despite this, only two stimulations were performed per experiment, and each experiment lasted less than 1 hour.

In other experiments, the lungs and spinotrapezius muscle were harvested for nitrotyrosine (NT) measurements, a marker for peroxynitrite. This was accomplished with dual-label immunofluorescence for NT and vWF, a positive marker for the endothelium. The lung was inflated with 2:1 optical coherence tomography (OCT) in a 20% sucrose and PBS solution and then cut along the mainstem bronchus, embedded in OCT, and frozen in an isopentane slurry on dry ice. The spinotrapezius muscle was embedded in OCT and then frozen in an isopentane slurry on dry ice. Frozen sections of spinotrapezius muscle and lung from rats exposed to 10 μg nano-TiO_2 or filtered air were stained for NT, generally the product of peroxynitrite reactions with cellular proteins. To further demonstrate the localization of NT relative to the vasculature, we stained the vascular endothelium for vWF as follows. Sections were cut with a cryostat, fixed in acetone, blocked with 10% donkey serum, and incubated overnight in the refrigerator with a primary antibody mixture containing a 1:50 dilution of rabbit anti-NT (Upstate, Temecula, CA) and a 1:200 dilution of sheep anti-vWF (Abcam, Cambridge, MA). The secondary antibodies were Alexa 594-labeled donkey anti-rabbit and Alexa 488-labeled donkey anti-sheep (Invitrogen, Carlsbad, CA). Slides were coverslipped with Prolong mounting media with 4′,6-diamidino-2-phenylindole (DAPI; Invitrogen, Carlsbad, CA). With this procedure, NT has red fluorescence, the vascular endothelium has green fluorescence, and nuclei fluoresce blue. The adjacent serial section was stained with Giemsa dye for identification of inflammatory cells. The filtered air–exposed sections used rabbit and sheep immunoglobulin G (IgG) in place of the primary antibodies and were otherwise treated identically to the sections for dual-label immunofluorescence.

EXPERIMENTAL PROTOCOL 3

In the last series of experiments, previously harvested blood was analyzed for circulating inflammatory markers and clotting potential.

In other experiments, the role of circulating neutrophils after PM exposure was assessed by depleting these cells prior to inhalation exposure. In this series of experiments, F-344 rats were used because an additional technique was attempted that required an inbred rat strain. However, that attempt was unsuccessful, and therefore only the role of circulating neutrophils was evaluated in this protocol. Cyclophosphamide (200 µg/g, i.p.) was administered three days prior to exposure. This dose has been previously shown to completely deplete circulating leukocytes in guinea pigs (Castranova et al. 1988). In order to properly characterize the effects of neutrophil depletion on microvascular function after PM exposure, four experimental groups were necessary: (1) i.p. saline and filtered-air exposure, (2) cyclophosphamide and filtered-air exposure, (3) i.p. saline and 10 µg nano-TiO_2, and (4) cyclophosphamide and 10 µg nano-TiO_2. Intravital microscopy experiments were performed on these groups 24 hours after exposure. Blood samples were taken via the carotid artery cannula.

In the last experiments of this protocol, the role of fast Na^+ channels in the arteriolar dysfunction that follows PM exposure was assessed in intravital microscopy experiments. Endothelium-dependent arteriolar dilation was assessed via intraluminal infusion of A23187 first under the normal superfusate (as previously described under experimental protocol 1). The fast Na^+ channel blocker TTX was then added to the superfusate (with a final bath concentration of 10^{-6} M) and allowed to incubate for 30 minutes. This concentration has been shown to completely block arteriolar vasoconstriction in the rat spinotrapezius muscle during direct perivascular nerve stimulation over a range of physiologic frequencies (Linderman and Boegehold 1998). Arteriolar A23187 infusions were then repeated during fast Na^+ channel blockade.

STATISTICAL METHODS AND DATA ANALYSIS

Variables in experiments with intravital microscopy were measured at 10-second intervals during all control and infusion periods. Whenever possible, raw data were used rather than derived data. However, there were instances in which the use of derived data was necessary. An example was when control diameters of different groups differed significantly for reasons associated with exposure or treatment. In this scenario, the two groups of microvessels were positioned at different locations on the length-tension curve, and, therefore, it was not representative to compare the raw data between the two groups. Resting vascular tone was calculated for each vessel as follows: tone = $[(D_{pass} - D_c)/D_{pass}] \times 100$, where passive diameter (D_{pass}) was the diameter under ADO, and control diameter (D_c) was the diameter measured during the control period. A tone of 100% represents complete vessel closure, whereas 0% represents the passive state. For comparisons of arteriolar responses to A23187 infusion among different treatments and experimental groups, responses were normalized as follows: the percentage change from control = $[(D_{ss}/D_c) - 1] \times 100$, where steady-state diameter (D_{ss}) is the steady-state diameter during A23187 exposure. Arteriolar dysfunction was normalized to the filtered air–exposed group among different exposure groups by evaluating arteriolar responsiveness to intraluminal infusion of A23187 at 40 psi as follows: arteriolar dysfunction = $(D_{40psi}/80\ \mu M) \times 100$, where D_{40psi} is the arteriolar diameter (in mm) during intraluminal infusion at 40 psi, and 80 µm is the arteriolar diameter in the filtered air–exposed group during the same stimulus.

All data are reported as means ± standard error (SE), where *n* represents the number of arterioles evaluated and *N* represents the number of rats studied. Statistical analysis was performed by commercially available software (Sigmastat, Jandel Scientific). One-way repeated-measures analysis of variance (ANOVA) was used to determine the effect of a treatment within a group or differences among groups. Two-way repeated-measures ANOVA was used to determine the effects of group, treatment, and group-treatment interactions on measured variables. For all ANOVA procedures, the Student-Newman-Keuls method for post hoc analysis was used to isolate pairwise differences among specific groups. Significance was assessed at the 95% confidence level ($P < 0.05$) for all tests.

RESULTS

Table 1 lists the TiO_2 exposure used for the current inhalation exposures, as well as the calculated and actual deposition values. The parameters used to calculate pulmonary deposition were aerosol concentration, exposure duration, minute ventilation, and estimated deposition fraction as described under Inhalation Exposure in the Methods section. The actual pulmonary deposition is used to identify experimental groups in subsequent tables and figures. Neither copper nor tin was detected in the pulmonary deposition measurement samples. This indicates that the components of the fluidized bed necessary to disperse bulk TiO_2 do not untowardly contaminate its generated aerosols.

The primary count mode for the nano-TiO_2 aerosols was 100 nm, whereas it was 710 nm for the fine-TiO_2 aerosols (Figure 4). When considering the whole-size distribution,

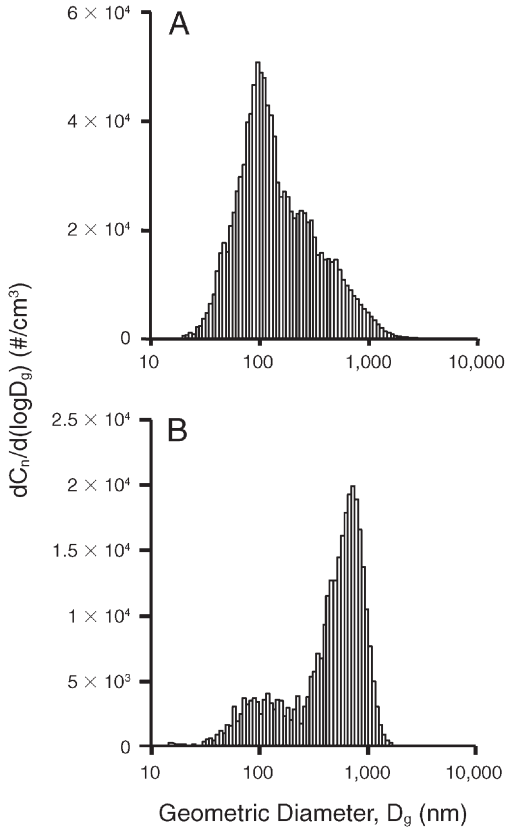

Figure 4. Particle-size distributions (geometric diameter [D_g]) of nano-TiO_2 (A) and fine-TiO_2 (B) aerosols generated by the inhalation exposure system. The nano-TiO_2 aerosol has a primary count mode at 100 nm and a secondary mode at 400 nm. The fine-TiO_2 aerosol has a primary mode at 710 nm and a secondary mode at 120 nm. These number-based size distributions were determined by combining the data from SMPS and APS. (Reprinted from Nurkiewicz et al. 2008).

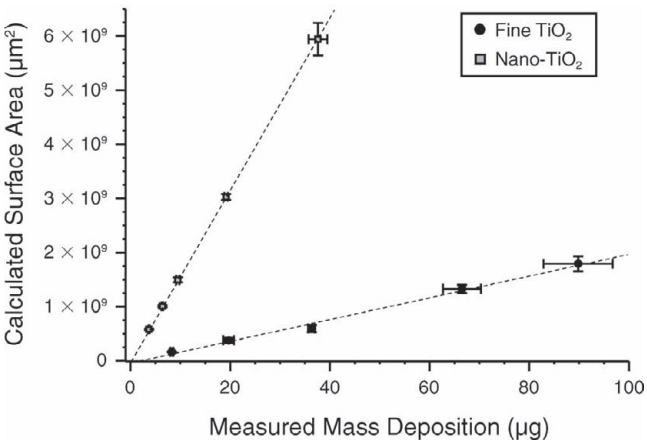

Figure 5. Particle mass deposition vs. surface area for all exposures used in the current study. The equations of first-order regressions lines are fine TiO_2, $y = 2.02e{+}7 \times (x) - 3.63e{+}7$, $r^2 = 0.99$; and nano-TiO_2, $y = 1.58e{+}8 \times (x) + 9.66e{-}7$, $r^2 = 1.0$. The line slope for nano-TiO_2 is significantly greater than that for fine TiO_2 ($P < 0.05$).

the former had a count geometric mean diameter of 138 nm and a geometric standard deviation of 2.2, and the latter had a count geometric mean diameter of 402 nm and a geometric standard deviation of 2.4. The raw data variables used to calculate the surface area of each of the doses are presented in Table 2. In order to characterize the deposited surface area available for interaction with biologic membranes in the lung, the mass deposition values from Table 1 were plotted against calculated surface area (Figure 5). As expected, nano-TiO_2 aerosols (as compared with fine-TiO_2 aerosols) produced a tremendously greater surface area at much lower mass depositions ($P < 0.05$).

Table 2. TiO_2 Aerosol Raw Data Variables

	Fine TiO_2	Nano-TiO_2
Measured mass concentration (mg/m^3)	0.01	0.01
Particle density (g/cm^3)	4.23	3.8
Particle diameter (μm)	0.71	0.1
Particle volume (cm^3)	1.87402×10^{-13}	5.23599×10^{-16}
Mass per particle (mg)	7.92709×10^{-10}	1.98968×10^{-12}
Surface area per particle (μm^2)	1.583676857	0.031415927
Particle per cm^3 of air (#/cm^3)	1.26×10^1	5.03×10^3
Surface area per cm^3 of air (μm^2/cm^3)	19.98	157.89
Specific surface area (μm^2/g), calculated	2.00×10^6	1.58×10^7
Measured specific surface area (m^2/g), reported by Sager et al. (2008)	2.34	48.08
Measured specific surface area (mean ± SE m^2/g)	2.49 ± 0.1	53.6 ± 0.3

PROTOCOL 1

The exposure concentrations selected for this study were those that did not alter BAL markers of pulmonary inflammation or lung damage. In the 150 μg nano-TiO_2 exposure group, BAL data were as follows: $N = 6$, AMs = 6.38 ± 0.33 (10^6 cells per rat), PMNLs = 0.1 ± 0.01 (10^6 cells per rat), albumin = 0.12 ± 0.01 mg/mL, LDH = 60 ± 12 U/l, total AM chemiluminescence (CM) = 8.42 ± 1.75, and NO-dependent CM = 0.45 ± 0.24. Where total AM CM = counts per minute × 10^5/0.25 × 10^6 AM/15 minutes. Because these BAL markers were usually measured in our highest exposure group and they were not significantly different from BAL data in either filtered air controls or animals exposed to lower concentrations of fine TiO_2 in our previous studies (Nurkiewicz et al. 2004, 2006), further BAL studies were not performed. Similarly, histopathologic examination did not identify significant inflammation in lung sections. The principal histopathologic alterations in the lung consisted of PM accumulation within AMs, the presence of anuclear macrophages, and an intimate association (contact) between PM-laden AMs and the alveolar wall. Anuclear AMs were not observed in any of the 21 filtered air–exposed rats. Anuclear AMs were identified in 1 of 20 rats exposed to nano-TiO_2 (a rat in the 38-μg exposure group) and in 16 of the 29 rats exposed to fine TiO_2 (Figure 6), including 1 of 6 rats in the 8-μg target exposure, 2 of 4 rats in the 20-μg target exposure, 5 of 6 rats in the 36-μg target exposure, 5 of 7 rats in the 67-μg target exposure, and 3 of 6 rats in the 90-μg target exposure. Because the macrophage cell membrane remains intact, anuclear macrophages are presumed to represent an apoptotic change.

Macrophages containing particles were frequently intimately associated (e.g., they had contact) with the alveolar wall (Figures 6 and 7), a location suggestive of, but not

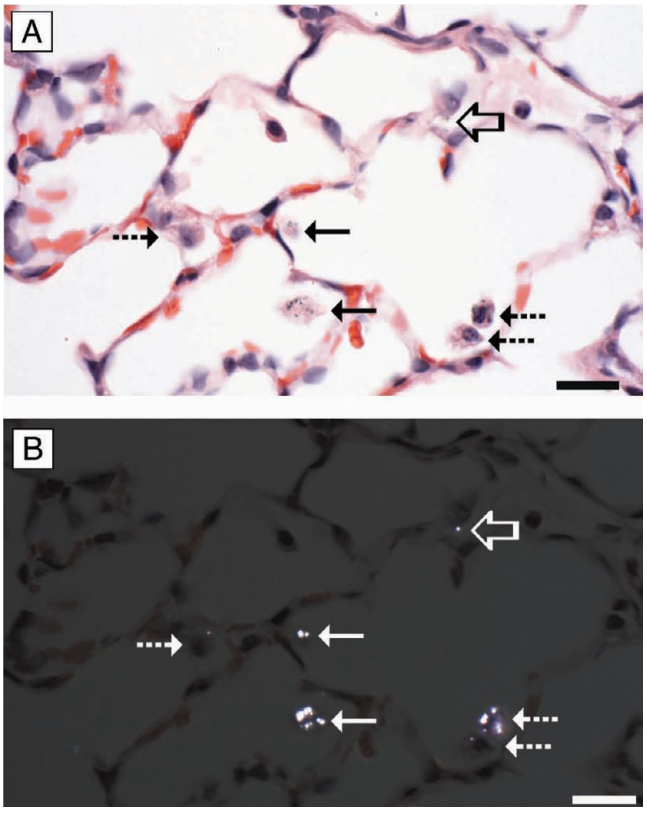

Figure 6. Histopathologic alterations in the lungs of rats inhaling fine TiO_2. These changes were subtle and principally consisted of PM accumulation. Particles were difficult to see using transmitted light **(A)** but were birefringent when visualized using cross-polarized light, enhancing their detection **(B)**. The particle accumulation included apparently free TiO_2 particles (open arrow), TiO_2 particles within morphologically normal alveolar macrophages (dashed arrows), and TiO_2 particles within macrophages without nuclei (anuclear macrophages, solid arrows). Both morphologically normal and anuclear macrophages were frequently in contact with the alveolar wall. Tissue sections are stained with H&E. Scale bar = 20 μm. (Reprinted from Nurkiewicz et al. 2008).

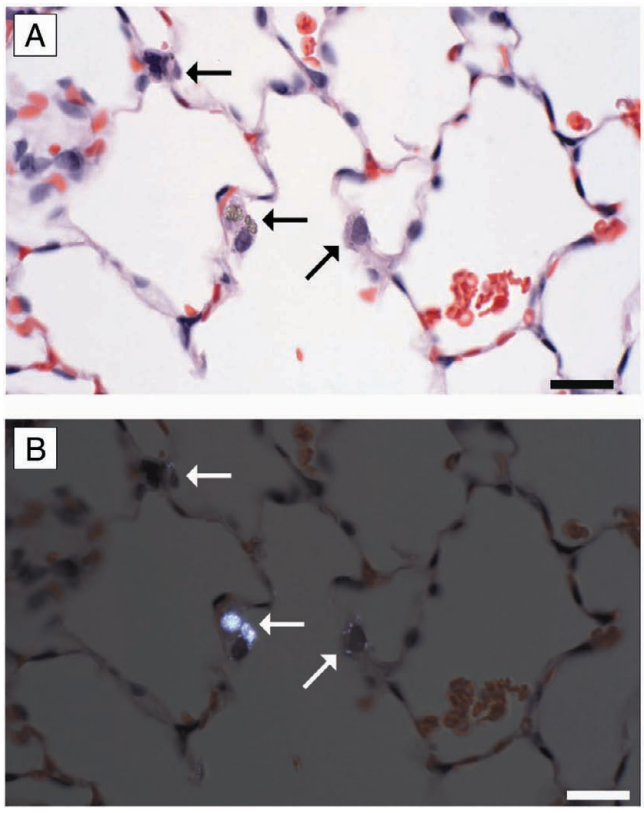

Figure 7. Histopathologic alterations in the lungs of rats inhaling nano-TiO_2. Nano-PM accumulation in alveolar macrophages (arrows) was subtle and was difficult to see with transmitted light **(A)**. Nano-PM accumulation within alveolar macrophages was more easily visualized as birefringent intracytoplasmic material using cross-polarized light **(B)**. Macrophages containing nano-TiO_2 particles were frequently in contact with the alveolar wall. Tissue sections are stained with H&E. Scale bar = 20 μm. (Reprinted from Nurkiewicz et al. 2008).

diagnostic of, macrophage activation. This change was difficult to quantify because it was dependent upon identifying the macrophages that were intimately associated with the alveolar wall. These macrophages were best demonstrated with cross-polarization to demonstrate the TiO_2 PM (Figures 6 and 7). Fine TiO_2 PM was distinctly birefringent in cross-polarized light and could be identified in both intracellular and extracellular locations, whereas nano-TiO_2 PM was faintly birefringent in polarized light and were only identified within macrophages (Figure 7). Because the size of nano-TiO_2 PM should be below the size visible in the light microscope, the observed nano-TiO_2 PM is presumed to represent agglomerates. Consistent with the nano-PM only being visible when agglomerated, nano-PM was not observed in filtered air–exposed rats or rats receiving the lowest exposure but was seen in 1 of 4 rats at the 6-μg target dose, 1 of 4 rats at the 10-μg target dose, 2 of 4 rats at the 19-μg target dose, and all rats receiving the 38-μg target dose. Conversely, fine-TiO_2 particles were seen in the lungs of all rats at every dose.

At the time of the intravital experiments, rats in the 38-μg nano-TiO_2 inhalation and 100-μg fine-TiO_2 i.t. groups were slightly older than rats in all other experimental groups (Table 3). Despite this subtle age difference, mean arterial pressure did not differ among the experimental groups. Resting diameter, passive diameter, and resting tone of arterioles were not affected by particle dose and size or by exposure route (Table 4).

Consistent with our previous findings in rats exposed to fine TiO_2 via i.t. instillation (Nurkiewicz et al. 2004, 2006), inhalation of fine TiO_2 impaired arteriolar dilation in response to A23187 infusion in a dose-dependent manner (Figure 8). Although significantly compromised, arteriolar dilation was still present after exposure to as much as 90 μg of fine TiO_2. The no-effect dose was determined to be 8 μg. At this dose, arteriolar dilation at each ejection pressure was identical to that observed in the filtered air–exposed group.

Inhalation of nano-TiO_2 impaired arteriolar dilation in response to A23187 infusion in a dose-dependent manner (Figure 9). This was most evident at the 38-μg dose, in which not only was dilation completely abolished, but significant arteriolar constriction resulted during A23187 infusion. The no-effect dose, the dose at which arteriolar

Table 3. Profiles of Sprague-Dawley Rats Used for Intravital Microscopy Studies

	Exposure Parameters						
TiO_2 Group / Dose	Route	Aerosol Concentration (mg/m^3)	Duration (min)	*n*	Age (days)[a]	Weight (grams)[a]	Arterial Pressure (mm Hg)[a]
Control	Inhalation	0	240	4	43 ± 1	206 ± 11	98 ± 9
Nano							
38 μg	Inhalation	10	720[b]	3	46 ± 3[c]	228 ± 29	98 ± 6
19 μg	Inhalation	12	240	5	40 ± 1	188 ± 9	95 ± 4
10 μg	Inhalation	6	240	4	42 ± 1	224 ± 7	103 ± 2
10 μg	Inhalation	3	480	22	43 ± 1	219 ± 5	99 ± 4
10 μg	Inhalation	12	120	5	42 ± 1	217 ± 6	107 ± 7
6 μg	Inhalation	3	240	3	42 ± 1	216 ± 9	93 ± 7
4 μg	Inhalation	1.5	240	3	42 ± 1	207 ± 8	96 ± 7
Fine							
90 μg	Inhalation	15	480	4	42 ± 1	233 ± 4	97 ± 2
67 μg	Inhalation	16	300	18	42 ± 1	214 ± 4	97 ± 3
36 μg	Inhalation	12	240	4	41 ± 1	213 ± 6	100 ± 4
20 μg	Inhalation	6	240	3	42 ± 1	209 ± 8	101 ± 3
8 μg	Inhalation	3	240	5	42 ± 1	233 ± 9	106 ± 6
100 μg	i.t.	n/a	n/a	5	50 ± 1[c]	275 ± 9[c]	108 ± 6

[a] Values are mean ± SE.

[b] Exposure was 4 hours/day for 3 days.

[c] $P < 0.05$ vs. all other experimental groups.

Table 4. Resting Variables for Arterioles from the Spinotrapezius Muscle of Sprague-Dawley Rats Studied in Intravital Microscopy Studies

TiO_2 Group / Dose	Exposure Parameters: Aerosol Concentration (mg/m^3)	Exposure Parameters: Duration (min)	*n*	Resting Diameter (μm)[a]	Passive Diameter (μm)[a]	Resting Tone (% of maximum)[a]
Control	0	240	8	40 ± 2	99 ± 4	59 ± 3
Nano						
38 μg	10	720[b]	9	42 ± 2	106 ± 5	60 ± 3
19 μg	12	240	11	42 ± 1	100 ± 5	57 ± 3
10 μg	6	240	41	42 ± 1	93 ± 2	54 ± 2
10 μg	3	480	10	40 ± 2	95 ± 4	57 ± 3
10 μg	12	120	10	45 ± 2	99 ± 7	54 ± 3
6 μg	3	240	7	39 ± 1	105 ± 5	62 ± 2
4 μg	1.5	240	9	38 ± 1	97 ± 4	60 ± 2
Fine						
90 μg	15	480	8	45 ± 1	106 ± 5	57 ± 3
67 μg	16	300	40	45 ± 1	99 ± 2	55 ± 1
36 μg	12	240	8	39 ± 2	100 ± 7	60 ± 3
20 μg	6	240	7	39 ± 1	92 ± 2	57 ± 2
8 μg	3	240	12	41 ± 1	100 ± 5	58 ± 2
100 μg, i.t.	n/a, i.t.	n/a, i.t.	9	45 ± 1	111 ± 4	59 ± 2

[a] Values are mean ± SE.

[b] Exposure was 4 hours/day for 3 days.

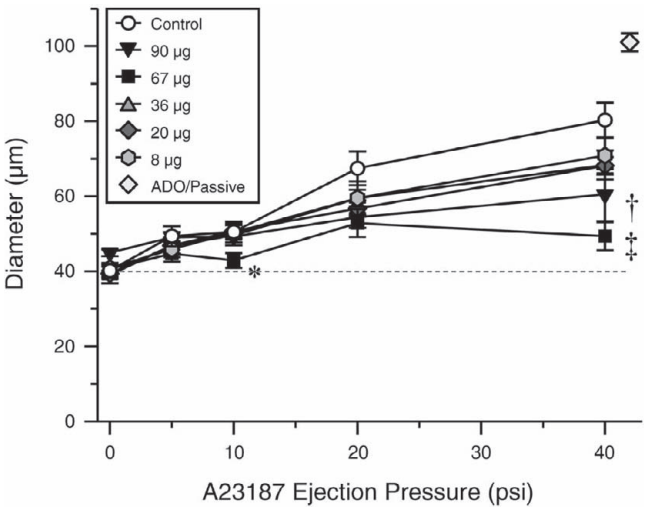

Figure 8. Impairment in systemic arteriolar dilation 24 hours after fine-TiO_2 inhalation exposure. Exposure metric is the measured particle mass (μg) deposited in the lungs. Filtered air, $n = 8$; 90 μg, $n = 8$; 67 μg, $n = 8$; 36 μg, $n = 8$; 20 μg, $n = 7$; 8 μg, $n = 12$. Values are mean ± SE. *, $P < 0.05$ vs. all groups. †, $P < 0.05$ vs. filtered air–exposed group. ‡, $P < 0.05$ vs. 8- to 36-μg groups. (Reprinted from Nurkiewicz et al. 2008).

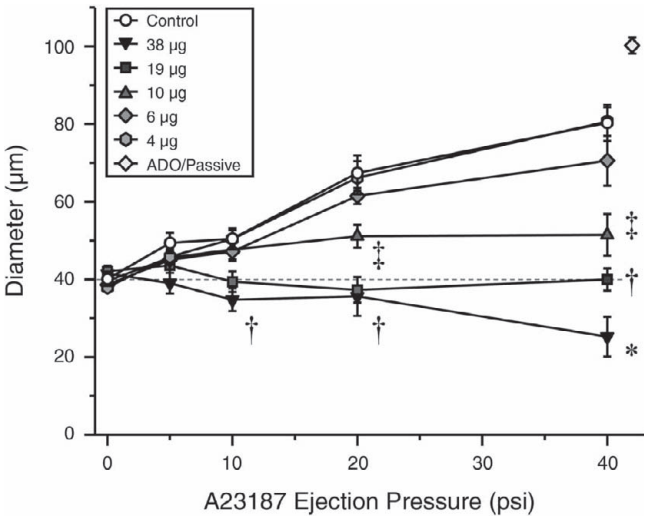

Figure 9. Impairment of systemic arteriolar dilation 24 hours after exposure to nano-TiO_2 inhalation in a dose-dependent manner. Exposure metric is the measured particle mass (μg) deposited in the lungs. Filtered air, $n = 8$; 38 μg, $n = 9$; 19 μg, $n = 11$; 10 μg, $n = 8$; 6 μg, $n = 7$; 4 μg, $n = 9$. Values are mean ± SE. *, $P < 0.05$ vs. 19 μg-group. †, $P < 0.05$ vs. 10 μg-group. ‡, $P < 0.05$ vs. 6 μg-group. (Reprinted from Nurkiewicz et al. 2008).

responsiveness was not different from responses observed in filtered air–exposed group, was determined to be 4 μg.

Because aerosol concentration and exposure time were manipulated to obtain an array of pulmonary depositions, the possibility existed that such manipulations could themselves contribute to the resultant microvascular dysfunction. To address this possibility, we performed additional exposures in which exposure duration (2–8 hours) and aerosol concentrations (3–12 mg/m^3) were manipulated to produce identical calculated pulmonary depositions. Three groups of rats displayed identical levels of microvascular dysfunction after exposure to 30 μg nano-TiO_2 via different conditions (Figure 10). This indicates that manipulation of exposure time or aerosol concentration within the parameters used in the current study neither attenuates nor augments the resultant microvascular dysfunction (i.e., the response is dependent on the duration × concentration product of exposure).

When arteriolar responses between rats exposed to similar doses of fine TiO_2 by different routes (90 μg via inhalation vs. 100 μg via i.t. instillation) were compared, no significant differences are apparent in the resultant microvascular dysfunction (Figure 11). This suggests that the method of PM introduction to the lungs does not artificially induce systemic microvascular dysfunction.

Because actual pulmonary mass deposition was determined and there was some overlap in the nano- and fine-PM mass, three pairwise comparisons of arteriolar responsiveness can be made between rats exposed to fine and nano-TiO_2 (Figure 12). At a deposition of 8 to 10 μg, fine TiO_2 produced no significant microvascular effects, whereas nano-TiO_2 significantly impaired arteriolar dilation at 20 and 40 psi of ejection pressure by 53% and 75%, respectively (Figure 12A). At a deposition of 19 to 20 μg, fine TiO_2 showed a trend towards an impaired dilation, whereas nano-TiO_2 produced arteriolar constrictions that were significantly different from the responses in both the filtered air–exposed and fine-TiO_2 groups (Figure 12B). At a deposition of 36 to 38 μg, effects similar to the 19- to 20-μg lung burden occurred, but the intensity of arteriolar constriction after exposure to nano-TiO_2 was more pronounced (Figure 12C). This suggests that at similar pulmonary burdens, nano-PM produces greater systemic microvascular dysfunction than fine PM.

Because mass deposition may not be the ideal dose metric, the arteriolar responses to 40 psi in each exposure group were normalized to the responses of control arterioles and expressed as a percentage (arteriolar dysfunction, Figure 13). These data were then plotted against either mass deposition (Figure 13, left), or calculated surface area (Figure 13, right). No relationship was evident between particle sizes when arteriolar dysfunction was plotted as a function of mass deposition. However, when plotted as a

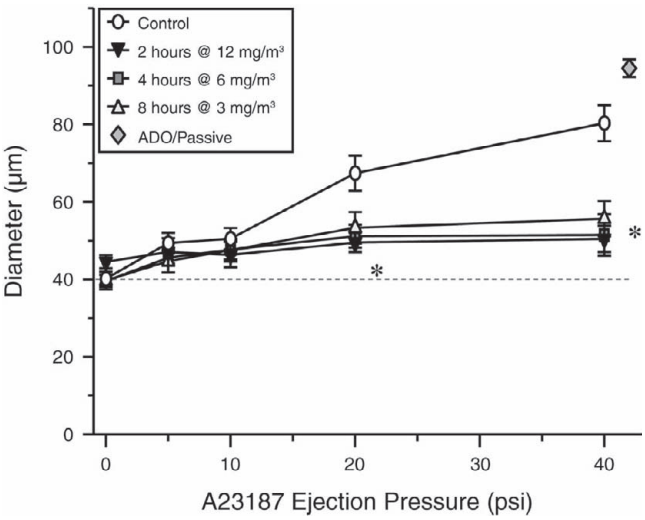

Figure 10. Effect of manipulation of nano-TiO_2 inhalation exposure time or aerosol concentration on impairment of systemic arteriolar dilation. A dose of 10 μg was selected for each group, but exposure time and concentration were manipulated as follows: 2 hr at 12 μg/m^3, n = 10; 4 hr at 6 μg/m^3, n = 8; 8 hr at 3 μg/m^3, n = 10. Values are mean ± SE. *, $P < 0.05$ vs. filtered air–exposed group. (Reprinted from Nurkiewicz et al. 2008).

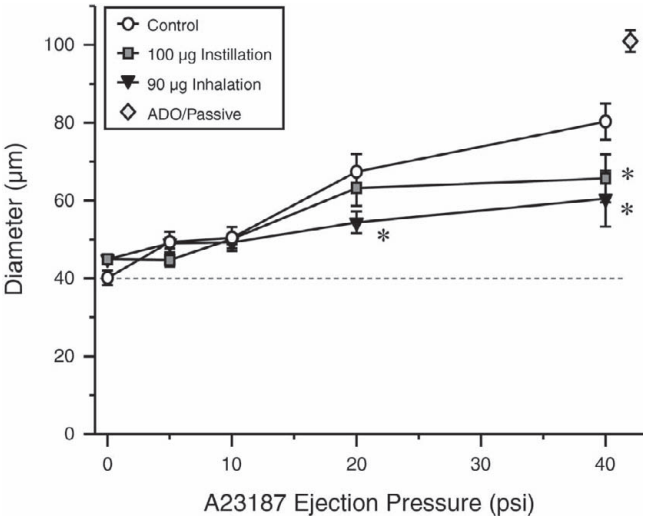

Figure 11. Inhalation and i.t. instillation-exposure to fine TiO_2 similarly impair systemic endothelium-dependent arteriolar dilation 24 hours after exposure. For inhalation exposure, metric is the measured particle mass (μg) deposited in the lungs. For instillation exposure, metric is the measured particle mass placed in suspension and then instilled. *, $P < 0.05$ vs. filtered air–exposed group.

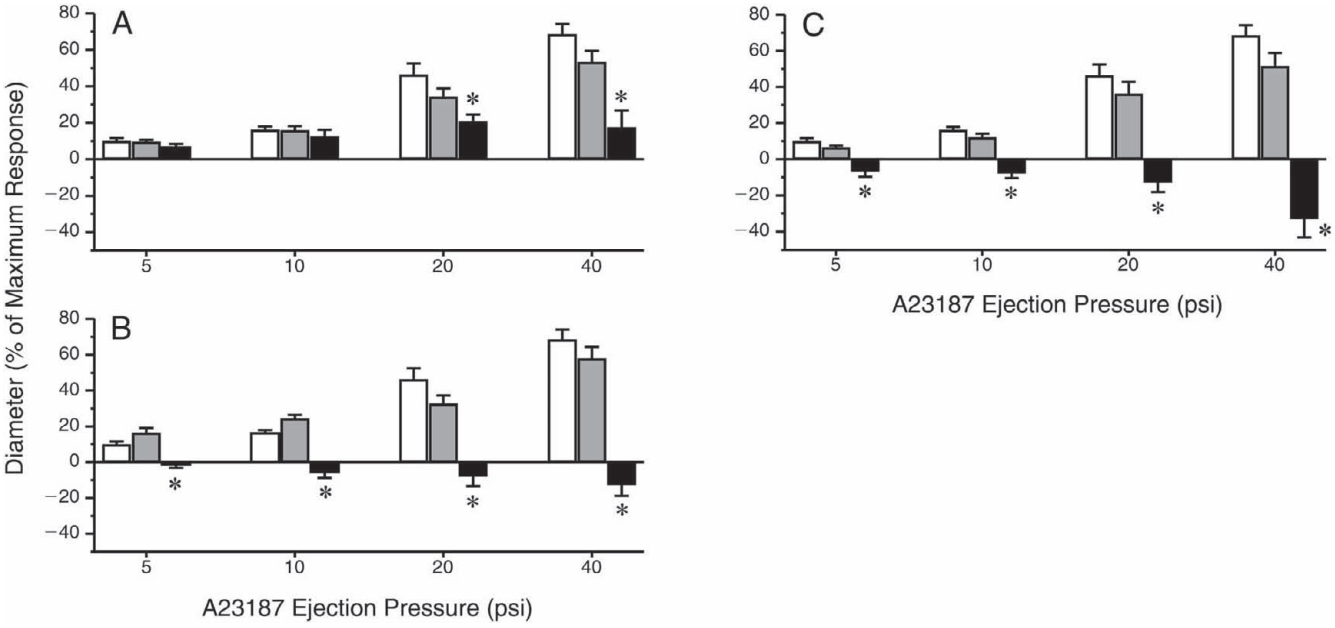

Figure 12. Systemic arteriolar dilation dose–response relationships at various inhalation exposure burdens of fine vs. nano-TiO_2. Exposure metric is the measured particle mass (μg) deposited in the lungs. Open bars in all panels indicate filtered air–exposed group. **(A)** Grey bars = 8 μg fine TiO_2; black bars = 10 μg nano-TiO_2. **(B)** Grey bars = 20 μg fine TiO_2; black bars = 19 μg nano-TiO_2. **(C)** Grey bars = 36 μg fine TiO_2; black bars = 38 μg nano-TiO_2. *, $P < 0.05$ vs. filtered air and fine TiO_2 at the same ejection pressure. Values are mean ± SE. (Reprinted from Nurkiewicz et al. 2008).

function of surface area, a clear relationship was evident that is consistent between both particle sizes. This suggests that in terms of predicting resultant arteriolar dysfunction after PM exposure, the more appropriate dose metric may be surface area.

Exposure doses of 67 μg fine TiO_2 and 10 μg nano-TiO_2 were selected for the remaining sets of experiments as they most closely represented the dose (pulmonary mass deposition for each particle size) at which endothelium-dependent arteriolar dilation was impaired by at least

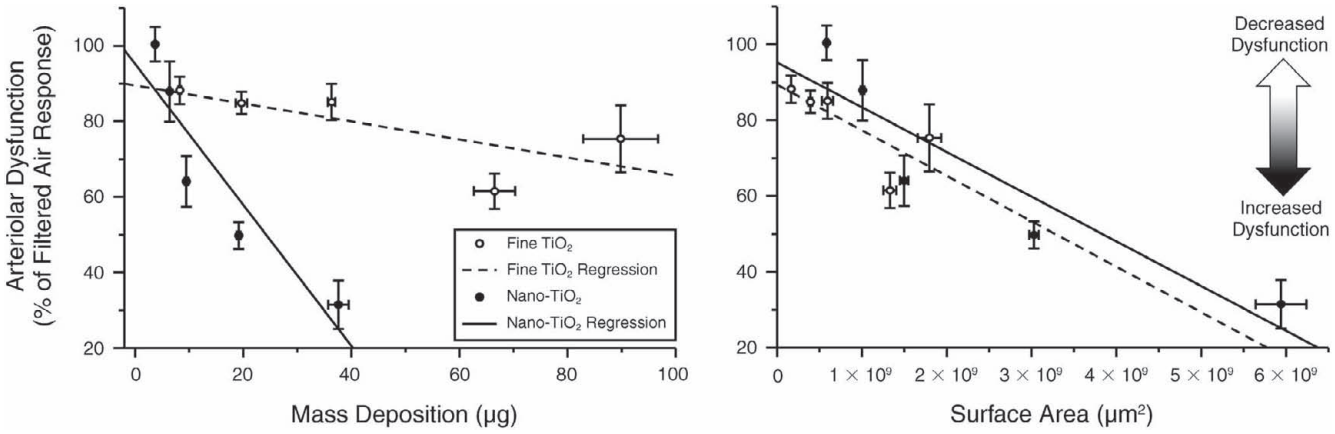

Figure 13. Comparison of different dose metrics as predictors of systemic arteriolar dysfunction. (Left) Equations of first-order regressions lines: fine TiO_2, $y = -0.24 \times (x) + 89.51$, $r^2 = 0.54$; and nano-TiO_2, $y = -1.86 \times (x) + 95.17$, $r^2 = 0.85$. The line slope for nano-TiO_2 is significantly greater than that for fine TiO_2 ($P < 0.05$). **(Right)** Equations of first-order regressions lines: fine TiO_2, $y = -1.20 \times (x) + 89.27$, $r^2 = 0.56$; and nano-TiO_2, $y = -1.18 \times (x) + 95.17$, $r^2 = 0.85$. The line slopes are not significantly different.

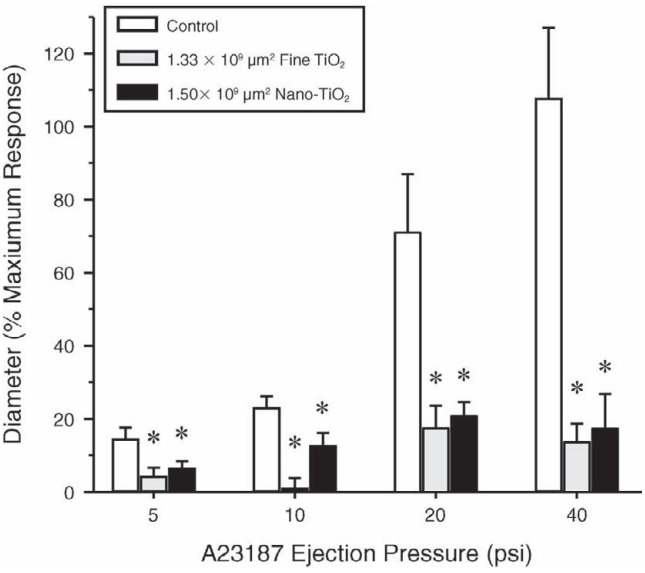

Figure 14. Comparison of arteriolar dysfunction between similar particle burden surface areas. Filtered air, $n = 8$; 67 μg fine TiO_2, $n = 8$; and 10 μg nano-TiO_2, $n = 10$. *, $P < 0.05$ vs. filtered air–exposed group at the same ejection pressure. (Reprinted from Nurkiewicz et al. 2009).

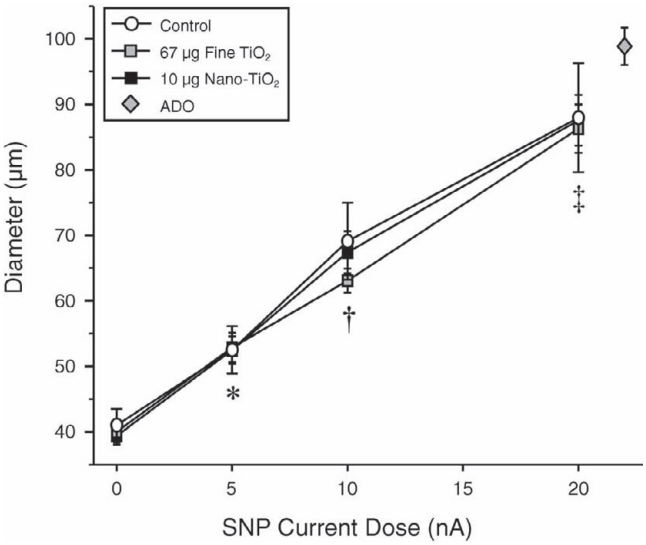

Figure 15. Arteriolar VSM NO sensitivity is not altered after particle inhalation. SNP was locally applied to individual arterioles via microiontophoresis and produced equivalent dose-dependent dilations in all groups that were near maximal (vs. ADO). Exposure metric is the measured particle mass (μg) deposited in the lungs. Filtered air, $n = 7$; 67 μg fine TiO_2, $n = 9$, and 10 μg nano-TiO_2, $n = 10$. *, $P < 0.05$ vs. 0 nA for all groups. †, $P < 0.05$ vs. 5 nA for all groups. ‡, $P < 0.05$ vs. 10 nA for all groups. Values are mean ± SE. (Reprinted from Nurkiewicz et al. 2009).

50% (approximately EC_{50}, Figure 14) using surface area as the dose metric. This was most evident at 40 psi. At the PM doses used in these experiments, equivalent levels of arteriolar dysfunction were found in the two exposure groups. This was most evident at 40 psi where arterioles in the filtered air–exposed group dilated up to 108 ± 20% of their original diameter, but arterioles in the fine and nano-TiO_2 exposure groups dilated to only 23 ± 8% and 24 ± 13% of their original diameters, respectively. The 40-psi ejection stimulus was also focused upon throughout the current study because the impact of PM exposure on microvascular function is most evident at this ejection pressure.

After PM exposure, arteriolar dilation in response to abluminal microiontophoretic application of SNP was not different from controls (Figure 15). Arteriolar dilations under these conditions were also not different among exposure groups, and all groups were near their maximal diameters at a dose of 20 nA. These findings are consistent with our previous findings in this microvascular bed after exposure to environmental PM (Nurkiewicz et al. 2004). Collectively, this verifies in our experimental models that VSM sensitivity to NO is not altered after exposure to a variety of PM or exposure routes.

Representative bright-field and fluorescent photomicrographs of the spinotrapezius-muscle microcirculation are presented in Figure 16, panels A through D. HE treatment of the spinotrapezius microcirculation revealed a significant increase in arteriolar ethidium bromide fluorescence (normalized to HE fluorescence) in both PM exposure groups (Figure 16, bottom). This ratio, as compared to the filtered air–exposed group (1.03 ± 0.01), was significantly increased after exposure to fine (1.09 ± 0.01) and nano-TiO_2 (1.09 ± 0.01). This increase in fluorescence verifies that the amount of ROS in the microvascular wall is elevated after PM exposure.

PROTOCOL 2

Stimulation of isolated microvessels from filtered air–exposed rats with a bolus dose of A23187 produced NO robustly (33 ± 5 nM/mg, Figure 17). During coincubation with L-NMMA, this response was significantly inhibited (decreasing by 65% to 11 ± 4 nM/mg). This verifies that the majority of the signal produced by the probes under these conditions was NO dependent. Stimulated NO production in isolated microvessels from rats exposed to either fine or nano-TiO_2 was significantly lower than in rats exposed to filtered air. This impairment was dose dependent in that as pulmonary particle deposition increased, the ability to produce NO was progressively compromised by 40 to 85% in the fine-TiO_2 groups and 30 to 88% in the nano-TiO_2 groups. Similar to filtered air, NO

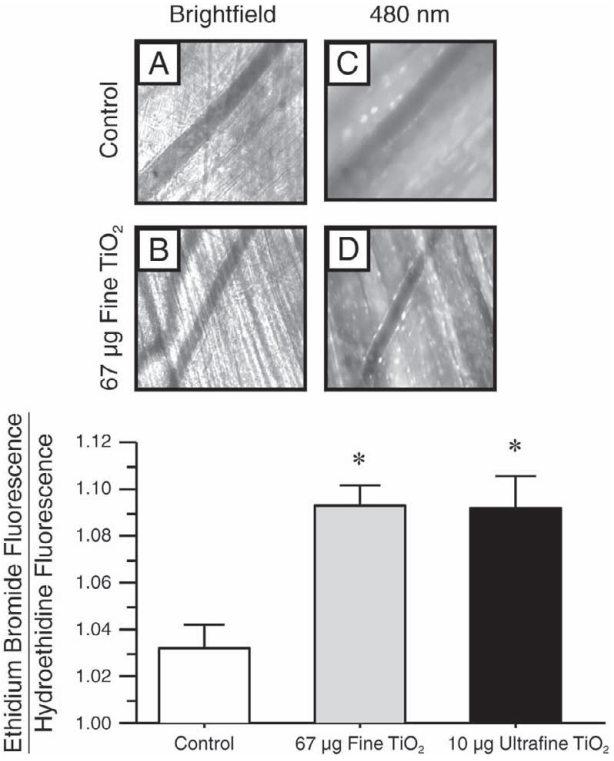

Figure 16. Increase in oxidative stress in the microvascular wall after particle inhalation. Exposure metric is the measured particle mass (µg) deposited in the lungs. **(Top)** Representative bright-field pictures for the filtered air–exposed **(A)** and 67 µg fine-TiO_2 groups **(B)**; and illumination at 480 nm for the filtered air–exposed **(C)** and 67 µg fine-TiO_2 groups **(D)**. Similar images were produced for the 10 µg nano-TiO_2 group (not shown). **(Bottom)** Ethidium bromide fluorescence (normalized to background fluorescence, hydroethidine). Filtered air, $n = 11$; 67 µg fine TiO_2, $n = 16$, and 10 µg nano-TiO_2, $n = 15$. *, $P < 0.05$ vs. filtered air–exposed group. Values are mean ± SE. (Reprinted from Nurkiewicz et al. 2009).

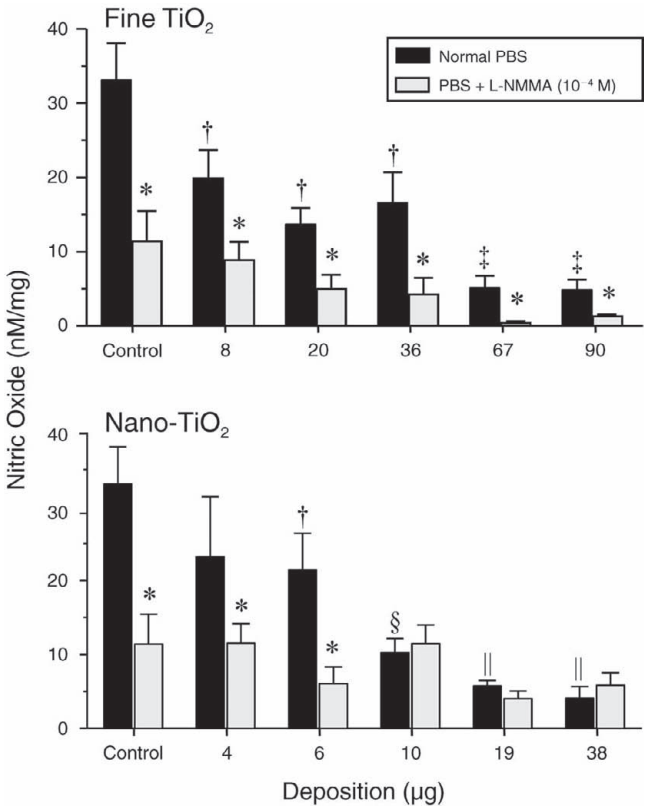

Figure 17. Attenuation of endogenous microvascular NO production after particle inhalation in a dose-dependent manner. Endothelial NO production was stimulated by a bolus dose of A23187 and measured in real time with an electrochemical sensor. NOS inhibition was accomplished by co-incubation with L-NMMA during measurements. Exposure metric is the measured particle mass (µg) deposited in the lungs. **(Top)** Fine TiO_2, 8 µg, $n = 9$; 20 µg, $n = 9$; 36 µg, $n = 7$; 67 µg, $n = 8$; 90 µg, $n = 9$; filtered air, $n = 34$. **(Bottom)** Nano-TiO_2, 4 µg, $n = 6$; 6 µg, $n = 8$; 10 µg, $n = 6$; 19 µg, $n = 6$; 38 µg, n = 6; filtered air, n = 34. *, $P < 0.05$ vs. normal PBS in the same group. †, $P < 0.05$ vs. filtered air–exposed group. ‡, $P < 0.05$ vs. 36 µg fine-TiO_2 group. §, $P < 0.05$ vs. 6 µg nano-TiO_2 group. ‖, $P < 0.05$ vs. 10 µg nano-TiO_2 group. Values are mean ± SE. (Reprinted from Nurkiewicz et al. 2009).

production was sensitive to NOS inhibition in that a significant portion of the NO produced under normal conditions (i.e., normal PBS) was decreased during coincubation with L-NMMA.

In further experiments, a single PM exposure dose was focused upon for each group (fine TiO_2, 67 µg; and nano-TiO_2, 10 µg) to better characterize what oxidant-generating mechanisms may be in isolated microvessels (Figure 18). At these exposure doses, stimulated NO production in isolated microvessels was 8 ± 2 and 10 ± 2 nM/mg for the fine-TiO_2 and nano-TiO_2 groups, respectively. Radical scavenging with TEMPOL and catalase similarly and significantly increased stimulated NO production in both groups to 34 ± 5 and 39 ± 12 nM/mg for the fine-TiO_2 and nano-TiO_2 groups, respectively. Inhibition of NADPH oxidase with apocynin significantly increased NO production in both groups to 44 ± 11 and 24 ± 7 nM/mg for the fine-TiO_2 and nano-TiO_2 groups, respectively. Although the NO response under apocynin was larger in the fine-TiO_2 group, the biologic relevance of this difference is unclear. Inhibition of MPO with ABAH significantly increased NO production in both groups to 46 ± 12 and 24 ± 6 nM/mg for the fine-TiO_2 and nano-TiO_2 groups, respectively. Again, although the NO response under ABAH was more potent in the fine-TiO_2 group, the biologic relevance of this difference is unclear. These agents did not significantly alter NO production in the filtered air–exposed group (data not shown).

As shown in Figure 19, the agents used to enhance stimulated NO production were superfused over the spinotrapezius muscle in order to evaluate their effectiveness on restoring endothelium-dependent arteriolar dilation.

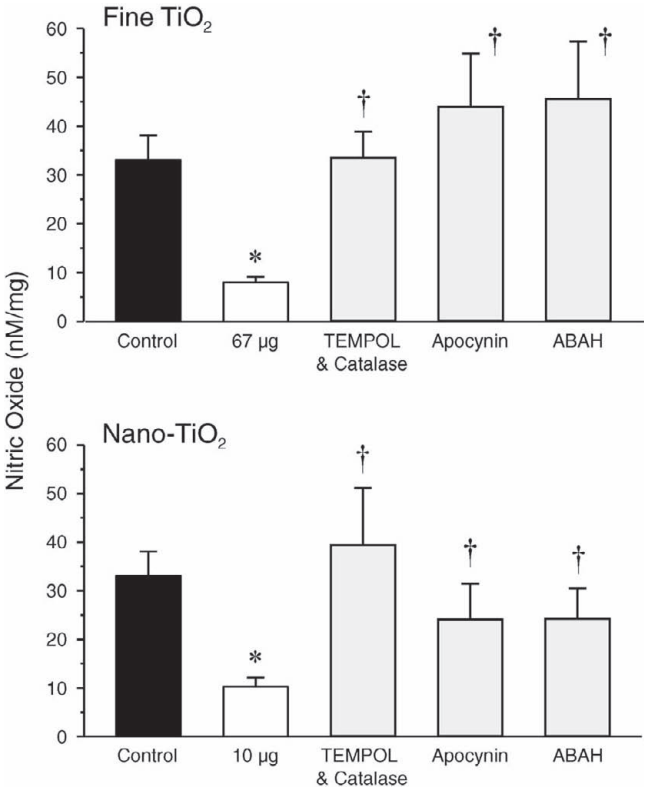

Figure 18. Restoration of endogenous NO production by radical scavenging or enzyme inhibition after particle exposure. Endothelial NO production was stimulated by a bolus dose of A23187 and measured in real time with an electrochemical sensor. Radical scavenging, NADPH oxidase, and myeloperoxidase inhibition were accomplished by coincubation during measurements with TEMPOL/catalase, apocynin, or ABAH, respectively. Exposure metric is the measured particle mass (µg) deposited in the lungs. **(Top)** Filtered air, n = 34; 67 µg fine TiO_2, n = 32; TEMPOL/catalase, n = 18; apocynin, n = 10; ABAH, n = 15. **(Bottom)** Filtered air, n = 34; 10 µg nano-TiO_2, n = 38; TEMPOL/catalase, n = 12; apocynin, n = 12; ABAH, n = 14. *, $P < 0.05$ vs. filtered air–exposed group. †, $P < 0.05$ vs. 67 µg fine TiO_2 or 10 µg nano-TiO_2 in the same panel. Values are mean ± SE. (Reprinted from Nurkiewicz et al. 2009).

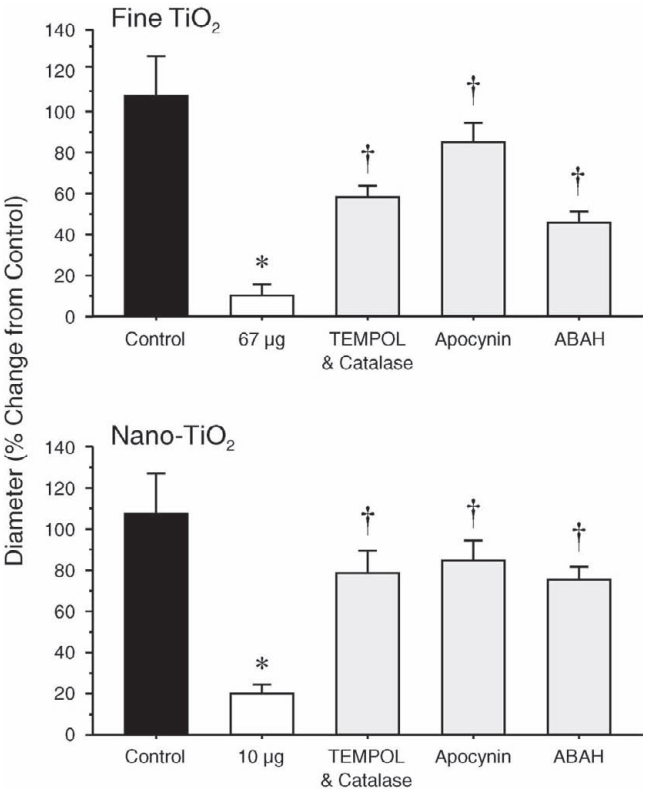

Figure 19. Restoration of arteriolar endothelium-dependent dilation by radical scavenging or enzyme inhibition after particle exposure. Responses were stimulated by intraluminal infusion of A23187 at 40 psi. Radical scavenging, NADPH oxidase, and myeloperoxidase inhibition were accomplished by coincubation during measurements with TEMPOL/catalase, apocynin, or ABAH, respectively. Exposure metric is the measured particle mass (µg) deposited in the lungs. **(Top)** Filtered air, n = 8; 67 µg fine TiO_2, n = 8; TEMPOL/catalase, n = 8; apocynin, n = 9; ABAH, n = 7. **(Bottom)** Filtered air, n = 8; 10 µg nano-TiO_2, n = 10; TEMPOL/catalase, n = 10; apocynin, n = 12; ABAH, n = 11. *, $P < 0.05$ vs. filtered air–exposed group. †, $P < 0.05$ vs. 67 µg fine TiO_2 or 10 µg nano-TiO_2 in the same panel. Values are mean ± SE. (Reprinted from Nurkiewicz et al. 2009).

Under control conditions with the normal superfusate, A23187 infusion (40 psi) produced significant arteriolar dilation in the filtered air–exposed group (108% ± 19% increase from control diameter). After exposure to either fine or nano-TiO_2, arteriolar dilation was limited to only 10% ± 5% or 20% ± 4% above control diameter, respectively. Radical scavenging with TEMPOL and catalase partially restored arteriolar dilation in both groups (increases from the control diameter of 58% ± 5% and 79% ± 11% for the fine-TiO_2, and nano-TiO_2 groups, respectively). NADPH oxidase inhibition with apocynin also partially restored arteriolar dilation in both groups (increases from the control diameter of 85% ± 9% and 85% ± 10% for the fine-TiO_2, and nano-TiO_2 groups, respectively). MPO inhibition with ABAH was also capable of partially restoring arteriolar dilation in both groups (increases from the control diameter of 46% ± 5% and 76% ± 6% for the fine-TiO_2, and nano-TiO_2 groups, respectively). These agents did not significantly alter arteriolar dilation in the filtered air–exposed group (data not shown).

The area (µm^2) of tissue containing NT was significantly elevated in the lung (Figure 20) and spinotrapezius-muscle microcirculation (Figure 21) after exposure to 10 µg nano-TiO_2. In both Figures 20 and 21, indirect immunofluorescence for NT is principally localized within discrete inflammatory cells. Because NT is a product of peroxynitrite-induced tyrosine nitration, the increased NT that follows PM exposure suggests oxidative injury within the lung and in the spinotrapezius-muscle microcirculation.

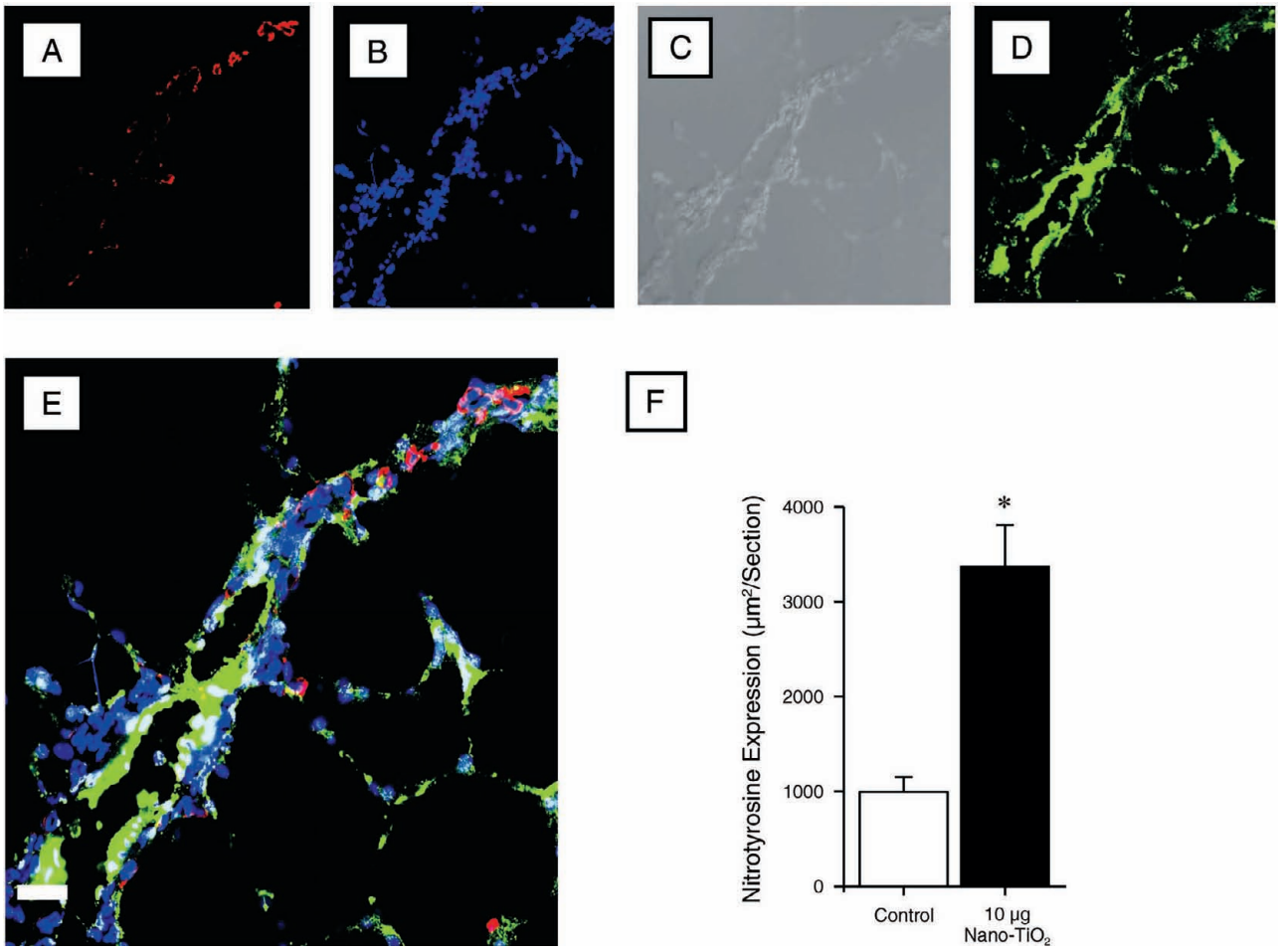

Figure 20. Indirect immunofluorescent and differential interference contrast (DIC) confocal microscopy of the lung and intrapulmonary vasculature from a rat exposed to 10 μg nano-TiO_2. Exposure metric is the measured particle mass (μg) deposited in the lungs. **(A)** Red fluorescence demonstrates NT and is localized within individual cells morphologically consistent with inflammatory cells. **(B)** Blue fluorescence is DAPI labeling of nuclei. **(C)** DIC confocal microscopy demonstrating lung structure with a large vessel traversing the section. The fishnet-like structure is an alveolus. **(D)** Green fluorescence cells indicate vWF, a marker of vascular endothelium in the intrapulmonary vasculature. **(E)** Triple label immunofluorescence. Coexpression of green and red gives a yellow color and indicates that these markers are within the same location. The majority of pulmonary NT expression is within discrete inflammatory cells in alveoli or near but only occasionally within, the vascular endothelium (the scale bar is 20 μm). **(F)** NT expression in the lung was increased by TiO_2 inhalation. Values are mean ± SE. (Reprinted from Nurkiewicz et al. 2009).

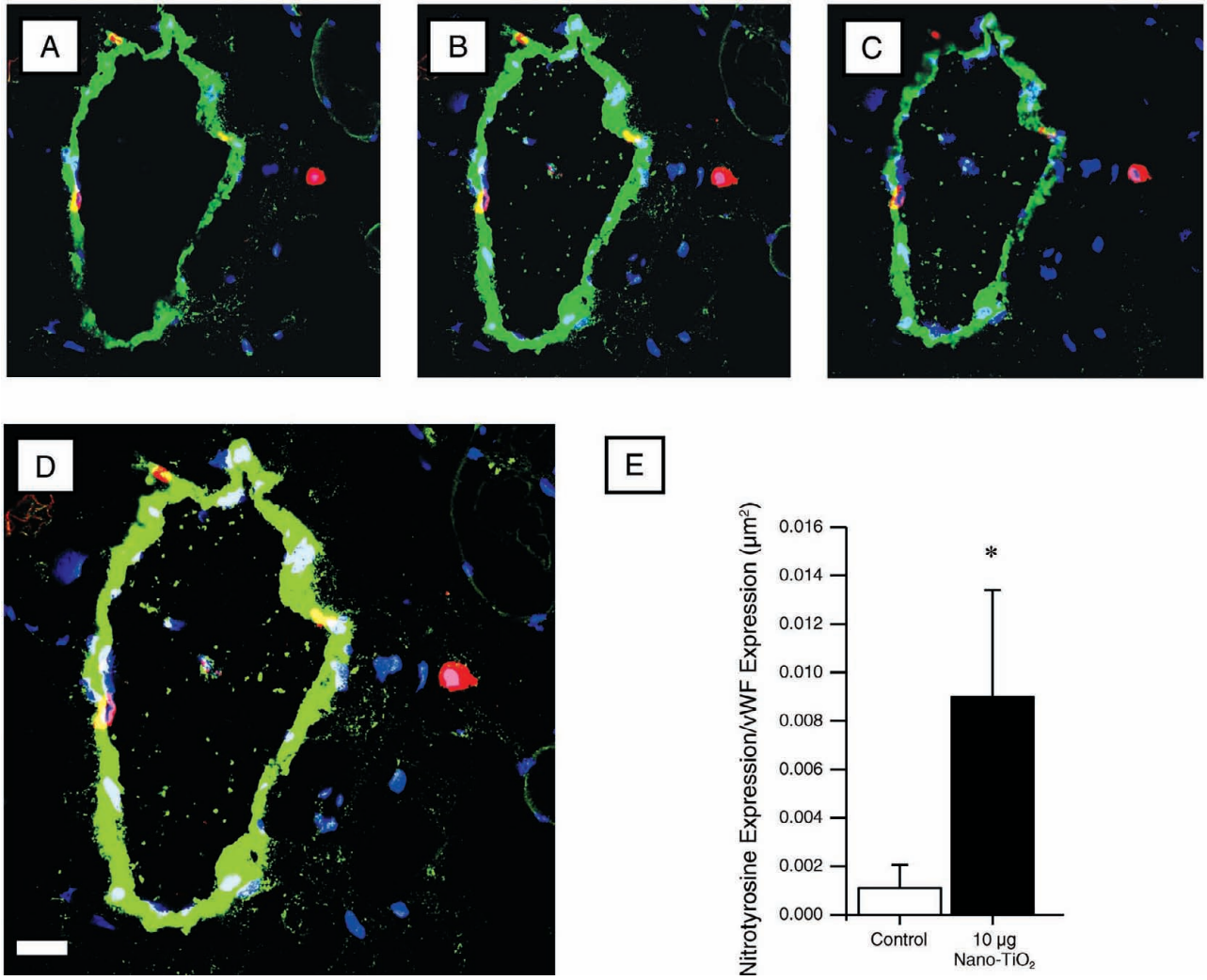

Figure 21. Indirect immunofluorescent confocal microscopy of the spinotrapezius-muscle microcirculation from a rat exposed to 10 μg nano-TiO_2. Exposure metric is the measured particle mass (μg) deposited in the lungs. **(A–D)** Longitudinal z stack of a microvessel. **(D)** Enlarged section. **(E)** NT expression in the microcirculation was increased by TiO_2 inhalation. Red fluorescence demonstrates NT and is localized within individual cells morphologically consistent with inflammatory cells. Green fluorescence cells indicate vWF, a marker of vascular endothelium. Coexpression of green and red gives a yellow color and indicates that these markers are within the same location (the scale bar is 20 μm). Values are mean ± SE. (Reprinted from Nurkiewicz et al. 2009).

PROTOCOL 3

Multiplex analysis of plasma from animals exposed to TiO_2 aerosol revealed significant increases in circulating cytokines 24 hours after exposure (Figure 22). Specifically, IL-2, IL-18, IL-13, and GRO-KC were elevated in rats exposed to fine TiO_2. Although some trends were noted in other variables, no changes in other cytokines and factors measured reached significance (data not shown).

The ETP assay measured the ability of rat plasma to generate thrombin and utilized a fluorogenic thrombin substrate. The total amount of thrombin generated over the duration of the readings is determined by measuring the area under the curve (AUC). The maximum amount of thrombin generated (peak thrombin generation) at any point in time was also determined. As compared with the filtered air–exposed rats, thrombin generation was significantly higher in rats exposed to either 10 µg nano-TiO_2 or 8 µg fine TiO_2 (Table 5). This effect was more pronounced in plasma from rats exposed to fine TiO_2.

Total thrombin generation was studied at various doses for the fine and nano-TiO_2 PM exposures over 24 hours. ETP was significantly higher in all exposure groups studied than in the filtered air–exposed group (Table 6). A dose–response relationship was not observed between exposure doses and ETP, as an increased effect was not seen as exposure increased. The most pronounced effect on thrombin generation occurred in the 10-µg group.

Table 5. Endogenous Thrombin Potential of Plasma Obtained from Rats Exposed to TiO_2 as Compared to Controls[a]

Group	*n*	Thrombin Generation (nM/min)	Peak Thrombin (nM)
Control	17	2972 ± 708	195 ± 45
Nano-TiO_2, 10 µg	13	3544 ± 332[b]	244 ± 24[b]
Fine TiO_2, 8 µg	8	4277 ± 156[b,c]	273 ± 13[b,c]

[a] This assay determines the ability of plasma to generate thrombin. *n* = number of animals with measurements performed in triplicate. Values are mean ± SD.

[b] Statistically significant difference between this group and control.

[c] Statistically significant difference between this group and all other exposed groups.

Using the Luminex assay, we saw very few differences between fibrinogen and vWF levels between exposed groups and the filtered air–exposed group (Table 7). This is partly explained by the variability of these assays, especially the fibrinogen assay. The exaggerated increase in fibrinogen in the 90-µg fine-TiO_2 group was explained by very high values in approximately two-thirds of the animals in this group. Other animals in this group had values that were more consistent with other groups. With the rat fibrinogen ELISA, no significant differences could be found between

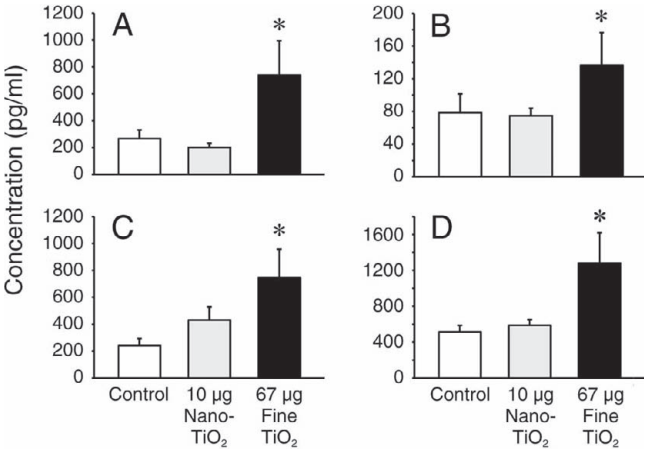

Figure 22. Alteration of plasma cytokine concentrations 24 hours after TiO_2 inhalation. Exposure metric is the measured particle mass (µg) deposited in the lungs. Cytokines were assessed by multiplex analysis. **(A)** IL-2. **(B)** IL-18. **(C)** IL-13. **(D)** GRO-KC. *, $P < 0.05$ vs. filtered air–exposed group. Values are mean ± SE.

Table 6. Endogenous Thrombin Potential of Plasma in Rats Exposed to Various Doses of Nano- and Fine TiO_2[a]

Group	*n*	Thrombin Generation (nM/min)
Control	15	2895 ± 705
Nano-TiO_2		
6 µg	5	3824 ± 285[b]
10 µg	8	4277 ± 182[b]
Fine TiO_2		
20 µg	9	3696 ± 354[b]
67 µg	11	3240 ± 791[b]
90 µg	5	3692 ± 264[b]

[a] *n* = number of animals with measurements performed in triplicate. Values are mean ± SD.

[b] $P < 0.05$ for the comparison between the exposed and control groups.

Table 7. Fibrinogen and vWF (Luminex Assay) of Plasma in Rats Exposed to Various Doses of Nano- and Fine TiO_2[a]

Group	Fibrinogen	vWF
Control	198,000 ± 301,868	105 ± 58
Nano-TiO_2		
6 µg	140,000 ± 187,621	135 ± 69
10 µg	82,000 ± 130,951	185 ± 130[b]
19 µg	100,000 ± 106,580	99 ± 65
38 µg	53,000 ± 44,247	138 ± 109
Fine TiO_2		
67 µg	110,000 ± 80,233	140 ± 92
90 µg	1,185,000 ± 630,111[c]	155 ± 95

[a] Values are mean fluorescent units ± SD.
[b] $P < 0.05$ for the comparison between this group and control.
[c] $P < 0.05$ for the comparison between this group and all other exposed groups.

Table 8. Plasma Fibrinogen (Rat Fibrinogen ELISA Assay) in Rats Exposed to Various Doses of Nano- and Fine TiO_2[a]

Group	Fibrinogen (µg/mL)
Control	51 ± 24
Nano-TiO_2	
10 µg	65 ± 26
19 µg	68 ± 27
Fine TiO_2	
67 µg	50 ± 12
90 µg	87 ± 8

[a] Values are mean ± SD.

Table 9. Troponin I and Troponin T Levels (Luminex Assay) in Plasma of Rats Exposed to Various Doses of Nano- and Fine TiO_2[a]

Group	Troponin I	Troponin T
Control	69,495 ± 2,801	6,178 ± 1,704
Nano-TiO_2		
6 µg	75,026 ± 5,237[b]	7,059 ± 404[b]
10 µg	70,116 ± 4,017	6,379 ± 617
19 µg	68,705 ± 3,446	6,467 ± 350
38 µg	71,639 ± 3,519	6,594 ± 779
Fine TiO_2		
67 µg	73,612 ± 4,150[b]	7,042 ± 1,070[b]
90 µg	67,793 ± 3,895	5,038 ± 975

[a] Values are mean fluorescent unit ± SD.
[b] $P < 0.05$ for the comparison between this group and control.

any of the groups (Table 8). For vWF measurements, only the 10-µg nano-TiO_2 group had values significantly higher than the filtered air–exposed group (Table 7).

Significant elevations were demonstrated in both troponin I and troponin T for the 67-µg fine-TiO_2 and 6-µg nano-TiO_2 groups (Table 9). Although these differences were significant, it is unclear if they truly reflect myocardial injury. There were no dose–response effects in either troponin I or troponin T in the exposed animals.

A separate group of F-344 rats were treated with cyclophosphamide 3 days prior to exposure. This treatment (10 µg nano-TiO_2) did not affect the weight or mean arterial pressure of any group (Table 10); in fact, these data were comparable to those for Sprague Dawley rats used in the majority of the experiments in the current study (Table 3). Cyclophosphamide treatment did significantly decrease circulating neutrophils (Figure 23). In rats exposed to filtered

Table 10. Profiles of F-344 Rats Used for Intravital Microscopy Studies[a]

Treatment	Inhalation Exposure	*n*	Age (days)	Weight (g)	Arterial Pressure (mm Hg)
Saline, i.p.	Filtered air	3	49 ± 1	203 ± 5	101 ± 19
Saline, i.p.	Nano-TiO_2, 10 µg	5	48 ± 1	211 ± 8	111 ± 9
Cyclophosphamide	Filtered air	3	49 ± 1	210 ± 5	100 ± 11
Cyclophosphamide	Nano-TiO_2, 10 µg	4	48 ± 1	205 ± 3	117 ± 6

[a] Values are mean ± SE.

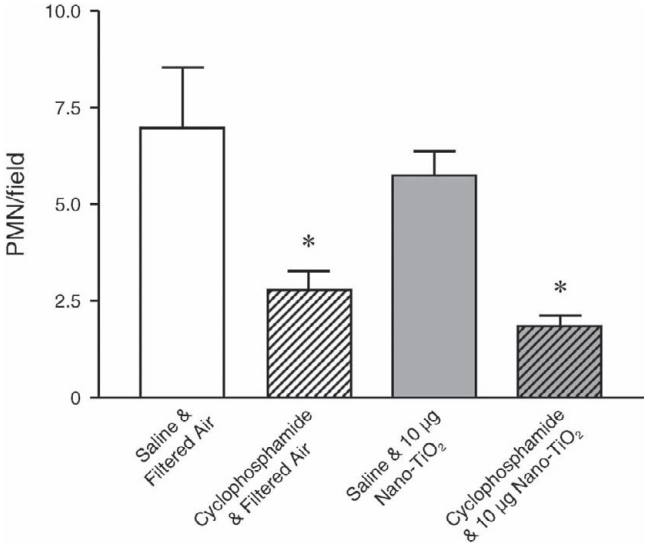

Figure 23. Cyclophosphamide treatment significantly decreases circulating neutrophils. Exposure metric is the measured particle mass (µg) deposited in the lungs. *, $P < 0.05$ vs. filtered air–exposed group at the same ejection pressure. Values are mean ± SE.

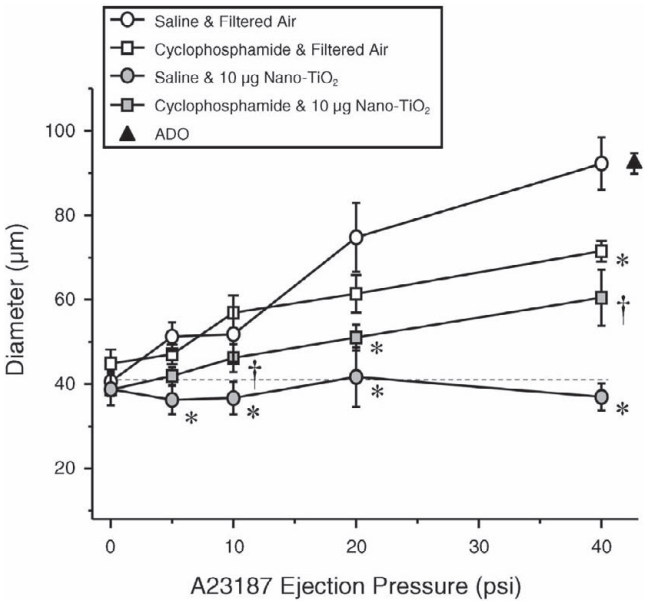

Figure 24. Partial vasoprotective effects on endothelium-dependent arteriolar dilation imparted by neutrophil depletion prior to nano-TiO_2 exposure. Exposure metric is the measured particle mass (µg) deposited in the lungs. Saline and filtered air, $n = 6$; saline and 10 µg nano-TiO_2, $n = 8$; cyclophosphamide and filtered air, $n = 9$; and cyclophosphamide and 10 µg nano-TiO_2, $n = 8$. *, $P < 0.05$ vs. saline and filtered air–exposed group at the same ejection pressure. †, $P < 0.05$ vs. saline and 10 µg nano-TiO_2 group at the same ejection pressure. Values are mean ± SE.

air, cyclophosphamide treatment produced an approximately 2.5-fold decrease in circulating neutrophils (Figure 23, white bar vs. white-hatched bar). Consistent with prior measurements in rats exposed to fine TiO_2 (Nurkiewicz et al. 2004), exposure to nano-TiO_2 also slightly decreased circulating neutrophils (Figure 23, gray bar vs. white bar). This subtle effect probably reflects increased leukocyte adhesion to the microvascular endothelium after PM exposure. In rats exposed to 10 µg nano-TiO_2, cyclophosphamide treatment similarly produced an approximately threefold decrease in circulating neutrophils (Figure 23, gray bar vs. gray-hatched bar). The passive diameters of the saline-treated rats exposed to filtered air were significantly greater than those for the other three groups (Table 11). This appears to be an artifact and the result of smaller n values associated with the group because the greater mean among filtered air–exposed rats is approximately 100 µm. Cyclophosphamide treatment was associated with a lower resting tone in both treated groups (Table 11). In intravital microscopy experiments, cyclophosphamide treatment did impair normal endothelium-dependent arteriolar dilation induced by A23187 (Figure 24, white squares

Table 11. Resting Variables for Arterioles from the Spinotrapezius Muscle of F-344 Rats Studied in Intravital Microscopy Studies[a]

Treatment	Inhalation Exposure	n	Resting Diameter (µm)	Passive Diameter (µm)	Resting Tone (% of maximum)
Saline, i.p.	Filtered air	5	41 ± 3	107 ± 5[b]	62 ± 3
Saline, i.p.	Nano-TiO_2, 10 µg	8	39 ± 4	92 ± 5	57 ± 5
Cyclophosphamide	Filtered air	9	45 ± 3	91 ± 4	50 ± 4[c]
Cyclophosphamide	Nano-TiO_2, 10 µg	8	39 ± 2	85 ± 6	53 ± 3[c]

[a] Values are mean ± SE.
[b] $P < 0.05$ vs. all other groups.
[c] $P < 0.05$ vs. i.p. saline and filtered air–exposed group.

vs. white circles). However, neutrophil depletion did partially protect endothelium-dependent arteriolar dilation after exposure to 10 μg nano-TiO_2 (Figure 24, gray squares vs. gray circles). Because alterations in resting tone can influence the length-tension relationship, the data were also compared as percentage change from filtered air. Expressing this data (data not shown) produced identical results to those presented in Figure 24. This is consistent with the hypothesis that active, circulating inflammatory cells are associated with the microvascular dysfunction that follows PM exposure. The endothelium-dependent responses observed in spinotrapezius-muscle arterioles of the i.p. saline group of F-344 rats was consistent with those we have observed in Sprague Dawley, Wistar-Kyoto, and Dahl salt-resistant rat strains in previous studies. This indicates that microvascular endothelial function is preserved across different rat strains (Boegehold 1993; Nurkiewicz and Boegehold 1998, 2004; Nurkiewicz et al. 2004, 2006, 2008, 2009).

In our last series of intravital microscopy experiments, fast Na^+ channels were blocked by adding TTX to the superfusate (Figure 25). In these experiments, TTX superfusion partially restored endothelium-dependent arteriolar dilation by as much as approximately 76% and 69% (at 20 and 40 psi, respectively) in rats exposed to 10 μg nano-TiO_2. TTX treatment did produce a slight decrease in resting diameter (indicating the influence of sympathetic nerve activity on resting tone), although this effect was not significant. As with the cyclophosphamide experiments, the disruption of resting tone or the balance of factors contributing to it can alter the length–tension relationship in arteriolar smooth muscle. Therefore, the data were also calculated as the percentage change from filtered air, and this produced identical results (data not shown). Collectively, this indicates that sympathetic activity in the peripheral microcirculation is altered after PM exposure.

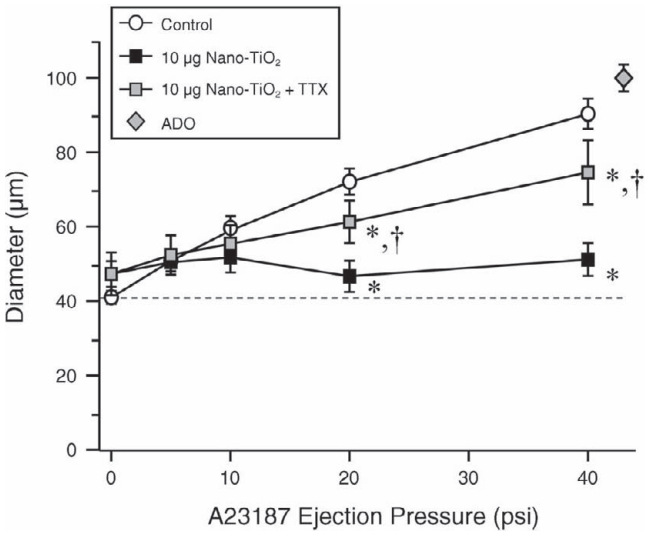

Figure 25. Partial restoration of endothelium-dependent arteriolar dilation after exposure to nano-TiO_2 by blocking fast Na^+ channel activity. Exposure metric is the measured particle mass (μg) deposited in the lungs. Saline and filtered air, $n = 5$; and 10 μg nano-TiO_2, $n = 8$. *, $P < 0.05$ vs. filtered air–exposed group at the same ejection pressure. †, $P < 0.05$ vs. 10 μg nano-TiO_2 group at the same ejection pressure. Values are mean ± SE.

DISCUSSION

These studies have directly identified an impaired vasodilator capacity in the systemic microcirculation after PM inhalation. We have also provided experimental evidence that links pulmonary exposure with a systemic effect (i.e., the smoking gun). In the current study, this may be represented by circulating neutrophils or associated inflammatory factors. It is equally possible that the activity of sympathetic projections to the microcirculation play a role in this process. Another important feature of the current report is that for the same pulmonary mass deposition, nano-PM produces significantly greater systemic microvascular dysfunction than their larger, fine counterparts of the same composition. The natural extension of this finding is our observation that the surface area of particles deposited in the lungs appears to be a stronger predictor of this dysfunction than the usually deposited particles.

Nano-PM inhalation attenuated systemic arteriolar dilation in a dose-dependent manner (Figure 9). This was most evident at a pulmonary deposition of 38 μg, in which arterioles constricted in response to intraluminal A23187 infusion. Arteriolar constriction during A23187 infusion is inconsistent with a healthy endothelium, because under healthy conditions, A23187 normally interacts only with endothelial cells to increase the intracellular Ca^{2+} concentration and subsequently stimulate NO production (Schneider et al. 2003). Altered endothelial integrity, permeability, or the two together could allow luminal A23187 to interact with smooth-muscle cells, thereby increasing intracellular Ca^{2+} concentration (Schuhmann et al. 1997) and ultimately stimulating vasoconstriction (Huang et al. 2000). Alternatively, endothelial integrity may be unaltered, but some aspect of PM exposure offsets the prevailing balance of vasoconstrictors and vasodilators. Indeed, A23187 has the potential to stimulate endothelial production of vasoconstrictor prostanoids (Huang and Koller 1996; Gluais et al. 2006). Future studies must determine whether endothelial integrity has been compromised, the

production of vasoconstrictor prostanoids has been altered by PM exposure, or both effects have occurred. Of equal importance, future investigations must characterize the ability of extrapulmonary particles to alter the bioavailability of vasoactive metabolites.

The loss of microvascular vasodilator capacity can have a profound influence on normal homeostasis in any organ. In its most basic sense, this microvascular impairment would decrease tissue perfusion and therefore compromise function (Frisbee 2003). Our current techniques and findings focus upon vasomotor function in single arterioles after pulmonary nano-PM exposure. To fully appreciate the net effect of alterations in vascular regulation, researchers must study total tissue or organ blood flow. These approaches can be challenging, and, as such, other hemodynamic variables that relate to tissue or organ blood flow can offer considerable insight into the systemic microvascular consequences that follow PM exposure. Mills and colleagues (2005) showed that diesel exhaust inhalation attenuates forearm blood flow responsiveness to vasodilators. Further, pulmonary exposure to diesel particles in the ultrafine range potentiates myocardial ischemia in patients with pre-existing coronary heart disease (Mills et al. 2007). Urch and colleagues (2005) have reported acute increases in diastolic blood pressure within 2 hours of PM exposure. Changes in diastolic blood pressure are achieved primarily by alterations within the resistance vasculature; Rundell and colleagues (2007) reported a deficit in hemoglobin reoxygenation after arterial occlusion. Taken together, these findings are highly suggestive of larger disturbances in microvascular blood flow regulation after PM exposure.

Brook and colleagues (2002) initially identified a subtle vasoconstriction of the brachial artery in humans who inhaled fine PM. Rundell and colleagues (2007) have reported that this conduit artery constricts similarly after ultrafine particle inhalation. Because the smaller particles studied by Rundell and colleagues did not appear to be associated with a more robust vasoconstriction than the larger particles used by Brook and colleagues, one might conclude that particle size does not dictate resultant vascular dysfunction. However, it is possible that this experimental model lacks sufficient sensitivity to reveal such differences or that fundamental differences in particle composition, exposure protocols, experimental group profiles, or a combination of all three prevent a meaningful comparison between the two studies.

Nano-TiO_2 has been shown to cause significantly greater airway inflammation than fine TiO_2 (de Haar et al. 2006). Based upon the count geometric mean diameter (Figure 4), nano-TiO_2 aerosols attenuate systemic endothelium-dependent arteriolar dilation to a greater degree than fine-TiO_2 aerosols (Figures 8, 9, 12, and 13) at similar lung burdens (Table 1). This observation is most evident at lung burdens of 36 µg and 38 µg for fine and nano-PM, respectively. In this case, nano-TiO_2 aerosol exposure was consistently associated with arteriolar constriction, whereas fine-TiO_2 inhalation was consistently associated with impaired arteriolar dilation (Figure 12C). This suggests that given the diverse nature of particle size, shape, and chemistry, the deposited particle mass may not be the ideal dose metric.

Data presented in the current study indicate that on an equivalent mass basis, nano-TiO_2 was approximately one order of magnitude more potent than fine TiO_2 in causing systemic microvascular dysfunction. Oberdorster (1996) has proposed that particle surface area per unit mass may be the more appropriate dose metric for pulmonary effects of nano-PM than mass. Therefore, we also analyzed the results on an equivalent surface area of PM deposited in the lungs. The analysis described by and named after Brunauer, Emmett, and Teller (BET analysis) (Brunauer et al. 1938) was used to determine that the surface area of nano-TiO_2 was 48.08 m^2/g, whereas that of fine TiO_2 was 2.34 m^2/g, that is, nano-TiO_2 had approximately 20 times more surface area per unit mass than fine TiO_2. Therefore, if one normalized the systemic microvascular response to equivalent total particle surface area, the fine TiO_2 would be more potent than the nano-TiO_2. This conclusion is likely the result of an overestimation of the total nano-TiO_2 surface area delivered to the lungs, because the BET method measures the gas absorptive surface area of the primary particles rather than the actual physical surface of the aerosolized agglomerates. Indeed, Shvedova and colleagues (2007) reported that the pulmonary response to ultrafine carbon black was significantly increased upon improved nano-PM dispersion.

The fundamental focus of the current report is upon the systemic microvascular effects of pulmonary particle exposure (rather than a focus upon pulmonary effects). Specifically, Oberdorster's proposition (that particle surface area per unit mass rather than mass may be the more appropriate dose metric for nano-PM) is being paraphrased to test its utility in the peripheral microcirculation (Oberdorster 1996). In this regard, the estimates in the previous paragraph are not sufficiently powerful to verify Oberdorster's proposition. Thus, we further analyzed the results on an equivalent surface area of deposited PM. The surface areas were calculated based on the modes (710 nm and 100 nm, respectively) of the fine and nano-PM–size distribution (Figure 4). Assuming that the particles are spherical, the specific surface area for the fine and nano-TiO_2 PM is determined to be 2.0 and 15.8 m^2/g, respectively, indicating that nano-TiO_2 had approximately eight

times more surface area per unit mass than fine TiO_2. The particle densities used in the calculation are 4.23 and 3.8 g/cm^3, respectively. With the actual pulmonary mass deposition data (Table 1) and the calculated specific surface area (Table 2) as the mass-to-area conversion factor, the arteriolar dysfunction in rats exposed to fine and nano-TiO_2 based on total surface area of the particles deposited in the pulmonary region can be compared to that based on the mass of particles deposited (Figures 12 and 13). It is evident from these data that particle surface area is a far better predictor of resultant arteriolar dysfunction than particle mass.

It is important to note that actual pulmonary particle deposition was significantly less than the calculated deposition (Table 1). This may be for several reasons. First, it is very likely that particle clearance occurs in the 24 hours after exposure and particularly during the 12-hour exposures that took place over 3 days. Second, biologic heterogeneity among rats may contribute to differences in the calculated versus the actual particle depositions. In this case, subtle differences in minute volumes or deposition fractions among rats could contribute to the divergent measurements. However, despite manipulation of aerosol concentration (3–12 mg/m^3) or exposure time (2–8 hr), the intensity of microvascular dysfunction did not differ among these groups 24 hours after exposure (Figure 10). This suggests that the ranges of variables used to obtain our target pulmonary loads were not responsible for the observed biologic effects in either the lungs or the systemic microcirculation.

This study presented the opportunity to directly compare the microvascular responses to two different exposure methods. When arteriolar responses between rats exposed to similar doses of fine TiO_2 (90 μg via inhalation vs. 100 μg via i.t. instillation [Nurkiewicz et al. 2006]) were compared, no significant differences were apparent in the resultant microvascular dysfunction (Figure 11). This suggests that the method of particle introduction to the lungs does not artificially induce systemic microvascular dysfunction.

Despite an obvious lack of difference (in terms of microvascular effects) between exposure techniques, the physiologic relevance of i.t. instillation is frequently questioned. Intratracheal instillation is a commonly used exposure method because it is rapid, economical, and consistent across multiple animals. Furthermore, i.t. instillation can produce a relatively uniform pulmonary particle distribution if exposure doses are kept low (Roberts et al. 2004). However, in regard to the true in vivo environment, i.t. instillation bypasses many important physiologic processes. Hence, the gold standard of particle exposure remains via inhalation.

We have reported that, as compared with fine-PM, nano-PM inhalation, at a similar mass pulmonary deposition, produces significantly greater microvascular dysfunction (Nurkiewicz et al. 2008). In the current study, this is most evident in that it required a fine PM deposition that was more than six times greater than the nano-PM deposition to produce equivalent levels of microvascular dysfunction (67 μg fine TiO_2 vs. 10 μg nano-TiO_2, Figure 13). Whether or not pulmonary mass deposition is the most appropriate metric to use for comparing such distinctly different particles remains to be determined (Warheit et al. 2007). Although a strong argument for surface area is presented in the current report, it is far from a definitive answer. In the absence of a definitive answer to this issue, and in order to establish the relevance of the current experimental conditions to human exposures, it is important to relate the aerosol concentrations and exposure times used in the current study to produce our doses in a single exposure (5 hours at 16 mg/m^3 and 4 hours at 6 mg/m^3 for fine TiO_2 and nano-TiO_2, respectively) to those to which people may be exposed over protracted periods of time. The current occupational exposure limit to fine TiO_2 is 5 mg/m^3. Therefore, a worker exposed at this level 8 hours/day for 5 working days would achieve a pulmonary burden equivalent to 67 μg (normalized for alveolar epithelial surface area [Stone et al. 1992] and assuming human pulmonary deposition of a 1-μm particle of 20% [Bates et al. 1966]). Levels of nano-TiO_2 have been measured in a production plant to be as high as 1.4 μg/m^3 (V.C. and Chuck Geraci, unpublished observations). Therefore, workers exposed to this level (1.4 μg/m^3) could achieve a pulmonary burden equivalent to 10 μg in the rat (normalized for alveolar epithelial surface area and assuming a deposition fraction of 45%) within 5 years. Although this may at first appear a tremendous burden, bear in mind that typical occupations (in which workers experience pulmonary exposures) last considerably longer than 5 years, and associated exposures frequently exceed those used in the current study by several-fold. Furthermore, not all workers are healthy, and typically they are not sedentary (which would lead to decreased ventilation and thus to decreased deposition) in an occupational environment. As such, the doses used in this study may be relevant in these regards. Regardless, it is important to indicate that acute exposure to higher particle concentrations may not be physiologically representative of the chronic exposure to low concentrations of particles that the general population may experience.

Because we reported an altered NO bioavailability after PM exposure, it was critical to define whether arteriolar smooth-muscle sensitivity to NO was altered. The microvascular dysfunction associated with exposure to either

fine TiO_2 or nano-TiO_2 is not due to altered arteriolar smooth-muscle responsiveness to NO (Figure 15). We have shown this to also be the case after exposure to residual oil fly ash (Nurkiewicz et al. 2004). Our finding of an unaltered smooth-muscle NO sensitivity after PM exposure is in agreement with findings in the rabbit carotid artery (Tamagawa et al. 2008) and mouse mesenteric artery and vein (Knuckles et al. 2008) but not the mouse septal artery (Campen et al. 2005), rat aorta (Bagate et al. 2004b), or rat intrapulmonary artery (Courtois et al. 2008). Multiple possibilities exist for this disparity in smooth-muscle sensitivity after PM exposure. First, the various tissues used possess inherently different levels of function as well as vascular reactivity that under certain artificial conditions prevent meaningful comparisons. However, studies do exist that report divergent sensitivities to different NO donors in the same vascular segment (Courtois et al. 2008). Second, the NO donors used across experiments can be different. In the current study, we used SNP, which donates NO via interaction with a biologic membrane at physiologic pH (Butler and Megson 2002; Ignarro et al. 2002), whereas diazeniumdiolates such as diethylamino-NONOate spontaneously release NO in a more controlled fashion (Ignarro et al. 2002; Miranda et al. 2005). Despite different mechanisms of NO donation, studies in the basilar and carotid arteries indicate that SNP is an effective NO donor, if not one of the most potent, NO donors (Salom et al. 1998, 1999). Ultimately, it is the activity of cyclic guanosine monophosphate (cGMP) in the VSM that is important in this regard, and studies with cGMP analogs indicate that PM exposure does not alter this sensitivity (Courtois et al. 2008). Third, the particles and conditions used in these and other studies are very different. The potential for one technique, particle, or emission condition to affect smooth-muscle NO sensitivity, whereas another does not, is high because numerous biologic mechanisms have been identified and advanced to help explain how a particle deposited in the lung can influence a systemic tissue (Dreher et al. 1997; Godleski et al. 2000; Watkinson et al. 2001; Brook et al. 2004; Oberdorster et al. 2004; Donaldson et al. 2005).

Microvascular oxidative stress is significantly increased after PM exposure (Figure 16), and this finding is consistent with findings in the aortic wall (Sun et al. 2008). An elevation of local ROS may potentially consume endothelium-derived NO and result in peroxynitrite radical formation (Forstermann and Munzel 2006). A stable product of peroxynitrite reactions with NO is NT (Beckman 1996; Beckman and Koppenol 1996). In Figure 21, microvascular NT formation is significantly increased in the microvascular wall after PM exposure. Taken together, these findings suggest that after PM exposure, oxidative stress in the microvascular wall consumes endothelial NO.

The logical corollary of the above findings is that endogenous NO production will be compromised after PM exposure because of radical quenching. Indeed, endogenous microvascular NO production is compromised after particle exposure in a dose-dependent relationship (Figure 17). To our knowledge, this is the first study to directly measure endogenous NO in real time and report that particle exposure attenuates this measurement. Since our first report that microvascular endothelium-dependent dilation is compromised after particle exposure (Nurkiewicz et al. 2004), it has become obvious that this effect is not limited to the microcirculation (Campen et al. 2005; Mills et al. 2005; Hansen et al. 2007; Rundell et al. 2007; Knuckles et al. 2008). Although the vascular effect is clearly not targeted at a singular level of the vasculature, it is imperative to note that endothelial stimulation produces numerous vasoactive agents other than NO, including cycloxygenase products, bradykinin, endothelium-derived hyperpolarizing factor, angiotensin, and endothelin. Moreover, the relative contribution of NO versus that of other vasodilators to endothelium-dependent dilation can be very different between vascular beds and even species. Therefore, it is not only critical to directly measure NO but also to characterize how the influence of other vasoactive agents is altered after particle exposure.

Making direct NO measurements is a time-consuming and particularly demanding experiment that, as with all experimental techniques, carries limitations (Zhang 2004; Davies and Zhang 2008). Additionally, NO sensors can be unreliable and sensitive to numerous artifacts. We used extreme caution in designing our experiments to avoid such complications. Specifically, the NO sensors used in the current study were calibrated before each experiment and no less than two sensors were simultaneously used in a single experiment (to verify that readings were not erroneous). The probes were also randomly calibrated throughout their lifespan (typically less than 2 weeks). Any probe that failed to consistently generate current (in the presence of SNAP) comparable to that produced by a fresh probe was removed. Perhaps a more important assumption we have made is that the NO measurements should be considered in a qualitative sense rather than attempting to precisely quantify the relationship between pulmonary deposition and microvascular NO production. In this regard, we caution the reader to interpret our findings only in the sense that the exposure doses used in our study produced a significant decrease in endogenous microvascular NO production. The presence of artifacts may be apparent in Figure 17, where the probes still measured an NO signal in the presence of L-NMMA. However, because this residual NO signal (in the presence of L-NMMA) was variable across the particle types and doses, it can

also be argued that NOS inhibition was incomplete under these conditions.

Given that PM exposure compromises endogenous NO production (Figure 17), it is essential to determine the fate of NO under this condition. In Figure 16, an increase in microvascular ROS is apparent after PM exposure. Because ROS are capable of consuming NO (Forstermann and Munzel 2006), we chose to indiscriminately scavenge radicals with TEMPOL and facilitate their ultimate conversion to H_2O via catalase. TEMPOL and catalase incubation partially restored endogenous NO production after exposure to either fine TiO_2 or nano-TiO_2 (Figure 18). Because HE was used as a marker of superoxide (Benov et al. 1998), it is reasonable to expect that a significant portion of the local ROS that was scavenged by TEMPOL was superoxide. The next logical step in this process was to determine the source of elevated superoxide. Superoxide generation can originate from NADPH oxidase activity (Sumimoto 2008), and apocynin has been shown to inhibit this activity (Johnson et al. 2002). In our experiments, apocynin incubation partially restored endogenous NO production after exposure to either fine TiO_2 or nano-TiO_2 (Figure 18). MPO is also capable of reducing bioavailable NO via generation of reactive substrate radicals (Eiserich et al. 2002) or chlorination of L-arginine (Zhang et al. 2001b). Incubation with the MPO inhibitor ABAH also partially restored endogenous NO production after exposure to either fine TiO_2 or nano-TiO_2 (Figure 18). Simultaneous incubation with ABAH, TEMPOL, and catalase did not produce a greater restoration of NO production (data not shown). This observation suggests that the majority of MPO-dependent microvascular dysfunction that follows PM exposure is due to radical generation rather than to decreasing NOS substrate (L-arginine). The ultimate test of physiologic relevance in this regard is whether these ROS scavengers and inhibitors are capable of restoring normal microvascular function after PM exposure. Indeed, incubation of the spinotrapezius muscle with each agent (TEMPOL and catalase, apocynin, ABAH) partially restores arteriolar endothelial dilation in rats exposed to either fine TiO_2 or nano-TiO_2 (Figure 19).

The ETP assay was utilized in the current studies because of the critical role thrombin plays in blood clotting. Thrombin catalyzes the conversion of fibrinogen, which circulates in the blood in a soluble form, to a fibrin clot. The ETP assay estimates the ability of plasma to generate thrombin and has clinical relevance in terms of determining the risk of clot formation (Baglin 2005). For example, individuals with certain diseases form clots because of excess thrombin generation. Taken together with the microvascular reactivity effects of PM exposure, the potential for a significant cardiovascular event is obvious. Differences in other important clotting proteins, including fibrinogen and vWF, were also determined between exposed and filtered air–exposed animals. We found variable changes in coagulation parameters for rats exposed to fine and nano-TiO_2 particles. The most consistent of these changes were seen when ETP was measured in rats exposed to the 8- to 10-μg doses of fine and nano-TiO_2, respectively. Those results suggest that these exposures favor increased thrombin generation, which has been associated with an increased ability to form clots (Tappenden et al. 2007). Other variable changes were seen for fibrinogen, which has been shown through clinical, experimental, and epidemiologic studies to be associated with an increased risk of clotting (Doutremepuich et al. 1998). No dose–response relationships were seen for any of the coagulation parameters studied. Differences in fibrinogen levels that were seen in some test animals as detected by Luminex assay (Table 7) could not be confirmed in experiments with separate animals with an ELISA. This could be explained by either differences in animal responsiveness to PM exposure between groups or by differences in the dynamic range of the fibrinogen measurement technique. Therefore, these results must be interpreted with caution because the limitations of measuring plasma fibrinogen with available assays are considerable.

Previous studies of blood coagulation parameters in rats exposed to ambient PM have had similar difficulties demonstrating consistent exposure-related effects (Nadziejko et al. 2002). As in our studies, several significant differences in clotting parameters have been described; however, these changes cannot be clearly labeled as adverse effects. The variable increases observed in our studies in clotting proteins that typically increase in concentration during inflammatory reactions, such as vWF and fibrinogen, have been described in other animal models after the short-term inhalation of ultrafine carbon black particles (Gilmour et al. 2004). It is unclear if these results translate to the human clotting system because all studies performed to date have utilized healthy rats. Humans who are exposed to particles through inhalation are in various states of health and may already have risk factors for clotting abnormalities; it is unclear how these individuals will respond to short- or long-term inhalation exposure.

The general mechanism that was tested by the collective group of experiments in this study is that the systemic inflammation that follows pulmonary particle exposure exerts a systemic microvascular effect. Given that we have documented pulmonary inflammation (Figures 6, 7, and 20) and systemic venular leukocyte adhesion and rolling after PM exposure (Nurkiewicz et al. 2004, 2006), it is reasonable to speculate that leukocytes are mediating these remote effects to some degree. In preliminary experiments,

we tested the notion that decreasing circulating leukocytes may decrease the severity of PM exposure. To this end, we pretreated rats with cyclophosphamide, exposed them to PM, and then evaluated endothelium-dependent arteriolar dilation. Although it was clear that this treatment decreased circulating leukocytes (Figure 23) and ameliorated the effects of pulmonary particle exposure on the microvascular system (Figure 24), it was unclear if the cyclophosphamide pretreatment had an effect on other circulating or resident cells. Future studies must be performed to address this issue.

Based on our results, normal microvascular function could not be completely restored by blocking or manipulating inflammatory mechanisms. Therefore, it is likely that pulmonary particle exposure also elicits systemic microvascular effects through noninflammatory pathways. In our final experiments, the role of sympathetic nerve activity was evaluated after particle exposure. In these experiments, TTX was used to locally block fast Na^+ channel activity in the spinotrapezius muscle. The result of these experiments was that TTX exposure partially restores endothelium-dependent arteriolar dilation in rats exposed to PM. This strongly suggests that pulmonary particle exposure perturbs the influence of autonomic nerve activity on microvascular function. Indeed, such a perturbation in sympathetic nerve activity is consistent with other studies that indicate more generally that autonomic activity (as characterized by heart-rate variability and baroreceptor responses) is affected by pulmonary particle exposure (Dockery 2001; Pope et al. 2004; Bartoli et al. 2009). The TTX experiments were also preliminary experiments that were performed because the opportunity to do so developed in the course of the funding period. As with cyclophosphamide, limitations with TTX use exist. Most notably, and despite the fact that TTX incubation did not significantly alter resting tone, the effect of TTX on filtered air–exposed animals must be established. Furthermore, additional TTX concentrations should be used to more clearly characterize its effects on arteriolar function. Finally, the use of adrenergic antagonists and agonists in a similar regard would produce further clarity in regards to the influence of sympathetic nerve activity on microvascular function after pulmonary particle exposure.

CONCLUSIONS

The critical findings in the current study are threefold: (1) microvascular NO bioavailability is compromised after nano-PM exposure, (2) nano-PM exposure increases ROS production in the microvascular wall, and (3) the microvascular dysfunction and decrease in NO bioavailability that follow nano-PM exposure are directly linked with discreet oxidant-generating mechanisms. In the time since we first reported that systemic microvascular dysfunction follows PM exposure (Nurkiewicz et al. 2004), nanotechnology products have become common in almost every aspect of daily life, and our attention to ultrafine ambient PM has further developed. It is also apparent now that the benefits of nanotechnology are far-reaching and growing rapidly, but exposure to ambient ultrafine PM remains a very serious risk. Unfortunately, not only are the precise mechanisms through which inhaled PM exerts systemic biologic effects unknown, but the scope of biologic targets and endpoints is also greater when nano-PM or ultrafines are considered. By definition, this latter observation may be largely because of particle size, but surface chemistry of particles must also be accounted for in future studies. Independent of the nomenclature used (nano-PM vs. ultrafine PM), the health concerns are quite similar. That is, are there health effects of inhaled PM and are any such effects related to particle size? In this regard, if nanotechnology is to truly benefit modern society (e.g., nanomedicine), the health effects of particles in this size range must first be established. Similarly, ambient ultrafine PM represents a potential health threat and, if it is to be properly addressed (i.e., we are to mitigate the health effects), we must first understand the health implications of exposure to ambient particles in this size range. Clearly, the two are not interchangeable, but our understanding of their influence on systemic microvascular function must start somewhere.

The nano-PM used in the current study represent engineered and manufactured metal-oxide particles in the nanosize range, and, after pulmonary deposition, they exerted a robust biologic effect. It is unclear at this time what the most appropriate dose metric is for particles in this size range, but it is apparent from our studies and many others that mass does not consistently appear to be the ideal metric. Our consistent observation that pulmonary particle exposure initiates systemic microvascular dysfunction is independent of the appropriate dose metric, and this observation is now extended to nano-PM.

In the absence of the appropriate particle dose metric, this study compared the biologic effects of pulmonary exposure to fine and nano-PM on the basis of their documented ability to cause microvascular dysfunction in a dose-dependent manner based on the mass deposited in the lungs. For many experiments we used EC_{50}. The fact that the fine PM dose was more than six times greater than the ultrafine dose in all experiments highlights the inherent toxic potential of particles in the nano range. Because endogenous NO production, its mechanisms of susceptibility, and the partial restoration of microvascular function after exposure are similar after pulmonary exposure

to either fine or nano-PM, it appears that these two particles exert their biologic effects through similar mechanisms. However, even the discrete mechanisms reported herein arise from very complex backgrounds, and further studies must venture to this level of mechanistic detail. In regards to normal physiology, blocking these mechanisms only partially restored normal microvascular function in PM-exposed animals. Future investigators must bear in mind that it is unlikely that the remaining mechanisms contributing to these effects are related to oxidative stress, NO, or even inflammatory mechanisms. In light of this study, it is readily apparent that sympathetic nerve activity is also altered after PM exposure. Taken together, it may be that the combined alterations in inflammatory and neural activities explain biphasic responses in the cardiovascular system after pulmonary particle exposure.

IMPLICATIONS OF FINDINGS

The question of the most appropriate dose metric to apply to PM exposure has gathered considerable attention and time in many laboratories, institutes, and agencies. A limited number of cardiovascular studies have made logical progress in this regard; however, they often lack direct evaluations of the important vascular endpoints. One implication that can be taken from this report is that particle surface per unit mass may be a more appropriate dose metric than mass when predicting systemic microvascular dysfunction. However, it is important to consider whether different TiO_2 particles (i.e., of different sizes and composition [anatase vs. rutile]) can be used in this context. Although this consideration is extremely valid, it is perhaps more important to indicate that the resultant pulmonary inflammation from exposure to both particle types was not severe. Rather, it was focalized. Therefore, until an ideal test particle is agreed upon, attention must be focused upon the biologic effects of exposure. Amongst these issues, and even if a definitive answer existed, the current study focuses on the lung as the organ of entry. Because particles may cause biologic effects independent of the lungs, as yet undetermined dose metrics may be required in the future to appropriately respond to specific toxicities.

It is also apparent that nano-PM is inherently more toxic in terms of resultant microvascular dysfunction. Although it may appear that both fine PM and nano-PM run parallel courses and have similar continuums when comparing surface area per unit mass and microvascular dysfunction, it should be emphasized that the fine PM aerosol concentrations required to produce a surface area per unit mass similar to that for a nano-PM aerosol are neither realistic nor practical. As such, finite limits exist for fine-PM and nano-PM aerosols, and the surface area produced by nano-PM will always be considerably greater than that for fine PM. Presently, the caveat to this statement is that after PM exposure, differential surface areas exist per given mass, and this may in part predict the resultant microvascular dysfunction.

Another implication of our findings is that NO bioavailability is compromised after PM exposure. Given the ubiquitous nature of NO in biologic systems, this implication is critical in bettering our understanding of the health effects of PM exposure. Our findings are the product of the first direct NO measurements made in the resistance vasculature after PM exposure, and we report that a significant component of vascular reactivity is compromised via NO-dependent pathways. This finding may contribute to prevention and treatment strategies targeting PM exposure. Most notably, if NO bioavailability can be preserved (or restored) by any of the mechanisms reported herein, the impact of the adverse relationship between PM exposure and ischemic events, blood pressure perturbations, and vascular reactivity may be attenuated.

In the current study, we have shown reasonable mechanistic linking between pulmonary particle exposure and systemic biologic effects. These links, although not conclusive, are an essential step in identifying how inhaled particles can contribute to a cardiac event. Identifying specific circulating inflammatory mediators after PM exposure will lead to direct investigations of their effects not only on the resistance vasculature but also on cardiac function. Similarly, the role of neutrophils in PM-dependent microvascular dysfunction is now obvious, and future studies must focus not only on the downstream targets of active neutrophils but also on determining what factors lead to their activation during a response to particle exposure. Lastly, the role of nerves in the systemic microvascular dysfunction that follows PM exposure must be aggressively investigated. Because disturbances in cardiac function are obvious after PM exposure, it is reasonable to expect that neural mechanisms are also contributing to microvascular dysfunction. Indeed, we discovered a considerable amount of dysfunction was associated with sympathetic activity, and future studies must focus on this aspect.

DISCLAIMERS

The findings and conclusions in this report are those of the authors and do not necessarily represent the views of the NIOSH.

Coagulation studies were supported by the Environmental Protection Agency (EPA #R832843, to P.L.P.).

ACKNOWLEDGMENTS

The authors thank Caroll McBride and Kimberly Wix tremendously for their expert technical assistance throughout this study, Syamala Jagannathan for her assistance with the coagulation studies, Victor Robinson for his assistance with the cyclophosphamide studies, and Lori Battelli and Sherri Friend for their assistance with the nitrotyrosine and pulmonary histology studies.

REFERENCES

Abu-Soud HM, Hazen SL. 2000. Nitric oxide is a physiological substrate for mammalian peroxidases. J Biol Chem 275:37524–37532.

Bagate K, Meiring JJ, Cassee FR, Borm PJ. 2004a. The effect of particulate matter on resistance and conductance vessels in the rat. Inhal Toxicol 16:431–436.

Bagate K, Meiring JJ, Gerlofs-Nijland ME, Vincent R, Cassee FR, Borm PJ. 2004b. Vascular effects of ambient particulate matter instillation in spontaneous hypertensive rats. Toxicol Appl Pharmacol 197:29–39.

Baglin T. 2005. The measurement and application of thrombin generation. Br J Haematol 130:653–661.

Baldus S, Eiserich JP, Brennan ML, Jackson RM, Alexander CB, Freeman BA. 2002. Spatial mapping of pulmonary and vascular nitrotyrosine reveals the pivotal role of myeloperoxidase as a catalyst for tyrosine nitration in inflammatory diseases. Free Radic Biol Med 33:1010–1019.

Baldus S, Eiserich JP, Mani A, Castro L, Figueroa M, Chumley P, Ma W, Tousson A, White CR, Bullard DC, Brennan ML, Lusis AJ, Moore KP, Freeman BA. 2001. Endothelial transcytosis of myeloperoxidase confers specificity to vascular ECM proteins as targets of tyrosine nitration. J Clin Invest 108:1759–1770.

Bartoli CR, Wellenius GA, Diaz EA, Lawrence J, Coull BA, Akiyama I, Lee LM, Okabe K, Verrier RL, Godleski JJ. 2009. Mechanisms of inhaled fine particulate air pollution-induced arterial blood pressure changes. Environ Health Perspect 117:361–366.

Bates DV, Fish BR, Hatch TF, Mercer TT, Morrow PE. 1966. Deposition and retention models for internal dosimetry of the human respiratory tract. Task group on lung dynamics. Health Phys 12:173–207.

Baudry N, Rasetti C, Vicaut E. 1996. Differences between cytokine effects in the microcirculation of the rat. Am J Physiol 271:H1186–H1192.

Beckman JS. 1996. Oxidative damage and tyrosine nitration from peroxynitrite. Chem Res Toxicol 9:836–844.

Beckman S, Koppenol WH. 1996. Nitric oxide, superoxide, and peroxynitrite: The good, the bad, and ugly. Am J Physiol 271:C1424–C1437.

Benov L, Sztejnberg L, Fridovich I. 1998. Critical evaluation of the use of hydroethidine as a measure of superoxide anion radical. Free Radic Biol Med 25:826–831.

Bindokas VP, Jordan J, Lee CC, Miller RJ. 1996. Superoxide production in rat hippocampal neurons: Selective imaging with hydroethidine. J Neurosci 16:1324–1336.

Boegehold MA. 1993. Effect of dietary salt on arteriolar nitric oxide in striated muscle of normotensive rats. Am J Physiol 264:H1810–H1816.

Boegehold MA, Bohlen HG. 1988. Arteriolar diameter and tissue oxygen tension during muscle contraction in hypertensive rats. Hypertension 12:184–191.

Brain JD, Knudson DE, Sorokin SP, Davis MA. 1976. Pulmonary distribution of particles given by intratracheal instillation or by aerosol inhalation. Environ Res 11:13–33.

Brian JE Jr, Faraci FM. 1998. Tumor necrosis factor-alpha-induced dilatation of cerebral arterioles. Stroke 29:509–515.

Brody AR, Bonner JC. 1991. Platelet-derived growth factor produced by pulmonary cells. Chest 99:50S–52S.

Brody AR, Bonner JC, Overby LH, Badgett A, Kalter V, Kumar RK, Bennett RA. 1992. Interstitial pulmonary macrophages produce platelet-derived growth factor that stimulates rat lung fibroblast proliferation in vitro. J Leukoc Biol 51:640–648.

Brook RD, Brook JR, Urch B, Vincent R, Rajagopalan S, Silverman F. 2002. Inhalation of fine particulate air pollution and ozone causes acute arterial vasoconstriction in healthy adults. Circulation 105:1534–1536.

Brook RD, Franklin B, Cascio W, Hong Y, Howard G, Lipsett M, Luepker R, Mittleman M, Samet J, Smith SC Jr, Tager I. 2004. Air pollution and cardiovascular disease: A statement for healthcare professionals from the Expert Panel on Population and Prevention Science of the American Heart Association. Circulation 109:2655–2671.

Brunauer S, Emmett PH, Teller E. 1938. Adsorption of gases in multimolecular layers. J Am Chem Soc 60:309–319.

Burnett RT, Smith-Doiron M, Stieb D, Cakmak S, Brook JR. 1999. Effects of particulate and gaseous air pollution on cardiorespiratory hospitalizations. Arch Environ Health 54:130–139.

Butler AR, Megson IL. 2002. Non-heme iron nitrosyls in biology. Chem Rev 102:1155–1166.

Campen MJ, Babu NS, Helms GA, Pett S, Wernly J, Mehran R, McDonald JD. 2005. Nonparticulate components of diesel exhaust promote constriction in coronary arteries from apoE$^{-/-}$ mice. Toxicol Sci 88:95–102.

Carreras MC, Riobo NA, Pargament GA, Boveris A, Poderoso JJ. 1997. Effects of respiratory burst inhibitors on nitric oxide production by human neutrophils. Free Radic Res 26:325–334.

Carter JD, Ghio AJ, Samet JM, Devlin RB. 1997. Cytokine production by human airway epithelial cells after exposure to an air pollution particle is metal-dependent. Toxicol Appl Pharmacol 146:180–188.

Castranova V, Robinson VA, DeLong DS, Mull J, Frazer DG. 1988. Pulmonary response of guinea pigs to inhalation of cotton dust: Effect of depletion of peripheral leukocytes. Proceedings of Endotoxin Inhalation Workshop, pp. 92–95. National Cotton Council, Memphis, TN.

Chen BT, Frazer DG, Stone S, Schwegler-Berry D, Cumpston J, McKinney W, Linsley W, Frazer A, Donlin M, Vandestouwe K, Castranova V, Nurkiewicz TR. 2006a. Development of a small inhalation system for rodent exposure to fine and ultrafine titanium dioxide aerosols. Proceedings of the 7th International Aerosol Conference, pp. 858–859. September 10–15, 2006. American Association for Aerosol Research, St. Paul, MN.

Chen HW, Su SF, Chien CT, Lin WH, Yu SL, Chou CC, Chen JJ, Yang PC. 2006b. Titanium dioxide nanoparticles induce emphysema-like lung injury in mice. FASEB J 20: 2393–2395.

Cheng YW, Kang JJ. 1999. Inhibition of agonist-induced vasocontraction and impairment of endothelium-dependent vasorelaxation by extract of motorcycle exhaust particles in vitro. J Toxicol Environ Health A 57:75–87.

Costa DL, Dreher KL. 1997. Bioavailable transition metals in particulate matter mediate cardiopulmonary injury in healthy and compromised animal models. Environ Health Perspect 105 Suppl 5:1053–1060.

Courtois A, Andujar P, Ladeiro Y, Baudrimont I, Delannoy E, Leblais V, Begueret H, Galland MA, Brochard P, Marano F, Marthan R, Muller B. 2008. Impairment of NO-dependent relaxation in intralobar pulmonary arteries: Comparison of urban particulate matter and manufactured nanoparticles. Environ Health Perspect 116:1294–1299.

Davies IR, Zhang X. 2008. Nitric oxide selective electrodes. Methods Enzymol 436:63–95.

de Haar C, Hassing I, Bol M, Bleumink R, Pieters R. 2006. Ultrafine but not fine particulate matter causes airway inflammation and allergic airway sensitization to co-administered antigen in mice. Clin Exp Allergy 36: 1469–1479.

Dockery DW. 2001. Epidemiologic evidence of cardiovascular effects of particulate air pollution. Environ Health Perspect 109 Suppl 4:483–486.

Donaldson K, Stone V, Seaton A, MacNee W. 2001. Ambient particle inhalation and the cardiovascular system: Potential mechanisms. Environ Health Perspect 109 Suppl 4:523–527.

Donaldson K, Tran L, Jimenez LA, Duffin R, Newby DE, Mills N, MacNee W, Stone V. 2005. Combustion-derived nanoparticles: A review of their toxicology following inhalation exposure. Part Fibre Toxicol 2:10.

Doutremepuich F, Aguejouf O, Belougne-Malfatti E, Doutremepuich C. 1998. Fibrinogen as a factor of thrombosis: Experimental study. Thromb Res 90:57–64.

Dreher KL, Jaskot RH, Lehmann JR, Richards JH, McGee JK, Ghio AJ, Costa DL. 1997. Soluble transition metals mediate residual oil fly ash induced acute lung injury. J Toxicol Environ Health 50:285–305.

Driscoll KE, Hassenbein DG, Carter J, Poynter J, Asquith TN, Grant RA, Whitten J, Purdon MP, Takigiku R. 1993. Macrophage inflammatory proteins 1 and 2: Expression by rat alveolar macrophages, fibroblasts, and epithelial cells and in rat lung after mineral dust exposure. Am J Respir Cell Mol Biol 8:311–318.

Driscoll KE, Maurer JK. 1991. Cytokine and growth factor release by alveolar macrophages: Potential biomarkers of pulmonary toxicity. Toxicol Pathol 19:398–405.

Driscoll KE, Maurer JK, Higgins J, Poynter J. 1995. Alveolar macrophage cytokine and growth factor production in a rat model of crocidolite-induced pulmonary inflammation and fibrosis. J Toxicol Environ Health 46:155–169.

Eiserich JP, Baldus S, Brennan ML, Ma W, Zhang C, Tousson A, Castro L, Lusis AJ, Nauseef WM, White CR, Freeman BA. 2002. Myeloperoxidase, a leukocyte-derived vascular NO oxidase. Science 296:2391–2394.

Eiserich JP, Hristova M, Cross CE, Jones AD, Freeman BA, Halliwell B, van der Vliet A. 1998. Formation of nitric

oxide-derived inflammatory oxidants by myeloperoxidase in neutrophils. Nature 391:393–397.

Fairley D. 1990. The relationship of daily mortality to suspended particulates in Santa Clara County, 1980–1986. Environ Health Perspect 89:159–168.

Fantone JC, Ward PA. 1982. Role of oxygen-derived free radicals and metabolites in leukocyte-dependent inflammatory reactions. Am J Pathol 107:395–418.

Fields LE, Burt VL, Cutler JA, Hughes J, Roccella EJ, Sorlie P. 2004. The burden of adult hypertension in the United States 1999 to 2000. A rising tide. Hypertension 44: 398–404.

Forstermann U, Munzel T. 2006. Endothelial nitric oxide synthase in vascular disease: From marvel to menace. Circulation 113:1708–1714.

Frisbee JC. 2003. Impaired skeletal muscle perfusion in obese Zucker rats. Am J Physiol Regul Integr Comp Physiol 285:R1124–R1134.

Fujii T, Hayashi S, Hogg JC, Vincent R, van Eeden SF. 2001. Particulate matter induces cytokine expression in human bronchial epithelial cells. Am J Respir Cell Mol Biol 25:265–271.

Garg R, Kumbkarni Y, Aljada A, Mohanty P, Ghanim H, Hamouda W, Dandona P. 2000. Troglitazone reduces reactive oxygen species generation by leukocytes and lipid peroxidation and improves flow-mediated vasodilatation in obese subjects. Hypertension 36:430–435.

Gaut JP, Byun J, Tran HD, Lauber WM, Carroll JA, Hotchkiss RS, Belaaouaj A, Heinecke JW. 2002. Myeloperoxidase produces nitrating oxidants in vivo. J Clin Invest 109: 1311–1319.

Geiser M, Rothen-Rutishauser B, Kapp N, Schürch S, Kreyling W, Schulz H, Semmler M, Im Hof V, Heyder J, Gehr P. 2005. Ultrafine particles cross cellular membranes by nonphagocytic mechanisms in lungs and in cultured cells. Environ Health Perspect 113:1555–1560.

Gilmour PS, Brown DM, Lindsay TG, Beswick PH, MacNee W, Donaldson K. 1996. Adverse health effects of PM_{10} particles: Involvement of iron in generation of hydroxy radical. Occup Environ Med 53:817–822.

Gilmour PS, Ziesenis A, Morrison ER, Vickers MA, Drost EM, Ford I, Karg E, Mossa C, Schroeppel A, Ferron GA, Heyder J, Greaves M, MacNee W, Donaldson K. 2004. Pulmonary and systemic effects of short-term inhalation exposure to ultrafine carbon black particles. Toxicol Appl Pharmacol 195:35–44.

Gluais P, Paysant J, Badier-Commander C, Verbeuren T, Vanhoutte PM, Feletou M. 2006. In SHR aorta, calcium ionophore A-23187 releases prostacyclin and thromboxane A2 as endothelium-derived contracting factors. Am J Physiol Heart Circ Physiol 291:H2255–H2264.

Godleski JJ, Verrier RL, Koutrakis P, Catalano P, Coull B, Reinisch U, Lovett EG, Lawrence J, Murthy GG, Wolfson JM, Clarke RW, Nearing BD, Killingsworth C. 2000. Mechanisms of Morbidity and Mortality from Exposure to Ambient Air Particles. Research Report 91. Health Effects Institute, Cambridge, MA.

Goldberg MS, Bailar JC III, Burnett RT, Brook JR, Tamblyn R, Bonvalot Y, Ernst P, Flegel KM, Singh RK, Valois MF. 2000. Identifying Subgroups of the General Population That May Be Susceptible to Short-Term Increases in Particulate Air Pollution: A Time-Series Study in Montreal, Quebec. Research Report 97. Health Effects Institute, Cambridge, MA.

Goldberg MS, Burnett RT, Bailar JC III, Tamblyn R, Ernst P, Flegel K, Brook J, Bonvalot Y, Singh R, Valois MF, Vincent R. 2001. Identification of persons with cardiorespiratory conditions who are at risk of dying from the acute effects of ambient air particles. Environ Health Perspect 109 Suppl 4:487–494.

Grassian VH, O'Shaughnessy PT, Adamcakova-Dodd A, Pettibone JM, Thorne PS. 2007. Inhalation exposure study of titanium dioxide nanoparticles with a primary particle size of 2 to 5 nm. Environ Health Perspect 115:397–402.

Gryglewski RJ, Palmer RM, Moncada S. 1986. Superoxide anion is involved in the breakdown of endothelium-derived vascular relaxing factor. Nature 320:454–456.

Gwinn MR, Vallyathan V. 2006. Nanoparticles: Health effects—pros and cons. Environ Health Perspect 114: 1818–1825.

Hampton MB, Kettle AJ, Winterbourn CC. 1996. Involvement of superoxide and myeloperoxidase in oxygen-dependent killing of *Staphylococcus aureus* by neutrophils. Infect Immun 64:3512–3517.

Hansen CS, Sheykhzade M, Moller P, Folkmann JK, Amtorp O, Jonassen T, Loft S. 2007. Diesel exhaust particles induce endothelial dysfunction in $apoE^{-/-}$ mice. Toxicol Appl Pharmacol 219:24–32.

Hazen SL, Zhang R, Shen Z, Wu W, Podrez EA, MacPherson JC, Schmitt D, Mitra SN, Mukhopadhyay C, Chen Y, Cohen PA, Hoff HF, Abu-Soud HM. 1999. Formation of nitric oxide-derived oxidants by myeloperoxidase in monocytes:

Pathways for monocyte-mediated protein nitration and lipid peroxidation in vivo. Circ Res 85:950–958.

Hedley AA, Ogden CL, Johnson CL, Carroll MD, Curtin LR, Flegal KM. 2004. Prevalence of overweight and obesity among US children, adolescents, and adults, 1999–2002. JAMA 291:2847–2850.

Huang A, Koller A. 1996. Both nitric oxide and prostaglandin-mediated responses are impaired in skeletal muscle arterioles of hypertensive rats. J Hypertens 14: 887–895.

Huang A, Sun D, Koller A, Kaley G. 2000. 17beta-estradiol restores endothelial nitric oxide release to shear stress in arterioles of male hypertensive rats. Circulation 101: 94–100.

Ibald-Mulli A, Stieber J, Wichmann HE, Koenig W, Peters A. 2001. Effects of air pollution on blood pressure: A population-based approach. Am J Public Health 571–577.

Ignarro LJ, Napoli C, Loscalzo J. 2002. Nitric oxide donors and cardiovascular agents modulating the bioactivity of nitric oxide: An overview. Circ Res 90:21–28.

Jimenez LA, Thompson J, Brown DA, Rahman I, Antonicelli F, Duffin R, Drost EM, Hay RT, Donaldson K, MacNee W. 2000. Activation of NF-κB by PM_{10} occurs via an iron-mediated mechanism in the absence of IκB degradation. Toxicol Appl Pharmacol 166:101–110.

Johnson DK, Schillinger KJ, Kwait DM, Hughes CV, McNamara EJ, Ishmael F, O'Donnell RW, Chang MM, Hogg MG, Dordick JS, Santhanam L, Ziegler LM, Holland JA. 2002. Inhibition of NADPH oxidase activation in endothelial cells by ortho-methoxy-substituted catechols. Endothelium 9:191–203.

Kadiiska MB, Mason RP, Dreher KL, Costa DL, Ghio AJ. 1997. In vivo evidence of free radical formation in the rat lung after exposure to an emission source air pollution particle. Chem Res Toxicol 10:1104–1108.

Kang YJ, Li Y, Zhou Z, Roberts AM, Cai L, Myers SR, Wang L, Schuchke DA. 2002. Elevation of serum endothelins and cardiotoxicity induced by particulate matter ($PM_{2.5}$) in rats with acute myocardial infarction. Cardiovasc Toxicol 2:253–261.

Klebanoff SJ. 1991. Myeloperoxidase: Occurrence and Biological Function. In: Peroxidases in Chemistry and Biology (Everse J, Everse KE, Grisham MB, eds). CRC Press, Boca Raton, FL.

Knaapen AM, den Hartog GJ, Bast A, Borm PJ. 2001. Ambient particulate matter induces relaxation of rat aortic rings in vitro. Hum Exp Toxicol 20:259–265.

Knuckles TL, Lund AK, Lucas SN, Campen MJ. 2008. Diesel exhaust exposure enhances venoconstriction via uncoupling of eNOS. Toxicol Appl Pharmacol 230:346–351.

Kodavanti UP, Schladweiler MC, Ledbetter AD, Hauser R, Christiani DC, McGee J, Richards JR, Costa DL. 2002. Temporal association between pulmonary and systemic effects of particulate matter in healthy and cardiovascular compromised rats. J Toxicol Environ Health A 65:1545–1569.

Kohen R, Nyska A. 2002. Oxidation of biological systems: Oxidative stress phenomena, antioxidants, redox reactions, and methods for their quantification. Toxicol Pathol 30: 620–650.

Lenda DM, Sauls BA, Boegehold MA. 2000. Reactive oxygen species may contribute to reduced endothelium-dependent dilation in rats fed high salt. Am J Physiol Heart Circ Physiol 279:H7–H14.

Linderman JR, Boegehold MA. 1998. Modulation of arteriolar sympathetic constriction by local nitric oxide: Onset during rapid juvenile growth. Microvasc Res 56:192–202.

Matsuki T, Beach JM, Klindt RL, Duling BR. 1993. Modification of vascular reactivity by alteration of intimal permeability: Effect of TNF-alpha. Am J Physiol 264: H1847–H1853.

Matsuki T, Duling BR. 2000. TNF-alpha modulates arteriolar reactivity secondary to a change in intimal permeability. Microcirculation 7:411–418.

Mayhan WG. 2002. Cellular mechanisms by which tumor necrosis factor-alpha produces disruption of the blood-brain barrier. Brain Res 927:144–152.

Maynard AD, Aitken RJ, Butz T, Colvin V, Donaldson K, Oberdorster G, Philbert MA, Ryan J, Seaton A, Stone V, Tinkle SS, Tran L, Walker NJ, Warheit DB. 2006. Safe handling of nanotechnology. Nature 444:267–269.

Metzger KB, Tolbert PE, Klein M, Peel JL, Flanders WD, Todd K, Mulholland JA, Ryan PB, Frumkin H. 2004. Ambient air pollution and cardiovascular emergency department visits. Epidemiology 15:46–56.

Mills NL, Tornqvist H, Gonzalez MC, Vink E, Robinson SD, Soderberg S, Boon NA, Donaldson K, Sandstrom T, Blomberg A, Newby DE. 2007. Ischemic and thrombotic effects of dilute diesel-exhaust inhalation in men with coronary heart disease. N Engl J Med 357:1075–1082.

Mills NL, Tornqvist H, Robinson SD, Gonzalez M, Darnley K, MacNee W, Boon NA, Donaldson K, Blomberg A, Sandstrom T, Newby DE. 2005. Diesel exhaust inhalation causes vascular dysfunction and impaired endogenous fibrinolysis. Circulation 112:3930–3936.

Miranda KM, Katori T, Torres de Holding CL, Thomas L, Ridnour LA, McLendon WJ, Cologna SM, Dutton AS, Champion HC, Mancardi D, Tocchetti CG, Saavedra JE, Keefer LK, Houk KN, Fukuto JM. Kass DA, Paolocci N, Wink DA. 2005. Comparison of the NO and HNO donating properties of diazeniumdiolates: Primary amine adducts release HNO in Vivo. J Med Chem 48:8220–8228.

Morgan AR, Evans DH, Lee JS, Pulleyblank DE. 1979. Review: Ethidium fluorescence assay. Part II. Enzymatic studies and DNA-protein interactions. Nucleic Acids Res 7:571–594.

Morris RD. 2001. Airborne particulates and hospital admissions for cardiovascular disease: A quantitative review of the evidence. Environ Health Perspect 109 Suppl 4: 495–500.

Nadziejko C, Fang K, Chen LC, Cohen B, Karpatkin M, Nadas A. 2002. Effect of concentrated ambient particulate matter on blood coagulation parameters in rats. Research Report 111. Health Effects Institute, Boston, MA.

National Research Council. 1998. The Committee's 10 highest-priority research recommendations. In: Research Priorities for Airborne Particulate Matter: I. Immediate Priorities and a Long-Range Research Portfolio. National Academy Press, Washington, D.C.

Nurkiewicz TR, Boegehold MA. 1998. High dietary salt alters arteriolar myogenic responsiveness in normotensive and hypertensive rats. Am J Physiol 275:H2095–H2104.

Nurkiewicz TR, Boegehold MA. 2000. Reinforcement of arteriolar myogenic activity by endogenous ANG II: Susceptibility to dietary salt. Am J Physiol Heart Circ Physiol 279:H269–H278.

Nurkiewicz TR, Boegehold MA. 2004. Calcium-independent release of endothelial nitric oxide: Onset during rapid juvenile growth. Microcirculation 11:453–462.

Nurkiewicz TR, Porter DW, Barger M, Castranova V, Boegehold MA. 2004. Particulate matter exposure impairs systemic microvascular endothelium-dependent dilation. Environ Health Perspect 112:1299–1306.

Nurkiewicz TR, Porter DW, Barger M, Millecchia L, Rao KM, Marvar PJ, Hubbs AF, Castranova V, Boegehold MA. 2006. Systemic microvascular dysfunction and inflammation after pulmonary particulate matter exposure. Environ Health Perspect 114:412–419.

Nurkiewicz TR, Porter DW, Hubbs AF, Cumpston JL, Chen BT, Frazer DG, Castranova V. 2008. Nanoparticle inhalation augments particle-dependent systemic microvascular dysfunction. Part Fibre Toxicol 5:1–12.

Nurkiewicz TR, Porter DW, Hubbs AF, Stone S, Chen BT, Frazer DG, Boegehold MA, Castranova V. 2009. Pulmonary nanoparticle exposure disrupts systemic microvascular nitric oxide signaling. Toxicol Sci 110:191–203.

Oberdorster G. 1996. Significance of particle parameters in the evaluation of exposure-dose-response relationships of inhaled particles. Inhal Toxicol 8 Suppl:73–89.

Oberdorster G, Oberdorster E, Oberdorster J. 2005. Nanotoxicology: An emerging discipline evolving from studies of ultrafine particles. Environ Health Perspect 113: 823–839.

Oberdorster G, Sharp Z, Atudorei V, Elder A, Gelein R, Kreyling W, Cox C. 2004. Translocation of inhaled ultrafine particles to the brain. Inhal Toxicol 16:437–445.

Peters A, Dockery DW, Muller JE, Mittleman MA. 2001. Increased particulate air pollution and the triggering of myocardial infarction. Circulation 103:2810–2815.

Podrez EA, Abu-Soud HM, Hazen SL. 2000. Myeloperoxidase-generated oxidants and atherosclerosis. Free Radic Biol Med 28:1717–1725.

Pope CA III, Hansen ML, Long RW, Nielsen KR, Eatough NL, Wilson WE, Eatough DJ. 2004. Ambient particulate air pollution, heart rate variability, and blood markers of inflammation in a panel of elderly subjects. Environ Health Perspect 112:339–345.

Porter DW, Barger M, Robinson VA, Leonard SS, Landsittel D, Castranova V. 2002. Comparison of low doses of aged and freshly fractured silica on pulmonary inflammation and damage in the rat. Toxicology 175:63–71.

Porter DW, Ramsey D, Hubbs AF, Battelli L, Ma J, Barger M, Landsittel D, Robinson VA, McLaurin J, Khan A, Jones W, Teass A, Castranova V. 2001. Time course of pulmonary response of rats to inhalation of crystalline silica: Histological results and biochemical indices of damage, lipidosis, and fibrosis. J Environ Pathol Toxicol Oncol 20 Suppl 1:1–14.

Rahman I, MacNee W. 1998. Role of transcription factors in inflammatory lung diseases. Thorax 53:601–612.

Riediker M, Cascio WE, Griggs TR, Herbst MC, Bromberg PA, Neas L, Williams RW, Devlin RB. 2004. Particulate matter exposure in cars is associated with cardiovascular effects in healthy young men. Am J Respir Crit Care Med 169:934–940.

Roberts JR, Taylor MD, Castranova V, Clarke RW, Antonini JM. 2004. Soluble metals associated with residual oil fly ash increase morbidity and lung injury after bacterial infection in rats. J Toxicol Environ Health A 67:251–263.

Rubanyi GM, Vanhoutte PM. 1986. Superoxide anions and hyperoxia inactivate endothelium-derived relaxing factor. Am J Physiol 250:H822–H827.

Rundell KW, Hoffman JR, Caviston R, Bulbulian R, Hollenbach AM. 2007. Inhalation of ultrafine and fine particulate matter disrupts systemic vascular function. Inhal Toxicol 19:133–140.

Sager TM, Kommineni C, Castranova V. 2008. Pulmonary response to intratracheal instillation of ultrafine versus fine titanium dioxide: Role of particle surface area. Part Fibre Toxicol 5:17.

Salom JB, Barbery D, Centeno JM, Orti M, Torregrosa G, Alborch E. 1998. Relaxant effects of sodium nitroprusside and NONOates in rabbit basilar artery. Pharmacology 57:79–87.

Salom JB, Barbery D, Centeno JM, Orti M, Torregrosa G, Alborch E. 1999. Comparative relaxant effects of the NO donors sodium nitroprusside, DEA/NO and SPER/NO in rabbit carotid arteries. Gen Pharmacol 32:75–79.

Salvi S, Blomberg A, Rudell B, Kelly F, Sandstrom T, Holgate ST, Frew A. 1999. Acute inflammatory responses in the airways and peripheral blood after short-term exposure to diesel exhaust in healthy human volunteers. Am J Respir Crit Care Med 159:702–709.

Samet JM, Dominici F, Curriero FC, Coursac I, Zeger SL. 2000a. Fine particulate air pollution and mortality in 20 U.S. cities, 1987–1994. N Engl J Med 343:1742–1749.

Samet JM, Zeger SL, Dominici F, Curriero F, Coursac I, Dockery DW, Schwartz J, Zanobetti A. 2000b. The National Morbidity, Mortality, and Air Pollution Study. Part II: Morbidity and Mortality from Air Pollution in the United States. Research Report 94. Health Effects Institute, Cambridge, MA.

Schneider JC, El Kebir D, Chereau C, Lanone S, Huang XL, Buys Roessingh AS, Mercier JC, Dall'Ava-Santucci J, Dinh-Xuan AT. 2003. Involvement of Ca^{2+}/calmodulin-dependent protein kinase II in endothelial NO production and endothelium-dependent relaxation. Am J Physiol Heart Circ Physiol 284:H2311–H2319.

Schuhmann K, Romanin C, Baumgartner W, Groschner K. 1997. Intracellular Ca^{2+} inhibits smooth muscle L-type Ca^{2+} channels by activation of protein phosphatase type 2B and by direct interaction with the channel. J Gen Physiol 110:503–513.

Schwartz J, Morris R. 1995. Air pollution and hospital admissions for cardiovascular disease in Detroit, Michigan. Am J Epidemiol 142:23–35.

Shieh KJ, Li M, Lee YH, Sheu SD, Liu YT, Wang YC. 2006. Antibacterial performance of photocatalyst thin film fabricated by defection effect in visible light. Nanomedicine 2:121–126.

Shvedova AA, Sager T, Murray A, Kisin E, Porter DW, Leonard SS, Schwegler-Berry D, Robinson VA, Castranova V. 2007. Critical issues in the evaluation of possible effects resulting from airborne nanoparticles. In: Nanotechnology: Characterization, Dosing and Health Effects (Monteiro-Riviere N and Tran L, eds). Informa Healthcare, Philadelphia, PA.

Stone KC, Mercer RR, Gehr P, Stockstill B, Crapo JD. 1992. Allometric relationships of cell numbers and size in the mammalian lung. Am J Respir Cell Mol Biol 6:235–243.

Sumimoto H. 2008. Structure, regulation and evolution of Nox-family NADPH oxidases that produce reactive oxygen species. FEBS J 275:3249–3277.

Sun D, Meng TT, Loong TH, Hwa TJ. 2004. Removal of natural organic matter from water using a nano-structured photocatalyst coupled with filtration membrane. Water Sci Technol 49:103–110.

Sun Q, Yue P, Ying Z, Cardounel AJ, Brook RD, Devlin R, Hwang JS, Zweier JL, Chen LC, Rajagopalan S. 2008. Air pollution exposure potentiates hypertension through reactive oxygen species-mediated activation of Rho/ROCK. Arterioscler Thromb Vasc Biol 28:1760–1766.

Suwa T, Hogg JC, English D, van Eeden SF. 2000. Interleukin-6 induces demargination of intravascular neutrophils and shortens their transit in marrow. Am J Physiol Heart Circ Physiol 279:H2954–H2960.

Suwa T, Hogg JC, Quinlan KB, Ohgami A, Vincent R, van Eeden SF. 2002. Particulate air pollution induces progression of atherosclerosis. J Am Coll Cardiol 39:935–942.

Tamagawa E, Bai N, Morimoto K, Gray C, Mui T, Yatera K, Zhang X, Xing L, Li Y, Laher I, Sin DD, Man SF, van Eeden

SF. 2008. Particulate matter exposure induces persistent lung inflammation and endothelial dysfunction. Am J Physiol Lung Cell Mol Physiol 295:L79–L85.

Tan WC, Qiu D, Liam BL, Ng TP, Lee SH, van Eeden SF, D'Yachkova Y, Hogg JC. 2000. The human bone marrow response to acute air pollution caused by forest fires. Am J Respir Crit Care Med 161:1213–1217.

Tappenden KA, Gallimore MJ, Evans G, Mackie IJ, Jones DW. 2007. Thrombin generation: A comparison of assays using platelet-poor and -rich plasma and whole blood samples from healthy controls and patients with a history of venous thromboembolism. Br J Haematol 139:106–112.

Terashima T, Wiggs B, English D, Hogg JC, van Eeden SF. 1997. Phagocytosis of small carbon particles (PM_{10}) by alveolar macrophages stimulates the release of polymorphonuclear leukocytes from bone marrow. Am J Respir Crit Care Med 155:1441–1447.

Tuma R, Durán WN, Ley K, eds. 2008. Handbook of Physiology: Microcirculation. Second edition. Academic Press, New York.

Ulrich MM, Alink GM, Kumarathasan P, Vincent R, Boere AJ, Cassee FR. 2002. Health effects and time course of particulate matter on the cardiopulmonary system in rats with lung inflammation. J Toxicol Environ Health A 65: 1571–1595.

United States Census Bureau. 2004. U.S. Interim Projections by Age, Sex, Race, and Hispanic Origin. Available from *www.census.gov/ipc/www/usinterimproj/*.

U.S. Environmental Protection Agency. 2002. Latest Findings on National Air Quality: 2001 Status and Trends. EPA 454/K-02-001. Office of Air Quality Planning and Standards, Research Triangle Park, NC.

Urch B, Silverman F, Corey P, Brook JR, Lukic KZ, Rajagopalan S, Brook RD. 2005. Acute blood pressure responses in healthy adults during controlled air pollution exposures. Environ Health Perspect 113:1052–1055.

van Eeden SF, Hogg JC. 2002. Systemic inflammatory response induced by particulate matter air pollution: The importance of bone-marrow stimulation. J Toxicol Environ Health A 65:1597–1613.

van Eeden SF, Tan WC, Suwa T, Mukae H, Terashima T, Fujii T, Qui D, Vincent R, Hogg JC. 2001. Cytokines involved in the systemic inflammatory response induced by exposure to particulate matter air pollutants (PM_{10}). Am J Respir Crit Care Med 164:826–830.

Vicaut E, Hou X, Payen D, Bousseau A, Tedgui A. 1991. Acute effects of tumor necrosis factor on the microcirculation in rat cremaster muscle. J Clin Invest 87:1537–1540.

Vogt W. 1996. Complement activation by myeloperoxidase products released from stimulated human polymorphonuclear leukocytes. Immunobiology 195:334–346.

von Klot S, Peters A, Aalto P, Bellander T, Berglind N, D'Ippoliti D, Elosua R, Hormann A, Kulmala M, Lanki T, Lowel H, Pekkanen J, Picciotto S, Sunyer J, Forastiere F. 2005. Ambient air pollution is associated with increased risk of hospital cardiac readmissions of myocardial infarction survivors in five European cities. Circulation 112: 3073–3079.

Warheit DB, Borm PJ, Hennes C, Lademann J. 2007. Testing strategies to establish the safety of nanomaterials: Conclusions of an ECETOC workshop. Inhal Toxicol 19: 631–643.

Watkinson WP, Campen MJ, Nolan JP, Costa DL. 2001. Cardiovascular and systemic responses to inhaled pollutants in rodents: Effects of ozone and particulate matter. Environ Health Perspect 109 Suppl 4:539–546.

Wichers LB, Nolan JP, Winsett DW, Ledbetter AD, Kodavanti UP, Schladweiler MC, Costa DL, Watkinson WP. 2004. Effects of instilled combustion-derived particles in spontaneously hypertensive rats. Part I: Cardiovascular responses. Inhal Toxicol 16:391–405.

Winterbourn CC, Vissers MC, Kettle AJ. 2000. Myeloperoxidase. Curr Opin Hematol 7:53–58.

Yeates DB, Mauderly JL. 2001. Inhaled environmental/occupational irritants and allergens: Mechanisms of cardiovascular and systemic responses. Introduction. Environ Health Perspect 109 Suppl 4:479–481.

Yoshioka T, Ichikawa I. 1989. Glomerular dysfunction induced by polymorphonuclear leukocyte-derived reactive oxygen species. Am J Physiol 257:F53–F59.

Zhang C, Patel R, Eiserich JP, Zhou F, Kelpke S, Ma W, Parks DA, Darley-Usmar V, White CR. 2001a. Endothelial dysfunction is induced by proinflammatory oxidant hypochlorous acid. Am J Physiol Heart Circ Physiol 281: H1469–H1475.

Zhang C, Reiter C, Eiserich JP, Boersma B, Parks DA, Beckman JS, Barnes S, Kirk M, Baldus S, Darley-Usmar VM, White CR. 2001b. L-arginine chlorination products inhibit endothelial nitric oxide production. J Biol Chem 276:27159–27165.

Zhang X. 2004. Real time and in vivo monitoring of nitric oxide by electrochemical sensors—from dream to reality. Front Biosci 9:3434–3446.

Zweifach BW. 1974. Quantitative studies of microcirculatory structure and function. I. Analysis of pressure distribution in the terminal vascular bed in cat mesentery. Circ Res 34:843–857.

Zweifach BW. 1991. Vascular resistance. In: The Resistance Vasculature (Bevan JA, Halpern W, Mulvany MJ, eds). Humana Press, Totowa, NJ.

Zweifach BW, Kovalcheck S, De Lano F, Chen P. 1981. Micropressure-flow relationships in a skeletal muscle of spontaneously hypertensive rats. Hypertension 3:601–614.

Zweifach BW, Lipowsky HH. 1977. Quantitative studies of microcirculatory structure and function. III. Microvascular hemodynamics of cat mesentery and rabbit omentum. Circ Res 41:380–390.

Zweifach BW, Lipowsky HH. 1984. Pressure-flow relations in blood and lymph microcirculation. In: Handbook of Physiology. The Cardiovascular System. Microcirculation, Vol 4, pp. 251–308. American Physiological Society, Bethesda, MD.

ABOUT THE AUTHORS

Timothy R. Nurkiewicz, Ph.D., is an associate professor of physiology and pharmacology at the West Virginia University (WVU) School of Medicine, where he is also an active member of the Center for Cardiovascular and Respiratory Sciences (CCRS). Dr. Nurkiewicz also has a joint appoint in the Department of Neurobiology and Anatomy. Dr. Nurkiewicz received his B.S. in exercise and sport science from the Pennsylvania State University in 1990. He received an M.S. in exercise physiology from West Virginia University in 1992. After a rotation at Allegheny Hospital in Pittsburgh, Pennsylvania; Dr. Nurkiewicz earned his Ph.D. in physiology in 1999. He spent 2 years as a postdoctoral fellow at Texas A&M University in the Department of Medical Physiology prior to returning to WVU. Dr. Nurkiewicz's interests in microvascular toxicology fueled his original studies with airborne particles and resulted in the seminal observation that endothelium-dependent dilation is impaired by particulate matter exposure. In 2005, he was awarded the Walter A. Rosenblith New Investigator Award by the HEI. During the execution of this prestigious award, Dr. Nurkiewicz was also recognized by the National Institute of Environmental Health Sciences as an Outstanding New Environmental Scientist. In addition to Dr. Nurkiewicz's academic and research appointments, he serves on the editorial boards of *Nanotoxicology*, *Cardiovascular Toxicology*, *Journal of Toxicology and Environmental Health*, and *Inhalation Toxicology*. Dr. Nurkiewicz is also the president of the cardiovascular toxicology specialty section of the Society of Toxicology, and the director of the WVU Inhalation Exposure Facility.

Dale W. Porter, Ph.D., is a research biologist in the Health Effects Laboratory Division of NIOSH, Morgantown, West Virginia. He is also an adjunct associate professor in the Department of Physiology and Pharmacology at WVU. Dr. Porter received a B.S. in biology from Allegheny College, Meadville, Pennsylvania, in 1986. He received a M.S. in agricultural biochemistry in 1988 and a Ph.D. in genetics and developmental biology in 1992, both from WVU. Dr. Porter received postdoctoral training as a National Research Council Research Associate and National Cancer Institute Intramural Research Fellow from 1992 to 1996. In 1996, Dr. Porter received a research staff position at NIOSH in Morgantown, West Virginia. Dr. Porter's research interests have concentrated on pulmonary toxicology and occupational lung disease. He has been a member of the Nanotoxicology Program in NIOSH since its inception in 2005. He has been an author or coauthor on 52 manuscripts and six book chapters.

Ann F. Hubbs, D.V.M., Ph.D., D.A.C.V.P., is a veterinary pathologist. She received her D.V.M. in 1981 from Texas A&M University, an M.S. from Purdue in 1986, and a Ph.D. from Colorado State University in 1989. In addition, she practiced veterinary medicine from 1981 to 1983, received a certificate of residency in veterinary pathology from Colorado State University in 1988, is board eligible in laboratory animal medicine, and became a diplomate of the American College of Veterinary Pathologists in 1991. In 1992, she joined NIOSH, Centers for Disease Control and Prevention (CDC) as a Toxicologist in the Division of Respiratory Disease Studies and was transferred to the Health Effects Laboratory Division in 1996, where she is a veterinary medical officer. She is also an adjunct associate professor in the Division of Animal and Veterinary Sciences and the Genetics and Developmental Biology Program at WVU. She has received numerous awards for her scientific publications and for assisting in the response to national emergencies, such as the anthrax events of 2001. She is the author of more than 100 peer-reviewed papers and abstracts, principally dealing with the toxicologic pathology of workplace agents.

Samuel Stone has a B.S. degree in electrical engineering from WVU. He has been employed by the NIOSH for over 10 years as a research engineer. Prior to working with

NIOSH, he was an engineer and technician for the Naval Surface Warfare Center for 10 years. He has been involved with many inhalation studies, including asphalt, welding, ozone, and carbon nanotubes. He has been an author on numerous abstracts and manuscripts associated with these exposures.

Amy M. Moseley has a B.S. degree in chemistry from WVU and is currently completing her M.S. degree in public health from WVU. She has been employed by the NIOSH for over 10 years as a laboratory technician. She has been involved with many inhalation studies including asphalt, welding, ozone, and carbon nanotubes. She has been an author on numerous abstracts and manuscripts associated with these exposures.

Jared L. Cumpston has a B.S. degree in criminal justice from Salem International University. He has been employed by the NIOSH for 5 years as a laboratory technician. He has been involved with many inhalation studies including ultrafine and fine particles, asphalt, welding, ozone, diesel, and single-wall and multi-wall carbon nanotubes. He has been an author on numerous abstracts and manuscripts associated with these exposures.

Adam G. Goodwill is a graduate student in the Department of Physiology and Pharmacology and in the CCRS at the WVU Health Sciences Center. He received his B.S. in molecular biology/biotechnology from Clarion University of Pennsylvania in 2003 and, after several years as a technician, entered into the interdisciplinary biomedical sciences doctoral program at WVU in 2006. He is currently under the mentorship of Jefferson C. Frisbee, Ph.D., studying the negative microvascular outcomes associated with obesity, insulin resistance, and the combined pathologic state of the metabolic syndrome.

Stephanie J. Frisbee, M.Sc., is a research instructor in the Department of Community Medicine (School of Medicine) and the Department of Dental Practice and Rural Health (School of Dentistry) and is a member of the CCRS at the WVU Health Sciences Center. She holds an undergraduate degree in biomedical sciences and a master's degree in consumer policy and affairs (applied economics) from the University of Guelph (Canada), and is currently working toward a Ph.D. in policy analysis in the Department of Political Science at WVU. Ms. Frisbee previously worked at Children's Hospital of Wisconsin where she managed the Outcomes Department and the National Outcomes Center, an analytic group that applied outcomes research and methodologic techniques to assess and improve the quality of care at the hospital and facilitate national, multisite studies and contracted projects. Ms. Frisbee's current research projects include investigating the potential health consequences of perfluorocarbon exposure in children, the cardiovascular and other related consequences of obesity in children, and associations between tobacco control policy and population health.

Peter L. Perrotta, M.D., is an associate professor in the Department of Pathology at WVU and medical director of the Clinical Laboratories at WVU Ruby Memorial Hospital. He obtained a B.S. in chemical engineering from WVU and an M.D. from the Pennsylvania State University, followed by residency training in anatomic and clinical pathology at Yale University. His research interests in nano include studying the potential effects of nanomaterials on the blood coagulation system.

Robert W. Brock, Ph.D., FAHA, is an associate professor and Wyeth research scholar in the Department of Physiology and Pharmacology and the CCRS, at the WVU School of Medicine. Dr. Brock earned his Ph.D. in medical biophysics from the University of Western Ontario, Canada, in 2001 where he was an Ontario Graduate Scholar. He joined the Lawson Health Research Institute in 2001 as a fellow of the Natural Sciences and Engineering Research Council of Canada to delineate the impact of type I diabetes on the regulation of blood flow dynamics in the skeletal-muscle microcirculation. In 2002, he was appointed as assistant professor of pharmacology and toxicology at the University of Arkansas for Medical Sciences where he acquired national funding from the American Heart Association and the National Institutes of Health (NIH) for his work. After a brief transition to WVU and the CCRS, Dr. Brock was appointed as a Wyeth research scholar to extend his explorations to the pathogenic mechanisms associated with the microvascular and endothelial dysfunction accompanying systemic inflammatory conditions. Specifically, this work focuses on understanding the pathways that influence blood flow regulation in the renal and hepatic microcirculations, as well as the kinetics of chemokine/cytokine signaling in normal and diseased states. Dr. Brock currently serves as chair of an American Heart Association national study section. He sits on the editorial boards of *Liver International* and *Reports in Medical Imaging*, as well as committees for the American Physiological Society, American Society for Pharmacology and Experimental Therapeutics, and the Microcirculatory Society. He recently was elected fellow of the Basic Cardiovascular Sciences Council of the American Heart Association.

Jefferson C. Frisbee, Ph.D., FAHA, is an associate professor in the Department of Physiology and Pharmacology at the WVU School of Medicine, where he is also an active member of the CCRS. He performed his graduate work in

biophysics at the University of Guelph (Canada) and completed a first postdoctoral fellowship in cardiovascular bioengineering at the University of Washington. He completed a second postdoctoral fellowship in microvascular physiology at the Medical College of Wisconsin, after which he assumed his first faculty position in their Department of Physiology before moving his research laboratory to WVU in 2004. His ongoing research program is supported by the NIH and the American Heart Association and is directed at the study of negative microvascular outcomes in obesity and insulin resistance and the combined pathologic state of the metabolic syndrome. His primary interests are integrating mechanistic alterations to vascular reactivity and network architecture to the regulation of skeletal-muscle perfusion.

Matthew A. Boegehold, Ph.D., received a B.S. in biology from the University of Michigan, and his Ph.D. in physiology from the University of Arizona. His postdoctoral training was in physiology and biophysics at Indiana University. Dr. Boegehold is currently professor and associate chair for research in the Department of Physiology and Pharmacology and director of the WVU CCRS. His research interests are focused on defining the microvascular control mechanisms that underlie tissue blood flow regulation and on gaining a better understanding of how these mechanisms can change with (1) the rapid vascular growth that accompanies juvenile maturation, (2) the development of salt-sensitive hypertension, and (3) high dietary salt intake in the absence of hypertension. Dr. Boegehold has had an active research program at WVU for 20 years. He has been continuously funded, as principal investigator by grants from the NIH or the American Heart Association for that entire period, with over 15 years of continuous NIH RO1 funding. Dr. Boegehold has also served on numerous study sections for the NIH and the American Heart Association and is currently serving on the editorial board of the journal *Microcirculation*.

David G. Frazer, Ph.D., received his B.S., M.S., and Ph.D. degrees in electrical engineering from the Pennsylvania State University in 1962, 1965, and 1970, respectively. He received another Ph.D. degree in physiology and biophysics from WVU in 1974. He is currently employed by NIOSH, Morgantown, WV, and is the leader of the developmental engineering research team. He also is an adjunct professor of electrical engineering and an adjunct assistant professor of physiology at WVU. His research interests include lung mechanics, the development of lung function testing methods, medical application of acoustics, aerosol science, and the development of small animal exposure systems.

Teh-Hsun "Bean" Chen, Ph.D., received a B.S. in physics from Tunghai University, Taiwan, and a Ph.D. in biophysics from the University of Rochester, New York. His postdoctoral training was in aerosol physics and inhalation toxicology at the Lovelace Inhalation Toxicology Research Institute, New Mexico. He has more than 30 years of experience in laboratory and applied research involving aerosol generation, sampling, and characterization methods; occupational safety and industrial hygiene practices; public health issues; and human health assessments. He has more than 100 peer-reviewed publications in these areas and was awarded two U.S. patents (No. 4,767,524 "virtual impactor" and No. 7,370,543, "air sampling device and method of use") based on his investigation on the phenomena of particle dynamics in air stream. He was the leader of the exposure monitoring team in the exposure assessment branch and is currently in charge of the nanoparticle inhalation exposure facility in the pathology and physiology research branch of the Health Effects Laboratory Division, NIOSH, CDC. As an American advisor in the International Science and Technology Center, he collaborated with Russian scientists through U.S. Department of Defense/Defense Threat Reduction Agency program on a project, entitled "a sampler for detection and express-identification of airborne microorganisms." He is currently served as a National Air and Space Administration science advisor on the lunar airborne dust toxicity advisory panel.

Vincent Castranova, Ph.D., is the Chief of the Pathology and Physiology Research Branch in the Health Effects Laboratory Division of the NIOSH, Morgantown, West Virginia. He holds the grade of a CDC Distinguished Consultant and received the Shepard Lifetime Scientific Achievement Award from CDC in 2008. He is also an adjunct professor in the Department of Basic Pharmaceutical Sciences at WVU and the Department of Environmental and Occupational Medicine at the University of Pittsburgh. Dr. Castranova received a B.S. in biology from Mount Saint Mary's College in 1970, graduating magna cum laude. He received a Ph.D. in physiology and biophysics in 1974 from WVU before becoming an NIH fellow and research faculty member in the Department of Physiology at Yale University. In 1977, Dr. Castranova received a research staff position at the NIOSH, Morgantown, West Virginia, and an adjunct faculty position at WVU. He has served at these institutions since that time. Dr. Castranova's research interests have concentrated on pulmonary toxicology and occupational lung disease. He has been coordinator of the nanotoxicology program in NIOSH since its inception in 2005. He has been a coeditor of four books and has coauthored over 450 manuscripts and book chapters.

OTHER PUBLICATIONS RESULTING FROM THIS RESEARCH

Chen BT, Frazer DG, Stone S, Schwegler-Berry D, Cumpston J, McKinney W, Lindsley W, Frazer A, Donlin M, Vandestouwe K, Castranova V, Nurkiewicz TR. 2006. Development of a small inhalation system for rodent exposure to fine and ultrafine titanium dioxide aerosols. Proceedings of the 7th International Aerosol Conference, pp. 858–859. September 10–15, 2006. St. Paul, MN.

LeBlanc AJ, Hu Y, Muller-Delp J, Chen BT, Frazer D, Castranova V, Nurkiewicz TR. 2008. Particulate matter inhalation impairs coronary microvascular reactivity. 25th European Conference on Microcirculation, pp. 13–17.

Nurkiewicz TR, Porter DW, Hubbs AF, Cumpston JL, Chen BT, Frazer DG, Castranova V. 2008. Nanoparticle inhalation augments particle-dependent systemic microvascular dysfunction. Part Fibre Toxicol 5:1.

Nurkiewicz TR, Porter DW, Hubbs AF, Stone S, Chen BT, Frazer DG, Boegehold MA, Castranova V. 2009. Pulmonary nanoparticle exposure disrupts systemic microvascular nitric oxide signaling. Toxicol Sci 110:191–203.

Prisby RD, Muller-Delp J, Delp MD, Nurkiewicz TR. 2008. Age, Gender and Hormonal Status Modulate the Vascular Toxicity of the Diesel Exhaust Extract Phenanthraquinone. J Toxicol Environ Health A 71:464–470.

ABBREVIATIONS AND OTHER TERMS

A23187	calcium ionophore
ABAH	4-aminobenzoic acid hydrazide
ADO	adenosine
AM	alveolar macrophage
ANOVA	analysis of variance
BAL	bronchoalveolar lavage
BET	Brunauer, Emmett, and Teller analysis
BH_4	tetrahydrobiopterin
Ca^{2+}	calcium
$CaCl_2$	calcium chloride
CAR bacteria	cilia-associated respiratory bacteria
CDC	Centers for Disease Control and Prevention
cGMP	cyclic guanosine monophosphate
Cl^-	chloride
CM	chemiluminescence
CO_2	carbon dioxide
DAPI	4′,6-diamidino-2-phenylindole
D_c	control diameter
DMSO	dimethylsulfoxide
D_{pass}	passive diameter
D_{ss}	steady-state diameter
EC_{50}	concentrations that produced 50% impairment of arteriolar dilation 24 hours after exposure
EDTA	ethylenediaminetetraacetic acid
ELISA	enzyme-linked immunosorbent assay
ETP	endogenous thrombin potential
F-344	Fischer 344 rat
G-CSF	granulocyte colony-stimulating factor
GM-CSF	granulocyte macrophage colony-stimulating factor
GRO-KC	growth-related oncogene-keratinocyte-derived-chemokine
H&E	hematoxylin and eosin
HE	hydroethidine
H_2O_2	hydrogen peroxide
HOCl	hypochlorous acid
IFN	interferon
IgG	immunoglobulin G
IL	interleukin
i.p.	intraperitoneal
i.t.	intratracheal
IP-10	chemokine ligand 10
ISO-NOP	isolated nitric oxide detection system
i.t.	intratracheal
K_2	dipotassium
KCl	potassium chloride
LDH	lactate dehydrogenase
L-NMMA	N^G-monomethyl-L-arginine
MCP	monocyte chemoattractant protein
MIP	macrophage inflammatory protein
MOUDI	micro-orifice uniform deposit impactors
MPO	myeloperoxidase
Na^+	sodium
Na_2EDTA	sodium ethylenediamine tetraacetate
NaCl	sodium chloride

NADPH	nicotinamide adenine dinucleotide phosphate
$NaHCO_3$	sodium bicarbonate
NF-κB	nuclear factor kappa-light-chain-enhancer of activated B cells
NIOSH	National Institute for Occupational Safety and Health
nm	nanometer
nM	nanomole
NO	nitric oxide
NOS	nitric-oxide synthase
NT	nitrotyrosine
O_2	oxygen
O_3	ozone
OCT	optical coherence tomography
PBS	phosphate-buffered saline
PM	particulate matter
$PM_{2.5}$	PM with an aerodynamic diameter $\leq$ 2.5 μm
PM_{10}	PM with an aerodynamic diameter $\leq$ 10 μm
PMNL	polymorphonuclear leukocyte
psi	pounds per square inch
RANTES	regulated upon activation, normal T-cell expressed, and secreted
ROFA	residual oil fly ash
ROS	reactive oxygen species
sICAM-1	soluble intercellular adhesion molecule-1
SNAP	S-nitroso-*N*-acetyl-D, L-penicillamine
SNP	sodium nitroprusside
TEMPOL	2,2,6,6-tetramethylpiperidine-*N*-oxyl
TiO_2	titanium dioxide
TNF α	tumor necrosis factor α
TTX	tetrodotoxin
U.S. EPA	U.S. Environmental Protection Agency
VEGF	vascular endothelial growth factor
VSM	vascular smooth muscle
vWF	von Willebrand Factor

Research Report 164, *Pulmonary Particulate Matter and Systemic Microvascular Dysfunction*, T.R. Nurkiewicz et al.

INTRODUCTION

Ambient particulate matter (PM*) is a complex mixture of solid and liquid airborne particles, ranging from approximately 5 nm to 100 µm in aerodynamic diameter. Although PM characteristics differ substantially from place to place, epidemiologic studies in diverse locations have reported associations between increases in levels of PM and short-term increases in cardiovascular morbidity and mortality. Short-term and long-term exposure to PM has also been associated with increased mortality from cardiopulmonary causes as well as from cancer (reviewed in U.S. Environmental Protection Agency [EPA] 2009).

On the basis of the epidemiologic findings, many governmental agencies have set regulatory standards or guidelines for levels of ambient PM classified by aerodynamic diameter. PM with an aerodynamic diameter ≤ 10 µm (PM_{10}) is of most concern because it is easily inhaled in the lower respiratory tract in humans. In the United States, to protect the general population and the groups considered most vulnerable to adverse effects from PM, the EPA monitors PM_{10} levels and has promulgated National Ambient Air Quality Standards for PM with an aerodynamic diameter ≤ 2.5 µm ($PM_{2.5}$, also referred to as fine particles), which is more likely to deposit in the alveolar region of the lung.

Current and past research on PM has aimed at identifying the pathophysiologic mechanisms responsible for their effects on health. Evidence from toxicologic studies has shown an association between PM exposure and a number of cardiac, vascular, and pulmonary outcomes, thus strengthening the epidemiologic evidence. Another important goal of research in this area has been to identify the characteristics of PM (including size and chemical composition) that are most responsible for toxicity. Some scientists believe that the subset of $PM_{2.5}$ made up of particles less than 100 nm in diameter may be especially toxic because although these particles are small, they can be present in large numbers and have a high surface area per unit mass. PM of this size found in ambient air is generally referred to as ultrafine particles, whereas engineered PM of this size is referred to as nanoparticles (nano-PM). For consistency with the Investigator's report, the latter term is used in this Critique.

In February 2005, Dr. Timothy R. Nurkiewicz submitted an application to HEI under Request for Applications 04-5 "Walter A. Rosenblith New Investigator Award." This award was established to provide support for an outstanding new investigator at the assistant professor level to conduct work in the area of air pollution and health and is unrestricted with respect to the specific topic of research. In his application, "Pulmonary Particulate Matter Exposure and Systemic Microvascular Disease," Nurkiewicz proposed to assess the effects of inhaled fine- and nano-sized titanium dioxide (TiO_2) on systemic microvascular circulation in rats. The goals of the study were to measure the effect of exposure to PM of different sizes on the severity of microvascular dysfunction and to investigate mechanisms associated with this effect. The HEI Research Committee recommended the proposal for funding because they believed that the project was innovative and that it would contribute toward the understanding of pathophysiologic mechanisms by which PM of different size fractions could cause adverse effects.

SCIENTIFIC BACKGROUND

At the time the proposal by Nurkiewicz and colleagues was considered for funding, a body of research was emerging that addressed cardiovascular effects of exposure to PM and their underlying mechanisms. Effects on the cardiovascular systems were hypothesized to be mediated by oxidative stress in the lung or by the direct translocation of PM or its components into the circulation. Oxidative stress was believed to activate and upregulate a number of proinflammatory mediators, including cytokines and

Dr. Timothy R. Nurkiewicz's 3-year study, "Pulmonary Particulate Matter Exposure and Systemic Microvascular Disease," began in July 1, 2005. Total expenditures were $300,000. The draft Investigators' Report from Nurkiewicz and colleagues was received for review in January 2009. A revised report, received in December 2009, was accepted for publication in May 2010. During the review process, the HEI Health Review Committee and the investigators had the opportunity to exchange comments and to clarify issues in both the Investigators' Report and the Review Committee's Critique.

* A list of abbreviations and other terms appears at the end of the Investigators' Report.

neutrophils, resulting in an inflammatory response in the lung, which would lead in turn to systemic inflammation (Brook et al. 2004). Systemic inflammation was thought to play a role in the dysfunction of the endothelial cells that line the interior surface of blood vessels and contribute to the development or progression of atherosclerosis and thrombosis (blood clots) (Utell et al. 2002).

Endothelial cells regulate vascular tone and help to maintain vascular homeostasis. A major vasodilator produced by endothelial cells is nitric oxide (NO); a major vasoconstrictor is endothelin (Davignon and Ganz 2004). Impairment of production of NO and associated endothelial dysfunction had been hypothesized to be one of the early signs of atherosclerosis (Davignon and Ganz 2004). Effects of air pollution on both vascular dilation and constriction had been observed in some studies, but the mechanisms underlying the rapid changes in vascular tone remained to be resolved (Brook et al. 2004). Nurkiewicz and colleagues (2004) had reported that intratracheal instillation of fine residual oil fly ash (ROFA) or fine TiO_2 caused vascular dysfunction (measured as changes in vascular dilation).

In some animal models of cardiovascular disease, exposure to PM caused more rapid progression of atherosclerotic lesions and increases in blood viscosity and markers of coagulation, such as fibrinogen (Bhatnagar 2004), relative to animals exposed to filtered air. Effects of PM on heart rate and heart-rate variability had been observed in many studies, suggesting that PM can alter the balance between the parasympathetic and sympathetic nervous systems by decreasing the parasympathetic input to the heart (Brook et al. 2004). However, a coherent mechanistic scheme linking all these outcomes was still to be formulated. Nano-PM was suspected of initiating an inflammatory effect that was larger than that of fine PM when considered on a mass basis because of its increased ratio of surface area to mass (Donaldson et al. 2001), but evidence for this differential effect was limited. Nurkiewicz proposed to build on his team's studies of exposure to ROFA by evaluating and comparing the effect of inhaled fine and nano-PM of TiO_2 on endothelium-dependent vascular dilation and the mechanisms associated with this effect.

This Critique is intended to aid the sponsors of HEI and the public by highlighting both the strengths and limitations of the study and by placing the Investigators' Report into scientific perspective.

SPECIFIC AIMS

The study had the following aims:

Specific Aim 1: Determine the severity of systemic microvascular dysfunction after PM exposure and characterize the influence of particle size in this dysfunction (Experimental Protocol 1)

Specific Aim 2: Determine whether pulmonary PM exposure reduces the capacity for endothelium-dependent microvascular NO production or vascular-smooth-muscle sensitivity to NO (Experimental Protocols 1 and 2)

Specific Aim 3: Determine whether systemic inflammation is associated with microvascular dysfunction after PM exposure (Experimental Protocol 3)

STUDY DESIGN

The study was designed to compare the effects of fine and nano-PM of the same composition with each other and a filtered air–exposed group. The investigators selected TiO_2 because it is used as a nanomaterial in many consumer products. This material has also been used often in toxicologic investigations.

The animals were exposed by inhalation to various concentrations of nano- and fine PM or filtered air for up to 12 hours. All observations were made 24 hours after the end of the exposure. To account for differences in deposition patterns between inhaled fine and nano-PM, the investigators decided to use the mass of particles deposited in the lungs (measured in a subset of animals in Experimental Protocol 1 as the primary exposure metric). From this measure they also derived an estimate of the surface area and used it as another metric of exposure. Nurkiewicz and colleagues evaluated the effect of PM exposure on microvascular function in rats as measured by dilation of peripheral arteriolar vessels in response to a vascular dilator (calcium ionophore A23187). They also sought to investigate whether PM exposure is associated with production of and sensitivity to NO in the microvasculature and whether generation of reactive oxygen species and inflammatory mediators in circulation or the lung contribute to microvascular dysfunction.

In the report, the investigators grouped their experiments into three main experimental protocols, which are described in the Critique Table. The methods used in these protocols are summarized below.

METHODS

EXPOSURE

Sprague Dawley rats were exposed by whole-body inhalation to fine (primary size, 1000 nm) and nano- (primary size, 21 nm) TiO_2 particles for 4 to 12 hours. The exposure

Critique Table. Summary of Results of the Study by Nurkiewicz and Colleagues[a]

Endpoints Measured (Sprague Dawley Rats)	TiO_2 Deposited Mass	Results		Figures and Tables of the Investigators' Report
		Fine TiO_2	Nano-TiO_2	
Microvascular Dysfunction				
Arteriolar dilation in response to infusion of calcium ionophore	8, 20, 36, 67, 90 µg fine 4, 6, 10, 19, 38 µg nano	Dose-dependent ↓ EC_{50} = 67 µg dose	Dose-dependent ↓ EC_{50} = 10 µg dose	Figures 8, 9
Microvascular NO Production and Sensitivity				
Arteriolar NO production	8, 20, 36, 67, 90 µg fine 4, 6, 10, 19, 38 µg nano	↓	↓	Figure 17
Arteriolar NO production with NO synthase inhibitor N^G-monomethyl-L-arginine	8, 20, 36, 67, 90 µg fine 4, 6, 10, 19, 38 µg nano	↓	↓	Figure 17
Arteriolar responsiveness to NO using the NO donor sodium nitroprusside	67 µg fine 10 µg nano	No effect	No effect	
Oxidative Stress				
Microvasculature oxidative stress (ethidium bromide fluorescence)	67 µg fine 10 µg nano	↑	↑	Figure 16
Arteriolar NO production in the presence of radical scavengers TEMPOL, catalase, NADPH oxidase inhibitor apocynin	67 µg fine 10 µg nano	↑	↑	Figure 18
Lung and vascular oxidative stress (nitrotyrosine level by immunofluorescence assay)	10 µg nano	ND	↑	Figures 20, 21
Systemic Inflammation and Clotting				
Systemic inflammation (levels of interleukins in plasma)	67 µg fine 10 µg nano	↑ IL-2, IL-18, IL-13, GRO-KC	No change	Figure 22
Markers of coagulation in plasma (thrombin potential, fibrinogen, von Willebrand factor, troponin I and T)	8, 20, 67, 90 µg fine 6, 10 µg nano	↑ Thrombin potential, no dose–response; small or no changes in the other markers	↑ Thrombin potential, no dose–response; small or no changes in the other markers	Tables 6, 7, 8, 9
Additional Findings				
Effect of neutrophil depletion (by phosphamide) on PM-induced decrease in arteriolar dilation (Fischer 344 rats)	10 µg nano	↓	↓	Figure 24
Arteriolar dilation after treatment with the channel blocker tetrodotoxin	10 µg nano	ND	↑	Table 11, Figure 25

[a] A downward arrow indicates a decrease and an upward arrow indicates an increase. ND denotes no data; EC_{50}, the concentration that produced 50% impairment of arteriolar dilation 24 hours after exposure; TEMPOL, 2,2,6,6-tetramethylpiperidine-*N*-oxyl; and NADPH, nicotinamide adenine dinucleotide phosphate oxidase.

concentrations ranged from 1.5 to 20 mg/m^3. The PM was generated using a fluidized-bed powder generator. Fischer 344 rats were used for a few endpoints.

DETERMINATION OF PM MASS DEPOSITED IN THE LUNGS AND SURFACE AREA

The mass of particles deposited in the lungs (also referred to here and in the Investigators' Report as the PM lung burden) was determined in lung extracts by inductively-coupled plasma-atomic emission spectroscopy and was also calculated according to the following equation: PM lung burden/rat = exposure concentration × exposure duration × rat ventilation rate × deposition fraction. The deposition fraction was assumed to be 10% for both fine and nano-PM. Surface area was calculated using the data presented in Table 2 of the Investigator's Report. Measurements of deposited PM surface area were obtained from the study by Sager and colleagues (2008) (also reported in Table 2 of the Investigators' Report).

MEASUREMENT OF MICROVASCULAR DILATION

Vascular dilation was evaluated in anesthetized rats by intravital microscopy of the microvasculature in the exteriorized spinotrapezius muscle enclosed in a tissue bath. The muscle was perfused during the duration of the experiment (up to 15 minutes). A23187, a vascular dilator that acts by increasing the activity of NO synthase (the enzyme that produces NO), was infused directly into selected microvessels (2–3 per rat) of the exteriorized muscle at various injection pressures for 2-minute periods, with a 2-minute recovery period between injections (Experimental Protocols 1 and 2). Arterial dilation was quantified from video images of each experiment in one to three microvessels per animal. The effect of exposure to PM was measured as the change in the ability of vessels in the exteriorized muscle to dilate in response to A23187, compared with the vessels from filtered air–exposed rats. It is reported as the mean of the vessel diameters or as the percentage of the diameter of vessels from PM-exposed rats relative to the diameter of the vessels from filtered air–exposed rats.

To clarify the mechanisms involved in the control of arterial dilation, the investigators used specific chemicals (either added to the superfusate or infused directly into the lumen of a microvessel) that are known to affect a specific pathway or the levels of a specific mediator. The compounds used were:

- Sodium nitroprusside: a donor of NO (from its breakdown in blood). Sodium nitroprusside was applied iontophoretically to selected microvessels to determine whether particle exposure altered vascular responsiveness to exogenous NO (Experimental Protocol 2).
- N^G-monomethyl L-arginine (L-NMMA): an inhibitor of NO synthase. L-NMMA was added to the superfusate to evaluate the role of NO synthase in the responsiveness to A23187 (Experimental Protocol 2).

NO PRODUCTION

NO production was measured in homogenized microvessels isolated from the spinotrapezius muscle at the end of the intravital microscopy experiments. A NO sensor probe was used to perform real-time electrochemical measurements of NO (Experimental Protocol 2).

SYSTEMIC AND LUNG INFLAMMATION

Systemic inflammation was assessed as changes in the level of circulating cytokines (including interleukin [IL]-4, IL-6, and tumor necrosis factor α), chemokines (such as growth-related oncogene-keratinocyte-derived-chemokine [GRO-KC], monocyte chemoattractant protein, and RANTES [regulated upon activation, normal T-cell expressed, and secreted]). In addition, other markers associated with vascular dysfunction (such as sE-Selectin and soluble intercellular adhesion molecule [sICAM-1]) were measured in some samples (Experimental Protocol 2). Lung inflammation was measured as the levels of lactate dehydrogenase and differential cell counts in bronchoalveolar lavage (BAL) fluid and by histopathologic examination of lung tissue (Experimental Protocol 2).

MICROVASCULAR AND LUNG OXIDATIVE STRESS

Microvascular oxidative stress was measured after addition of hydroxyethidine (HE) to the muscle infusate in intravital miscroscopy studies. HE permeates the vessels' membranes and, in the presence of oxidants, is converted to ethidium bromide, which binds to DNA. After a 30-minute incubation with HE, the muscle was perfused with HE-free buffer, and ethidium bromide fluorescence in arteriolar walls was detected with a mercury lamp with appropriate filters and was quantified using an imaging software (Experimental Protocol 2).

Another measure of oxidative stress was the production of nitrotyrosine (the product of nitration of tyrosine by peroxynitrite). Frozen sections of the spinotrapezius muscle and the lung from PM-exposed and filtered air–exposed rats were stained with an immunofluorescent antibody and examined by confocal microscopy. In addition, free radical scavengers (such as superoxide dismutase mimetic 2,2,6,6-tetramethylpiperidine-*N*-oxyl [TEMPOL] and

catalase) were added to the infusate to evaluate whether oxidative stress was responsible for the inhibition of NO production (Experimental Protocol 2).

BLOOD CLOTTING MARKERS

The following markers were quantified in platelet-poor plasma: endogenous thrombin potential, fibrinogen, von Willebrand factor, troponin I, and troponin T. Thrombin, fibrinogen, and von Willebrand factor play roles in various stages of blood clotting. Troponins are indicators of injury to cardiac tissue (Experimental Protocol 3).

ROLE OF CIRCULATING NEUTROPHILS

Neutrophils are part of the subset of leukocytes (white blood cells) referred to as granulocytes, and they play a key role in the inflammatory response. In order to evaluate whether neutrophils play a role in microvascular dysfunction, the investigators treated a subset of rats with cyclophosphamide (a compound that causes depletion of leukocytes) before they were exposed to PM or filtered air. The investigators used intravital microscopy to assess and compare the dilation of microvessels in PM-exposed and filtered air–exposed rats that were, or were not, treated with cyclophosphamide. Only nano-TiO_2 was used (Experimental Protocol 3).

ROLE OF FAST SODIUM CHANNELS

The investigators used tetrodotoxin (TTX), which prevents nerve cell depolarization by blocking membrane fast sodium channels, to determine the role of these channels in arterial vasodilation using intravital microscopy. Tetrodoxin was added to the perfusate for 30 minutes. The treatment was followed by infusion with A23187. Only nano-TiO_2 was used (Experimental Protocol 3).

DATA ANALYSES

In all the analyses, the exposure metric was the deposited dose, which was determined in Experimental Protocol 1 for a set of exposure concentrations and durations (shown in Table 1 of the Investigator's Report) and was assumed to be the same for a given exposure concentration in all subsequent experiments. The investigators used the individual number of arterioles in their analyses of the results of intravital microscopy even if some vessels were from the same animals; their rationale was that the anatomy and physiology of the microvascular beds are very heterogeneous within an animal and can therefore be considered as independent observations. One- and two-way repeated-measures analysis of variance was used to evaluate differences within a group and the group–treatment interaction, respectively. For all these analyses, the Student-Newman-Keuls method was used to isolate pairwise differences between specific groups.

MAIN RESULTS

The main results reported by Nurkiewicz and colleagues are described below according to the individual aims. A summary is provided in the Critique Table.

EXPOSURE CHARACTERIZATION AND DOSE METRICS

Results of measurements inside the exposure chamber showed that the peak of the number-based size distribution of nano-PM was 100 nm. The number-based size distribution of fine PM was bimodal and had a major peak at 710 nm and a minor peak at 100 nm (Figure 4 of the Investigators' Report). Measured and calculated lung burdens did not agree (see Table 1 of the Investigator's Report): the measured lung burden was lower than the calculated one. The measured lung burden at the same TiO_2 concentration and exposure duration was lower after exposure to nano-PM than to fine PM. Measured and calculated surface areas were similar for fine PM but did not agree for nano-PM (the calculated surface area of nano-PM was smaller than the measured surface area, as shown in Table 2 of the Investigator's Report).

MICROVASCULAR DYSFUNCTION

As described in Specific Aim #1 and carried out in Experimental Protocol 1, the investigators evaluated the severity of microvascular dysfunction after PM exposure and the influence of particle size on the degree of dysfunction. They found that inhalation of either fine or nano-TiO_2 particles impaired arteriolar dilation in response to infusion with A23187 (Figures 8 and 9 of the Investigators' Report). The effect was dose dependent. Similar effects were observed after exposure to nano-PM for different combinations of exposure durations and concentrations that yielded the same deposited dose of 10 µg (Figure 10 of the Investigators' Report). The study confirmed earlier findings regarding the effects of exposure to fine and nano-TiO_2 administered by intratracheal instillation (Nurkiewicz et al. 2006).

At similar deposited PM mass, nano-PM produced greater inhibition of microvascular dilation than did fine PM (see Figure 12 of the Investigators' Report). The level at which there was no effect was determined to be 8 µg (corresponding to 3 mg/m^3 for 4 hours) for fine PM and 4 µg (corresponding to 1.5 mg/m^3 for 4 hours) for nano-PM.

The deposited mass that caused a 50% decrease in dilation was 67 µg for fine PM and 10 µg for nano-PM. The exposure concentrations that yielded these lung burdens were used in several of the subsequent experiments (as shown in the Critique Table). The investigators concluded from these results that nano-PM impairs arteriolar dilation to a greater degree (more than sixfold) than fine TiO_2 at similar lung mass burdens.

When the vascular dilation response in the PM-exposed rats — expressed as percentage of the response in rats exposed to filtered air — was plotted as a function of the deposited PM mass, the slopes of the dose–response curves were different between the two types of particles. However, when the response was plotted as a function of the calculated deposited PM surface area, the dose–response relation was the same for the two types of particles (see Figure 13 of the Investigator's Report). The investigators conclude that the deposited PM surface area was a better predictor of arterial dysfunction than the deposited PM mass. However, they also noted that the results regarding the relative potency of nano- versus fine PM would be different if the measured, rather than the calculated, surface area had been used (fine PM would be more potent than nano-PM).

MICROVASCULAR NO PRODUCTION AND SENSITIVITY

As described in Specific Aim #2 and carried out in Experimental Protocols 1 and 2, the investigators evaluated NO production by the microvascular endothelium and its responses to exogenous NO in PM-exposed and filtered air–exposed rats. They found that NO production was inhibited in the presence of A23187 as a function of different doses of fine and nano-PM (see Figure 17 of the Investigators' Report, black bars). In separate experiments, the NO synthase inhibitor L-NMMA was added to the perfusate. The results showed that L-NMMA decreased NO production in vessels from filtered air–exposed animals, indicating that the endothelial response to A23187 was in large part dependent on NO. L-NMMA also further impaired NO production after exposure to PM, especially at low particle doses (see Figure 17 of the Investigators' Report, white bars). The results after infusion of the NO donor sodium nitroprusside showed that endothelial sensitivity to NO was not altered after exposure to either fine or nano-PM (Figure 15 of the Investigators' Report).

OXIDATIVE STRESS

Other experiments in exteriorized microvessels showed that NO production increased in the presence of radical scavengers (see Figure 18 of the Investigators' Report) and that the presence of radical scavengers in the perfusate combined with infusion A23187 partially reduced the inhibition of arterial dilation caused by PM exposure (Figure 19 of the Investigators' Report). These findings were supported by the increase in arteriolar ethidium bromide fluorescence and by increased staining for nitrotyrosine (two markers of oxidative stress) after exposure to either fine or nano-PM. Nurkiewicz and colleagues noted that pulmonary nitrotyrosine staining was localized in inflammatory cells in the alveoli or near the vascular endothelium (see the legend of Figure 20 of the Investigators' Report).

MARKERS OF SYSTEMIC INFLAMMATION AND CLOTTING

Experiments conducted in Experimental Protocol 3 showed that the plasma inflammatory mediators IL-2, IL-18, IL-13, and GRO-KC were elevated after exposure to fine PM but not to nano-PM (Figure 22 of the Investigators' Report). Effects of PM on clotting markers were variable and for the most part negative (Table 7 of the Investigators' Report). The investigators noted that the only consistent finding was the increase of thrombin potential at a deposited mass of 8 and 10 µg of fine and nano-PM respectively, but no dose–response relation was observed.

ADDITIONAL FINDINGS

Nurkiewicz and colleagues report that markers of lung inflammation in BAL were not altered by exposure to either fine or nano-PM, and histopathology of lung slices did not show effects of TiO_2 exposures on inflammation (the data are not shown in the Investigators' Report). The investigators noted that histopathologic analysis of lung tissue slices revealed the presence of macrophages containing PM. Although fine TiO_2 particles were seen inside the macrophages as well as in the extracellular matrix, nano-TiO_2 particles were always within macrophages in aggregates. Based on the observation that some macrophages were anucleated and that nitrotyrosine staining was localized in lung inflammatory cells (as mentioned above), the authors state that the study showed evidence of lung inflammation.

Neutrophil depletion (resulting from treatment of the animals with cyclophosphamide) partially prevented the PM-induced decrease in endothelium-dependent arteriolar dilation as measured by intravital microscopy (Figure 23 of the Investigators' Report). The addition of the sodium channel blocker TTX to muscle superfusate partially reversed the inhibitory effect of nano-PM (fine PM was not tested) on arteriolar dilation, but the change was not statistically significant.

HEI REVIEW COMMITTEE EVALUATION

The HEI Review Committee, in its independent review of the study, thought that it had been well conducted and used novel approaches. For example, the selection of the measured lung burden as a dose metric was valuable because it accounted for differences in deposition patterns between fine and nano-PM. Moreover, the technique of ex vivo intravital microscopy that the investigators used has the potential to provide valuable insights on microvascular health in response to particulate exposures. One drawback, however, is that this experimental setup requires general anesthesia and surgical manipulation, which in themselves could have influenced the effects investigated in this study. The use of inhalation exposures and two different sizes of particles were also strengths of the study. The Committee thought that although TiO_2 is not representative of ambient PM or of the vast array of nano-PM used in the nanotechnology industry, it was useful for investigating mechanisms of action and establishing proof of principle in this study.

EXPOSURE

The Review Committee considered the exposure generation system adequate. The number-based size distribution indicates that the nano-TiO_2 in the exposure chamber did not consist of single primary particles; instead, it consisted of agglomerates of larger sizes than the primary particles. This could be a consequence of the high concentration of PM, the method of generating them, or both. It is not known whether the deposition and clearance of these aggregates are the same as for the single particles. The fine TiO_2 particles in the chamber were smaller than the primary particles. This also could be a result of the method for generating the particles.

PM concentrations between 1.5 and 20 mg/m^3 for 4 to 12 hours were used; the intent was to deliver a high burden of TiO_2 particles to the lung in a short period of time (hours), although this is not reflective of low-level protracted exposure in a real-world situation. The concentrations of fine TiO_2 used are not far from the current occupational exposure limits recommended by the National Institute for Occupational Health and Safety (NIOSH) (2.4 mg/m^3 time-weighted averaged concentrations for up to 10 hr/day during a 40-hour work week), but the concentrations of nano-TiO_2 used are higher that those recommended by NIOSH (0.3 mg/m^3 for nano-TiO_2 time-weighted averaged concentrations for up to 10 hr/day during a 40-hour work week) (NIOSH 2011). For both PM sizes, the concentrations used are several orders of magnitude higher than ambient PM concentrations.

MAIN RESULTS

Several important outcomes of this study provide new and significant information. The study demonstrated that the degree of systemic microvascular dysfunction associated with PM exposure is related to the size and lung burden of the particles and that nano-PM is more potent than fine PM at an equivalent lung burden. Whether this effect is related to particle surface area, as the investigators concluded, cannot be firmly established because of the uncertainties in the determination of this metric. Another important result is the demonstration that the impairment of microvasculature dilation after PM exposure is related to a decrease in bioavailable NO rather than to alteration of vascular-smooth-muscle responsiveness to NO; this finding indicates that dilation is mediated by the endothelium.

These results are consistent with the available evidence from the literature relating exposure to PM and endothelium-dependent vascular dilation, which has recently been reviewed by Brook and colleagues (2010). In their review (which considered the results presented in this report and previously published [Nurkiewicz et al. 2008 among many others]), Brook and colleagues concluded that "the available studies suggest that short-term and long-term particle exposure can impair conduit and resistance arterial endothelium-dependent vasodilation."

The experiments reported here also demonstrate that PM-induced impairment of microvascular function is likely related to enhanced oxidative stress (that is, to the formation of reactive oxygen species) in the microvasculature and the lung. The investigators hypothesize that oxidative stress consumes NO by producing peroxynitrite, which in turn is converted to a more stable product, nitrotyrosine. The fact that Nurkiewicz and colleagues found an increase in nitrotyrosine staining in the microvascular wall after exposure to PM is consistent with their hypothesis. Several other studies with different types of PM have also shown that reactive oxygen species are generated in the vasculature (reviewed by Araujo 2011; Brook et al. 2010). However, those studies have generally found an association between oxidative stress and systemic inflammation, whereas in the study by Nurkiewicz and colleagues, the systemic inflammatory response was mild or nonexistent. A puzzling finding is that increases in some plasma cytokines were observed with fine TiO_2 but not with nano-TiO_2. Whether nano- and fine PM caused lung inflammation under the exposure conditions is unclear. However, the fact that no changes in BAL cell types (in particular neutrophil counts) were observed would lead to the conclusion that inflammation was not present since increase in neutrophil is considered a more sensitive and quantitative

indicator of lung inflammatory response than histopathology, at least for these acute short-term effects.

Markers of coagulation were for the most part unaffected by the exposure. The investigators measured these markers because they have been associated with exposure to PM and are involved in the processes leading to clot formation. However, no mechanistic interpretation linking them to arteriolar dilation is provided by the authors.

The investigators note that the results after cyclophosphamide treatment — showing a reduction in circulating neutrophils and a protective effect of PM on vasodilation — suggested that neutrophils play a role in impairing arteriolar dilation (Figure 23 of the Investigators' Report). The Review Committee commented that, although cyclophosphamide reduced the number of circulating neutrophils, it could also have had profound effects on many other circulating or resident cells. It is therefore difficult to attribute the vasoprotective effect observed after cyclophosphamide administration to neutrophil depletion. Moreover, although neutrophil depletion alleviated microvascular dysfunction with PM exposure, the results reported by Nurkiewicz and colleagues do not establish cause and effect because the data do not demonstrate that PM exposure influences neutrophil number or function (or pulmonary inflammation) per se, and there was no clear relationship between PM exposure and most circulating inflammatory cytokines.

The Committee thought that the investigators' conclusion that mechanisms related to the action of the sympathetic nervous system are involved in microvascular dysfunction seemed tenuous. The conclusions were based on the ability of TTX (a blocker of fast sodium channels) to provide vasoprotection after nano-TiO_2 exposure. However, the study did not include an experiment with filtered air exposure plus TTX to evaluate effects of TTX on basal microvascular tone. More importantly, the use of a single concentration of a single pharmacologic agent to dissect a mechanism can be misleading. Additional experiments using adrenergic antagonists or agonists to identify sympathetic effects on vasculature after PM exposure would be needed to support a conclusion that the sympathetic nervous system is involved in the observed effect.

The Review Committee agreed with the investigators' conclusion that the results demonstrate that nano-PM at similar doses produces greater systemic microvascular dysfunction than fine PM. The Committee raised the possibility, given the bimodal distribution of the fine TiO_2 aerosol, that the biologic effects of fine PM exposure observed in this study could be due primarily to the low concentrations of the smaller particles, rather than to the much higher concentrations of the larger particles. Another possible explanation is that there may be substantial clearance of particles after PM exposure and that such clearance may differentially affect the deposition of nano- and fine PM; the Committee felt that this issue was not adequately discussed in the Investigators' Report. Another unresolved question that requires further study is whether the nano-PM enters into the systemic circulation and directly affects vascular endothelial function.

It is also possible that the differences in toxicity are related to different composition of the two types of PM, as suggested by the results reported in a review of the mechanisms of action of TiO_2 by Johnston and colleagues (2009), showing that a mixed sample of anastase (80%) and rutile (20%) TiO_2 of the same size was capable of eliciting the release of lactate dehydrogenase after intratracheal instillation, whereas a sample of rutile TiO_2 was not.

The interpretation of the results reported by Nurkiewicz and colleagues is also difficult, in part, because of the question of whether the different TiO_2 particles can readily be compared with each other; instead, different dose–response relationships may exist based on surface area and mass, composition, and mechanisms of translocation. Also, there may be different mechanisms at play for any particle, including the mediators induced and released in the respiratory tract.

DOSE METRICS

The fact that the measured and calculated lung burdens in the study did not agree could be due to uncertainties in the method used to estimate the deposited mass, as well as to the extent of PM clearance that occurred during the 24-hour period between the end of the exposure and the lung burden analyses. The finding that — at the same mass concentration and exposure duration — the lung burden of fine PM was greater than that of nano-PM is somewhat surprising since nano-PM would be expected to have a higher deposition fraction than fine PM, based on a human deposition model (Oberdorster et al. 2005). However, the behavior of nano-PM aggregates could be different from that of single particles, and, as noted above, nano-PM may have a different rate and mechanisms of clearance than fine PM (Möller et al. 2009).

The investigators conclude that deposited PM surface area is a more appropriate metric of exposure than deposited PM mass. The Review Committee did not think that the study results convincingly supported this conclusion, however. The calculation of surface area was based on an average size of the particles, but the size distribution covered a wide range of sizes. As noted by the authors, a different conclusion would be reached regarding the potency of fine PM versus nano-PM if one used the measured, instead of the calculated, surface area.

STATISTICAL ANALYSES

For the analyses of vasodilation responses, the investigators treated each vessel as if it were an independent observation, although several vessels were measured in each rat. The Review Committee was concerned about this method of analysis because such clustering of observations can, if not taken into account, distort the results and in particular can lead to the underestimation of uncertainty. The investigators justified this approach nonetheless on the grounds that considerable heterogeneity was observed between vessels.

Because the investigators kindly provided some of their data (those underlying Figure 9 in the Investigators' Report), the Committee was able to evaluate the impact of clustering on these results. There was indeed heterogeneity among vessels (intra-animal) but not as much as there was heterogeneity among rats (interanimal). That is, there was evidence of clustering of observed outcomes by rat. For example, in the observations of diameter at 40-psi ejection pressure (Figure 9 of the Investigators' Report), 30% of the variance between vessels within the same exposure group was explained by "rat" effects — that is, by interanimal variation.

The Committee repeated the analyses reported in Figure 9 in the Investigators' Report by including random "rat" effects (i.e., a mixed model). The results did not show much of an effect on the point estimates, probably because most animals had similar numbers of vessels measured (two or three), but revealed that the original analysis underestimated the standard errors by 10–20% and hence of the *P* values obtained. Thus some *P* values reported as $P < 0.05$ were no longer significant when retested in the mixed model (those for the comparison of 19 with 10 and 38 with 19 $\mu g/m^3$, respectively, at 40 psi and 10 with 6 $\mu g/m^3$ at 20 psi). The broad pattern of the results in Figure 9 in the Investigators' Report was, however, robust in the analysis that adjusted for clustering.

Thus the Committee noted that the issue of clustering of observations from individual rats in this study did not substantially affect the interpretation of the results. Nevertheless, the Committee thinks good statistical practice is to take account of such clustering because — until clustering is adjusted for — it is impossible to be sure what affect it may have had on the results. The simplest method to account for clustering is to carry out the analysis on mean outcomes for each rat; in the Committee's analysis, this method produced results that were broadly similar to those of the random effects model applied to these data. The Committee, however, thought that random effect models such as the one it used for such analyses are somewhat preferable.

OVERALL SUMMARY AND CONCLUSIONS

Overall, this was a thorough and well-conducted study. Each of the specific aims was achieved. The use of fluorescent intravital microscopy to measure vascular dilation and oxidative stress is a novel approach and may be useful in future investigations. A potential drawback of this procedure is that the use of general anesthesia and surgical manipulations used to obtain the measurements may themselves affect microvascular function.

A strength of the study is the measurement of the PM deposited in the lung after each exposure condition and the use of this metric for comparing effects of nano- and fine PM. Also of interest is the use of deposited particle surface area as an alternative exposure metric. However, the Review Committee did not think that the results convincingly supported the investigators' conclusion that surface area is a more appropriate metric of exposure than deposited mass.

The type of PM used, TiO_2, is relatively insoluble and is considered to have low reactivity. Although it is used extensively in the nanotechnology industry, it should not be considered representative of nanoengineered PM in general. The TiO_2 PM also should not be considered to be representative of fine or nano-PM in ambient air, which contains a variety of reactive metals, polycyclic aromatic hydrocarbons, and other organic compounds. The concentrations used in the study are very high in relation to the PM levels that are generally encountered in ambient air; however, they are not far from the current occupational exposure limits recommended by NIOSH for TiO_2.

An important finding reported by Nurkiewicz and colleagues is that acute high-dose–inhalation exposure to nano- and fine TiO_2 impairs the ability of the skeletal-muscle microvasculature to dilate in response to a stimulus and that this effect is mediated by decreased NO production by endothelial cells. Also of importance is the finding that at the same pulmonary mass deposition, nano-PM produced significantly greater systemic microvascular dysfunction than the fine PM. Whether this effect is related to particle surface area cannot be firmly established. The impairment in NO production appears to be related to enhanced oxidative stress in both lung tissue and the vasculature. Although oxidative stress has been linked to both lung and systemic inflammation in several studies, evidence of lung inflammation was weak in this study and a role of systemic inflammatory mediators was not clearly established. The Review Committee cautioned extrapolating from the effects and mechanisms observed in rats after short-term exposure to high concentrations of the TiO_2 PM to effects in humans after either short-term or long-term exposure to lower concentrations and to different types of PM.

The Review Committee considered the investigators' conclusions that circulating neutrophils and sympathetic neurogenic mechanisms are involved in the systemic microvascular dysfunction observed after PM exposure to be tenuous and preliminary. More mechanistic studies will be required to assess possible inflammatory pathways and role of the sympathetic nervous system in these effects.

The study provides insights into the pathophysiologic ramifications of inhalation of TiO_2 nano-PM and the comparison of various dose metrics. Future mechanistic studies might usefully focus on addressing the effects of ambient and engineered PM, not only on the systemic resistance vessels but also on coronary endothelial function at lower concentrations.

ACKNOWLEDGMENTS

The Health Review Committee thanks the ad hoc reviewers for their help in evaluating the scientific merit of the Investigators' Report. The Committee is also grateful to Annemoon van Erp for her oversight of the study, to Maria Costantini for her assistance in preparing its Critique, to Trina Arpin for science editing of this Report and its Critique and to Suzanne Gabriel, Barbara Gale, Fred Howe, Bernard Jacobson, and Flannery Carey McDermott for their roles in preparing this Research Report for publication.

REFERENCES

Araujo JA. 2011. Particulate air pollution, systemic oxidative stress, inflammation, and atherosclerosis. Air Qual Atmos Health 4:79–93.

Bhatnagar A. 2004. Cardiovascular pathophysiology of environmental pollutants. Am J Physiol Heart Circ Physiol 286:H479–H485.

Brook RD, Franklin B, Cascio W, Hong Y, Howard G, Lipsett M, Luepker R, Mittleman M, Samet J, Smith SC Jr, Tager I; Expert Panel on Population and Prevention Science of the American Heart Association. 2004. Air pollution and cardiovascular disease: A statement for healthcare professionals from the Expert Panel on Population and Prevention Science of the American Heart Association. Circulation 109:2655–2671.

Brook RD, Rajagopalan S, Pope CA III, Brook JR, Bhatnagar A, Diez-Roux AV, Holguin F, Hong Y, Luepker RV, Mittleman MA, Peters A, Siscovick D, Smith SC Jr, Whitsel L, Kaufman JD; American Heart Association Council on Epidemiology and Prevention, Council on the Kidney in Cardiovascular Disease, and Council on Nutrition, Physical Activity and Metabolism. 2010. Particulate matter air pollution and cardiovascular disease: An update to the scientific statement from the American Heart Association. Circulation 121:2331–2378.

Davignon J, Ganz P. 2004. Role of endothelial dysfunction in atherosclerosis. Circulation 109:III27–III32.

Donaldson K, Stone V, Seaton A, MacNee W. 2001. Ambient particle inhalation and the cardiovascular system: Potential mechanisms. Environ Health Perspect 109 Suppl 4:523–527.

Johnston HJ, Hutchison GR, Christensen FM, Peters S, Hankin S, Stone V. 2009. Identification of the mechanisms that drive the toxicity of TiO(2) particulates: The contribution of physicochemical characteristics. Part Fibre Toxicol 6:33.

Möller W, Kreyling WG, Schmid O, Semmler-Behnke, Schulz H. 2009. Deposition, retention and clearance, and translocation of inhaled fine and nano-sized particles. In: Particle and Lung Interactions. Second Edition. (Gehr P, Mühlfeld C, Rothen-Rutishauser B, Blank F, eds.) Informa Health Care, New York, NY.

National Institute for Occupational Safety and Health. 2011. Occupational exposure to titanium dioxide. Current Intelligence Bulletin 63 (DHHS Publication No. 2011-160). Available from *www.cdc.gov/niosh/docs/2011-160/pdfs/2011-160.pdf.*

Nurkiewicz TR, Porter DW, Barger M, Castranova V, Boegehold MA. 2004. Particulate matter exposure impairs systemic microvascular endothelium-dependent dilation. Environ Health Perspect 112:1299–1306.

Nurkiewicz TR, Porter DW, Barger M, Millecchia L, Rao KM, Marvar PJ, Hubbs AF, Castranova V, Boegehold MA. 2006. Systemic microvascular dysfunction and inflammation after pulmonary particulate matter exposure. Environ Health Perspect 114:412–419.

Nurkiewicz TR, Porter DW, Hubbs AF, Cumpston JL, Chen BT, Frazer DG, Castranova V. 2008. Nanoparticle inhalation augments particle-dependent systemic microvascular dysfunction. Part Fibre Toxicol 5:1–12.

Oberdorster G, Oberdorster E, Oberdorster J. 2005. Nanotoxicology: An emerging discipline evolving from studies of ultrafine particles. Environ Health Perspect 113: 823–839.

Sager TM, Kommineni C, Castranova V. 2008. Pulmonary response to intratracheal instillation of ultrafine versus fine titanium dioxide: Role of particle surface area. Part Fibre Toxicol 5:17.

U.S. Environmental Protection Agency. 2009. Integrated Science Assessment for Particulate Matter. EPA/600/R-08/139F. Office of Research and Development, Research Triangle Park, NC.

Utell MJ, Frampton MW, Zareba W, Devlin RB, Cascio WE. 2002. Cardiovascular effects associated with air pollution: Potential mechanisms and methods of testing. Inhal Toxicol 14:1231–1247.

RELATED HEI PUBLICATIONS: PARTICULATE MATTER

Number	Title	Principal Investigator	Date*
Research Reports			
159	Role of Neprilysin in Airway Inflammation Induced by Diesel Exhaust Emissions	S.S. Wong	2011
151	Pulmonary Effects of Inhaled Diesel Exhaust in Young and Old Mice: A Pilot Project	D.L. Laskin	2010
147	Atmospheric Transformation of Diesel Emissions	B. Zielinska	2010
145	Effects of Concentrated Ambient Particles and Diesel Engine Exhaust on Allergic Airway Disease in Brown Norway Rats	J.R. Harkema	2009
138	Health Effects of Real-World Exposure to Diesel Exhaust in Persons with Asthma	J. Zhang	2009
136	Uptake and Inflammatory Effects of Nanoparticles in a Human Vascular Endothelial Cell Line	I.M. Kennedy	2009
135	Mechanisms of Particulate Matter Toxicity in Neonatal and Young Adult Rat Lungs	K.E. Pinkerton	2008
134	Black-Pigmented Material in Airway Macrophages from Healthy Children: Association with Lung Function and Modeled PM_{10}	J. Grigg	2008
129	Particle Size and Composition Related to Adverse Health Effects in Aged, Sensitive Rats	F.F. Hahn	2003
128	Neurogenic Responses in Rat Lungs After Nose-Only Exposure to Diesel Exhaust	M.L. Witten	2005
126	Effects of Exposure to Ultrafine Carbon Particles in Healthy Subjects and Subjects with Asthma	M.W. Frampton	2004
124	Particulate Air Pollution and Nonfatal Cardiac Events		2005
	Part I. Air Pollution, Personal Activities, and Onset of Myocardial Infarction in a Case–Crossover Study	A. Peters	
	Part II. Association of Air Pollution with Confirmed Arrhythmias Recorded by Implanted Defibrillators	D. Dockery	
120	Effects of Concentrated Ambient Particles on Normal and Hypersecretory Airways in Rats	J.R. Harkema	2004
118	Controlled Exposures of Healthy and Asthmatic Volunteers to Concentrated Ambient Particles in Metropolitan Los Angeles	H. Gong Jr.	2003
117	Peroxides and Macrophages in Toxicity of Fine Particulate Matter	D.L. Laskin	2003
112	Health Effects of Acute Exposure to Air Pollution	S.T. Holgate	2003
	Part I. Healthy and Asthmatic Subjects Exposed to Diesel Exhaust		
	Part II. Healthy Subjects Exposed to Concentrated Ambient Particles		

Continued

** Reports published since 1999.*
Copies of these reports can be obtained from the Health Effects Institute and many are available at http://pubs.healtheffects.org.

RELATED HEI PUBLICATIONS: PARTICULATE MATTER

Number	Title	Principal Investigator	Date*
110	Particle Characteristics Responsible for Effects on Human Lung Epithelial Cells	A.E. Aust	2002
106	Effects of Combined Ozone and Air Pollution Particle Exposure in Mice	L. Kobzik	2001
105	Pathogenomic Mechanisms for Particulate Matter Induction of Acute Lung Injury and Inflammation in Mice	G.D. Leikauf	2001
104	Inhalation Toxicology of Urban Ambient Particulate Matter: Acute Cardiovascular Effects in Rats	R. Vincent	2001
96	Acute Pulmonary Effects of Ultrafine Particles in Rats and Mice	G. Oberdörster	2000
91	Mechanisms of Morbidity and Mortality from Exposure to Ambient Air Particles	J.J. Godleski	2000
Special Report			
17	A Critical Review of the Health Effects of Traffic-Related Air Pollution		2010
HEI Communications			
10	Improving Estimates of Diesel and Other Emissions for Epidemiologic Studies		2003
7	Diesel Workshop: Building a Research Strategy to Improve Risk Assessment		1999
HEI Perspectives			
	Understanding the Health Effects of Components of the Particulate Matter Mix: Progress and Next Steps		2002

** Reports published since 1999.*
Copies of these reports can be obtained from the Health Effects Institute and many are available at http://pubs.healtheffects.org.

HEI BOARD, COMMITTEES, and STAFF

Board of Directors

Richard F. Celeste, Chair *President Emeritus, Colorado College*

Sherwood Boehlert *Of Counsel, Accord Group; Former Chair, U.S. House of Representatives Science Committee*

Enriqueta Bond *President Emeritus, Burroughs Wellcome Fund*

Purnell W. Choppin *President Emeritus, Howard Hughes Medical Institute*

Michael T. Clegg *Professor of Biological Sciences, University of California–Irvine*

Jared L. Cohon *President, Carnegie Mellon University*

Stephen Corman *President, Corman Enterprises*

Gowher Rizvi *Vice Provost of International Programs, University of Virginia*

Linda Rosenstock *Dean, School of Public Health, University of California–Los Angeles*

Henry Schacht *Managing Director, Warburg Pincus; Former Chairman and Chief Executive Officer, Lucent Technologies*

Warren M. Washington *Senior Scientist, National Center for Atmospheric Research; Former Chair, National Science Board*

Archibald Cox, Founding Chair *1980–2001*

Donald Kennedy, Vice Chair Emeritus *Editor-in-Chief Emeritus,* Science*; President Emeritus and Bing Professor of Biological Sciences, Stanford University*

Health Research Committee

David L. Eaton, Chair *Associate Vice Provost for Research and Director, Center for Ecogenetics and Environmental Health, School of Public Health, University of Washington–Seattle*

David T. Allen *Gertz Regents Professor in Chemical Engineering; Director, Center for Energy and Environmental Resources, University of Texas–Austin*

David Christiani *Elkan Blout Professor of Environmental Genetics, Harvard School of Public Health*

David E. Foster *Phil and Jean Myers Professor, Department of Mechanical Engineering, Engine Research Center, University of Wisconsin–Madison*

Uwe Heinrich *Professor, Medical School Hannover; Executive Director, Fraunhofer Institute for Toxicology and Experimental Medicine, Hanover, Germany*

Grace LeMasters *Professor of Epidemiology and Environmental Health, University of Cincinnati College of Medicine*

Sylvia Richardson *Professor of Biostatistics, Department of Epidemiology and Public Health, Imperial College School of Medicine, London, United Kingdom*

Richard L. Smith *Director, Statistical and Applied Mathematical Sciences Institute, University of North Carolina–Chapel Hill*

James A. Swenberg *Kenan Distinguished Professor of Environmental Sciences, Department of Environmental Sciences and Engineering, University of North Carolina–Chapel Hill*

HEI BOARD, COMMITTEES, and STAFF

Health Review Committee

Homer A. Boushey, Chair *Professor of Medicine, Department of Medicine, University of California–San Francisco*

Ben Armstrong *Reader in Epidemiological Statistics, Public and Environmental Health Research Unit, Department of Public Health and Policy, London School of Hygiene and Tropical Medicine, United Kingdom*

Michael Brauer *Professor, School of Environmental Health, University of British Columbia, Canada*

Bert Brunekreef *Professor of Environmental Epidemiology, Institute of Risk Assessment Sciences, University of Utrecht, the Netherlands*

Mark W. Frampton *Professor of Medicine and Environmental Medicine, University of Rochester Medical Center*

Stephanie London *Senior Investigator, Epidemiology Branch, National Institute of Environmental Health Sciences*

Armistead Russell *Georgia Power Distinguished Professor of Environmental Engineering, School of Civil and Environmental Engineering, Georgia Institute of Technology*

Lianne Sheppard *Professor of Biostatistics, School of Public Health, University of Washington–Seattle*

Officers and Staff

Daniel S. Greenbaum *President*
Robert M. O'Keefe *Vice President*
Rashid Shaikh *Director of Science*
Barbara Gale *Director of Publications*
Jacqueline C. Rutledge *Director of Finance and Administration*
Helen I. Dooley *Corporate Secretary*

Kate Adams *Staff Scientist*
Aaron J. Cohen *Principal Scientist*
Maria G. Costantini *Principal Scientist*
Philip J. DeMarco *Compliance Manager*
Suzanne Gabriel *Editorial Assistant*
Hope Green *Editorial Assistant (part time)*
L. Virgi Hepner *Senior Science Editor*
Anny Luu *Administrative Assistant*
Francine Marmenout *Senior Executive Assistant*
Nicholas Moustakas *Policy Associate*
Hilary Selby Polk *Senior Science Editor*
Sarah Rakow *Science Administrative Assistant*
Evan Rosenberg *Staff Accountant*
Robert A. Shavers *Operations Manager*
Geoffrey H. Sunshine *Senior Scientist*
Annemoon M.M. van Erp *Senior Scientist*
Katherine Walker *Senior Scientist*
Morgan Younkin *Research Assistant*

HEALTH
EFFECTS
INSTITUTE

101 Federal Street, Suite 500
Boston, MA 02110, USA
+1-617-488-2300
www.healtheffects.org

RESEARCH
REPORT

Number 164
December 2011